

LANSOPRAZOLE AND ITS METABOLITES IN THE TREATMENT OF TNBC AND THE
CONTRIBUTION OF ABCG2 TO CC-115 RESISTANCE

Jennifer Diane Beebe

Submitted to the faculty of the University Graduate School

in partial fulfillment of the requirements

for the degree

Doctor of Philosophy

in the Department of Pharmacology & Toxicology

Indiana University

August 2019

Accepted by the Graduate Faculty, Indiana University, in partial
fulfillment of the requirements for the degree of Doctor of Philosophy.

Doctoral Committee:

Jian-Ting Zhang, Ph.D., Chair

Travis Jerde, Ph.D.

Ahmad Safa, Ph.D.,

Jingwu Xie, Ph.D.,

Melissa Fishel, Ph.D.

May 13, 2019

© 2019

Jennifer Diane Beebe

ACKNOWLEDGEMENTS

My mentor, Dr. Zhang, has been supportive and helpful over the past several years to ensure the successful completion of my work. He has been instrumental in developing my critical thinking and scientific communication skills. Additionally, my committee members, Dr. Jerde, Dr. Safa, Dr. Xie, and Dr. Fishel contributed to my development and expertise by guiding me to learn and to grow as a doctoral candidate.

I would like to thank all my present and former lab mates for their assistance. They were not only able to provide me with help in solving technical problems in lab, but they also contributed to discussions about my projects and helped to determine potential avenues to pursue for my research. They have been invaluable, providing support and helping me to navigate graduate school.

I would like to thank the entire IUSM support staff who assisted me every step of the way. Lauren Easterling, Tara Hobson-Prater, Brandy Wood, and Britney Heiser from the graduate office were there whenever required and helped set up events for graduate students and post docs. Amy Lawson, Joanna Plew, and Lisa King helped with all the administrative tasks and answered any questions I may have had. Rob Lawson was always able to address my computer problems, and I appreciated his willingness to help whenever an issue arose. Andy Boyll supported me by submitting all my grant applications.

Thank you to ISUM graduate division travel grants, CSCO Young Investigator Award, and IU Simon Cancer Center Training Fellowship for supporting me during graduate school and providing necessary funds to attend international conferences. I

would also like to thank Pharmacology and Toxicology professors who took the time to teach me how to critically read scientific papers and how to interpret scientific data.

Lastly, I would like to thank all my family and friends who have all been very supportive throughout this process, especially my mom who was always willing to lend an ear when I needed to talk through issues. I have made lasting friendships while in graduate school and maintained some since childhood. These friends have been there to support me, and, without them, this process would have been extremely difficult. My final thank you goes out to my dog, Mocha, for always being there and providing me with a distraction after working for hours on end. She made me get up and stay active.

Jennifer Diane Beebe

LANSOPRAZOLE AND ITS METABOLITES IN THE TREATMENT OF TNBC AND THE
CONTRIBUTION OF ABCG2 TO CC-115 RESISTANCE

Triple-negative breast cancer (TNBC) is a highly aggressive form of breast cancer with a dismal prognosis. Targeted therapies for breast cancer with expression of estrogen receptor (ER), progesterone receptor (PR), and human epidermal growth factor receptor 2 (HER2) are currently available; however, due to the lack of ER, PR, and HER2 in TNBC, targeted therapies are limited. While surgery and traditional chemotherapy remain the standard of care, development of a new treatment strategy for TNBC is needed to improve clinical outcomes. Fatty acid synthase (FASN) has been implicated as a metabolic oncogene and has given cancer cells a survival advantage by increasing NHEJ repair. Recently, it has been shown that FDA-approved proton pump inhibitors, used for the treatment of acid related digestive diseases, have antitumor effects. Here, I show that a metabolite of lansoprazole, 5-hydroxy lansoprazole sulfide, has increased potency over parent compound lansoprazole. 5-hydroxy lansoprazole sulfide inhibits FASN, leading to a decrease in PARP and NHEJ DNA repair activity in TNBC. Ultimately, this leads to an increase in DNA damage and cell death via apoptosis. These findings suggest that 5-hydroxy lansoprazole sulfide, as a metabolite of lansoprazole, may have better activity in suppressing TNBC cells and that 5-hydroxy lansoprazole sulfide may be developed as a therapeutic for TNBC treatment.

Furthermore, due to the role of FASN in increasing NHEJ repair, we hypothesized that FASN played a role in resistance to CC-115, a dual mTOR/DNA-PK inhibitor currently

in clinical trials, by increasing DNA-PK activity. However, it was found that ABCG2, an ATP-binding cassette transporter, and not FASN, has a role in CC-115 resistance. ABCG2 effluxes CC-115 from cancer cells, increasing resistance to treatment. Inhibition of ABCG2 by FTC or PZ39C8 led to accumulation of CC-115 within cells and sensitization to treatment. Therefore, ABCG2 status should be assessed to stratify patients into treatment groups, increasing the efficacy of CC-115 treatment.

Jian-Ting Zhang, Ph.D., Chair

TABLE OF CONTENTS

LIST OF TABLES	xi
LIST OF FIGURES	xii
LIST OF ABBREVIATIONS	xv
CHAPTER 1: INTRODUCTION.....	1
Section 1.A: Breast Cancer.....	1
Section 1.B: Fatty Acid Synthase.....	10
Section 1.C: FASN and Cancer.....	18
Section 1.D: Inhibitors of FASN.....	22
Section 1.E: CC-115 and NHEJ.....	28
Section 1.F: ATP-binding cassette transporters and drug resistance	32
CHAPTER 2: MATERIALS AND METHODS	38
Section 2.A: Reagents	38
Section 2.B: Cell Culture	40
Section 2.C: Western Blot.....	44
Section 2.D: RT-PCR	46
Section 2.E: Proliferation and Survival Assays	47
2.E.1 Methylene Blue.....	47
2.E.2 MTT	48
2.E.4 Apoptosis Assay	48
2.E.5 Cell Cycle Analysis	49
Section 2.F: Drug Accumulation Assay	50

Section 2.G: Confocal Microscopy	50
2.G.1 Quantification of puncta staining.....	51
Section 2.H: NHEJ Activity Assay.....	52
2.H.1 Plasmid Prep.....	53
Section 2.I: FASN Activity Assays	53
2.I.1 Free Fatty Acid Quantification Assay	53
Section 2.J: Measurement of Reactive Oxygen Species	54
Section 2.K: Statistical Analysis.....	55
CHAPTER 3: RESULTS.....	56
Section 3.A: 5-Hydroxy Lansoprazole Sulfide.....	56
3.A.1 Lansoprazole and its metabolite 5-Hydroxy Lansoprazole Sulfide have cytotoxic effects in TNBC cell lines.	56
3.A.2 5-Hydroxy Lansoprazole Sulfide causes apoptosis	64
3.A.3 Treatment with 5-Hydroxy Lansoprazole Sulfide increases DNA double strand breaks	70
3.A.4 Reactive oxygen species scavenger NAC reverses DNA damage and apoptosis	74
3.A.5 5-Hydroxy Lansoprazole Sulfide does not produce reactive oxygen species	76
3.A.6 5-Hydroxy Lansoprazole Sulfide treatment decreases NHEJ repair activity	79
3.A.7 5-Hydroxy Lansoprazole Sulfide inhibits Fatty Acid Synthesis.....	83

Section 3.B CC-115	87
3.B.1 FASN does not play a role in resistance to DNA-PK inhibitor Nu7441 or CC-115	87
3.B.2 Identification of ABCG2 as a contributor to CC-115 resistance	91
3.B.3 Inhibition of ABCG2 reverses CC-115 resistance by increasing accumulation of drug.....	95
3.B.4 Overexpression of ABCG2 in MCF7 and HEK293 cells increases resistance to CC-115	98
3.B.5 CC-115 is also a substrate of ABCB1	105
CHAPTER 4: DISCUSSION	108
Section 4.A: 5-hydroxy lansoprazole Sulfide	108
Section 4.B: CC-115.....	116
Future Directions	118
REFERENCES	123
CURRICULUM VITAE	

LIST OF TABLES

Table 1: Buffers	38
Table 2: Reagent list	38
Table 3: Cell lines and Media.....	41
Table 4: Breast Cancer subtype for each cell line and identification of plasmids used for stable transfection.....	43
Table 5: Identification of Non-cancerous cell lines utilized and their origin	44
Table 6: Antibodies.....	46
Table 7: RTPCR Primers	47

LIST OF FIGURES

Figure 1: ErbB signaling	9
Figure 2: Overview of cellular metabolism.....	13
Figure 3: Reactions of Fatty Acid Synthesis	15
Figure 4: Schematic of the DNA-PK pathway (A) and mTOR pathway (B).....	30
Figure 5: ABCG2 dimerization and oligomerization allows for active transport of substrates across the membrane	35
Figure 6: Metabolic Pathways for Proton Pump Inhibitors	58
Figure 7: Lansoprazole's Metabolites.....	59
Figure 8: Effect of Lansoprazole and its Metabolites on Breast Cancer Cell lines	61
Figure 9: Lansoprazole and 5-Hydroxy Lansoprazole Sulfides effect on TNBC cell and non-cancerous breast cell lines	63
Figure 10: Treatment of TNBC cell line MDA-MB-231 with lansoprazole of 5- hydroxy lansoprazole sulfide does not affect cell cycle.....	64
Figure 11: Treatment with 5-hydroxy lansoprazole sulfide induces apoptosis in MDA-MB-231 cells.....	67
Figure 12: Treatment with 5-hydroxy lansoprazole sulfide induces apoptosis in MDA-MB-468.....	68
Figure 13: Treatment with MDA-MB-231 induces cleavage of PARP and caspase 3.....	69
Figure 14: Treatment of MDA-MB-468 with lansoprazole and 5-hydroxy lansoprazole sulfide induces cleaved PARP and cleaved caspase 3	70

Figure 15: 5-hydroxy lansoprazole sulfide reduces PARP expression and increases γ H2AX	72
Figure 16: 5-hydroxy lansoprazole sulfide treatments leads to DNA double strand breaks as indicated by γ H2AX puncta staining	73
Figure 17: Lansoprazole and 5-hydroxy lansoprazole sulfide does not create DNA double strand breaks, as indicated by γ H2AX, or induce cleavage of PARP in non-cancerous breast epithelial cells lines	74
Figure 18: ROS scavenger NAC abrogates apoptosis in MDA-MB-231 cells treated with 5-hydroxy lansoprazole sulfide.....	75
Figure 19: ROS scavenger NAC reduces cleavage of PARP and caspase 3.....	76
Figure 20: 5-hydroxy lansoprazole sulfide does not produce ROS.....	79
Figure 21: Treatment of MDA-MB-231 and MDA-MB-468 cells with lansoprazole and 5-hydroxy lansoprazole sulfide reduces mRNA levels of PARP	80
Figure 22: Depiction of the NHEJ assay	82
Figure 23: 5-Hydroxy Lansoprazole Sulfide decreases NHEJ activity.....	82
Figure 24: 5-hydroxy lansoprazole sulfide treatment reduces the free fatty acid content in MDA-MB-231 cells.	84
Figure 25: Hypothetical schematic of pathway	86
Figure 26: FASN does not affect the potency of CC-115	89
Figure 27: FASN does not affect the potency of DNA-PK specific inhibitor NU7441.....	90
Figure 28: CC-115 inhibition of mTOR and expression profile of efflux pumps	91
Figure 29: Absorbance and Fluorescence of CC-115	92

Figure 30: CC-115 Accumulation is decreased in M3K cells as compared to MCF7	94
Figure 31: ABCG2 decreases cellular accumulation of CC-115	96
Figure 32: Inhibition of ABCG2 sensitizes M3K cells to CC-115 and increases inhibition of mTOR signaling.....	98
Figure 33: Overexpression of ABCG2 in HEK293 and MCF7 cells reduces accumulation increases resistance to CC-115	100
Figure 34: ABCG2 increases resistance to CC-115 inhibition of mTOR.....	101
Figure 35: ABCG2 expression	102
Figure 36: Inhibition of ABCG2 in HEK293 cells restores CC-115 accumulation.....	104
Figure 37: Inhibition of ABCG2 in HEK293 cells reverses mTOR inhibition and sensitizes HEK293/ABCG2 to CC-115.....	105
Figure 38: CC-115 is a substrate for ABCB1.....	106

LIST OF ABBREVIATIONS

5HLS	5-Hydroxy Lansoprazole Sulfide
ABC	ATP-binding cassette
ABCB1	Multi-drug resistance protein 1
ABCC1	MRP1
ABCG2	ATP-binding cassette G2
ACC	Acetyl-coenzyme A carboxylase
ACP	Acyl carrier protein
AML	Acute myelogenous leukemia
AMP	Adenosine monophosphate
ANOVA	Analysis of variance
ATP	Adenosine triphosphate
BBB	Blood-brain barrier
BCRP	Breast cancer resistant protein
BRCA1/2	Breast cancer
CML	Chronic myeloid leukemia
CNS	Central nervous system
DH	β -hydroxylacyl dehydratase
DNA	Deoxyribonucleic acid
DNA-PK	DNA protein kinase
DSB	Double strand break
EGCG	Epigallocatechin-3-gallate

EGFR	Epidermal growth factor receptor
ER	Estrogen receptor
ER	Enoyl Reductase
ERK	Extracellular signal-regulated kinase
FA	Fatty Acids
FASN	Fatty acid synthase
FBS	Fetal Bovine Serum
FFA	Free fatty acids
FTC	Fumitremorgin C
HER2	Human epidermal growth factor receptor 2
HS	Horse Serum
IGF	Insulin-like growth factor
Insig	Insulin induced gene
KR	β -ketoacyl reductase
KS	β -ketoacyl synthase
Lans	Lansoprazole
MAPK	Mitogen-activated protein kinase
MAT	Malonyl/acetyl transferase
MDR	Multi-drug resistance
MEF	Mouse embryonic fibroblast
NAC	N-acetyl-L-cysteine
NBD	Nucleoside binding domain

NHEJ	Nonhomologous end joining
OD	Optical density/absorbance
OA	Oncogenic Antigen
PARP	Poly- (ADP) ribose polymerase
PI	Propidium iodide
PPI	Proton Pump inhibitor
PR	Progesterone receptor
RNA	Ribonucleic acid
ROS	Reactive Oxygen Species
Scap	SREBP-cleavage-activating protein
shRNA	small or short hairpin RNA
SREBP-1c	Sterol regulatory element-binding protein 1c
TE	Thioesterase
TNBC	Triple negative breast cancer
vATPase	Vacuolar-type H ⁺ ATPase

CHAPTER 1: INTRODUCTION

Section 1.A: Breast Cancer

The abnormal growth of cells that can spread to other areas of the body is called cancer. Cancer makes up a group of diseases that can affect all areas of the body. There are six hallmarks of cancer cells which distinguishes them from normal healthy cells. These hallmarks include: the ability of cells to evade apoptosis, self-sufficiency in growth signals, insensitivity to anti-growth signals, sustained angiogenesis, limitless replicative potential, and, the capability for tissue invasion and metastasis [1]. Over time, cells acquire DNA mutations which allow them to sustain these traits, leading to multiple types of malignancies in the body.

Breast cancer is the second most commonly diagnosed malignancy in women, after skin cancer, and has the second highest death rate in the U.S., behind lung cancer. It is estimated that 250,000 cases of invasive breast cancer are diagnosed a year and about 40,000 women die each year from breast cancer (breastcancer.org). Risk factors for breast cancer include weight, diet, alcohol use, smoking, age, family history, pregnancy, and breastfeeding. One genetic risk factor for breast cancer is a mutation in the breast cancer 1 and 2 genes (BRCA1 and BRCA2). BRCA1/2 are genes involved in activation of DNA repair processes. Mutations in these genes lead to an accumulation of DNA damage and neoplastic progression [2]. 2-6% of all breast cancers patients have a mutation in BRCA1 or BRCA2 [2]. While only 2-6% of breast cancers are affected by BRCA1/2, women who carry a mutation in one of these genes have a 40-57% lifetime risk of developing breast cancer [3]. This is a significant increase from about 12% of

women developing breast cancer in their lifetime without these mutations (breastcancer.org). Therefore, having this mutation results in the need for earlier onset of mammograms and regular breast exams.

Upon a breast cancer diagnosis, survival is highly dependent on the stage at which the cancer is diagnosed and the histological grade of the tumor cells. The earlier the cancer is detected, the better the chance of survival. Stage 0 breast cancer indicates that the abnormal, or cancer cells, remain within the duct of the breast. With increasing stages, I-III, the tumor begins to grow and invade nearby tissues, including the lymph nodes. At stage III, breast cancer is more advanced and harder to treat than at lower stages. Once the tumor has spread to distant areas of the body, it is considered stage IV. With increasing stages, there is a decrease in 5-year survival rate. 5-year survival rates are as follows: stage 0-1, nearly 100%; stage II, 93%; stage III, 72%; and, finally, stage IV, 22%.

The histological grade of a tumor is a measurement of how different tumor cells are from benign cells and explains the differentiation state of the tumor. The more the tumors resemble benign cells, the lower the grade. The grade becomes higher as tumor cells show more abnormal characteristics and increased growth rate [4]. In breast cancer, the grade of a tumor is determined by the degree of gland formation, the variability in the size and shape of cells, as well as the mitotic count [5]. Grade I tumors maintain a tubular structure, resembling normal ducts and are not growing rapidly. Grade II tumors are beginning to lose glandular structure and acquire an abnormal phenotype, with an increase in growth rate as compared to benign cells. Grade III

tumors are very abnormal and have a very high proliferation index [6]. Both stage and grade are taken into account when physicians develop a course of treatment. Typically, a higher-grade tumor will require a more aggressive and immediate treatment course. The stage and grade will also help to determine which patients will benefit from adjuvant chemotherapy and those that will not.

Breast cancer progression typically occurs in stages. The first stage being ductal hyperplasia of the ductal epithelial. Eventually, this hyperplasia becomes atypical and cells begin to populate the luminal duct. This stage of breast cancer is known as ductal carcinoma in-situ. If left untreated the cancer cells will spread outside the duct to the surrounding breast tissue where it will be classified as invasive ductal carcinoma. Breast cancer then becomes metastatic when it has spread to distant areas of the body outside the breast [7, 8]. There are several genetic alterations that have been implicated in breast cancer progression including mutations in BRCA, ATM, TP53, PTEN, AKT, and PI3KCA [7, 9-12].

Epigenetic changes also play a role in breast cancer progression. The main forms of epigenetic change that occur in breast cancer is DNA methylation or demethylation of CpG islands in gene promoter regions and histone modifications [13]. DNA methylation in the promoter region of a gene will shut off expression due to an inability of transcription factors to bind to these regions. On the other hand, demethylation of a promoter will allow for its expression. Hypermethylation of genes involved in apoptosis, cell cycle regulation (CCND2, CDKN2A), DNA repair (GSTP1, BRCA1), hormone mediated cell signaling, and tissue invasion and metastasis have been observed in breast cancer

[14, 15]. Hypomethylation has also been observed in MDR1, NOTCH1 and NAT1 [7, 13, 16, 17]. Increased DNA methylation of promoter regions of the DNA has been shown to be a risk factor for developing breast cancer [18]. Furthermore, a distinct pattern of hyper- and hypo- methylation of specific genes has emerged in the progression from ductal hyperplasia to atypical hyperplasia to ductal carcinoma in-situ and finally to metastatic breast cancer [14, 19-21]. An increase in methylation occurs in genes such as APC and CDH1 during progression while there is a decrease in methylation of LINE1 during progression [22, 23]. TNBC specifically, is associated with hypermethylation of CD44, CDKN2B, RB, and p73, and hypomethylation of GSTP1, MSH2, TWIST1, DLC1, MSH6, and ID4 [24]. Additionally, an analysis of TNBC methylated regions showed that the hypomethylated profile was associated with better survival within the first 5 years compared to hypermethylated profile being associated with worse prognosis [15].

Another form of epigenetic change, that has not been studied as extensively in breast cancer, is alterations of histones by post-transcriptional modifications. Acetylation or methylation of histones can lead to open or closed DNA, allowing for transcription or repressing transcription of genes [25]. Studies in breast cancer cell lines compared to non-cancerous cells lines have shown an increase in H3K4ac and H3K4me in TNBC potentially suggesting increased metastatic potential [26]. A genome-wide analysis of histones, their modifications, and their location has provided information on histones, modifications, and genes at specific sites that may be involved in cancer initiation and progression [27]. Further study in the epigenetics of breast cancer may

yield new treatment strategies and help to divide breast cancer into specific treatment groups.

Using DNA microarrays, breast tumors have been divided into four main distinct subtypes of breast cancer [28]. These subtypes correspond to histological grade of tumors and clinically observed features. These distinct features have been shown to influence patterns of response to different treatment strategies. Therefore, the subtype of breast cancer will help to determine course of treatment as well as patient prognosis. The main subclasses of breast cancers are luminal, which is broken up into luminal A and B, human epidermal growth factor receptor 2 (HER2) positive, and triple-negative (TNBC) breast cancer [29]. Microarray data revealed that luminal type tumors express luminal cytokeratins and other markers of epithelial cells. On the other hand, TNBC do not express ER, PR, or markers of luminal epithelial cells but several express basal cytokeratins such as CK5, and increased growth factor receptor expression [28]. Furthermore, microarray comparative genomic hybridization classified basal-like tumors as having an increased copy-number variation, but also low-level copy-number gains. This indicates more genetic instability because there are increased copy-number of genes throughout the genome that do not occur in the same pattern between samples [30, 31]. In contrast, luminal B and HER2 type had high level amplifications at specific gene sites [30].

The most common type of breast cancer is luminal A breast cancer, comprising about 50-60% of all breast cancer cases. Luminal A cancers are typically characterized by high levels of estrogen receptor (ER) and/or progesterone receptor (PR) and are known

to grow slower than other subtypes, classifying them as low-grade tumors [32]. The majority of luminal B breast cancers are ER-positive and some express HER2. Luminal B cancers differ from luminal A by a marked increase in proliferative ability and increased expression of growth receptors [33]. Luminal B cancers are tumors with intermediate to high-grade differentiation, and make up about 15-20% of all breast cancers [34]. A third subset of breast cancer is the HER2-positive breast cancers. HER2-positive tumors make up 15-20% of all breast cancer cases and are high-grade breast cancers [34]. Lastly, TNBC is characterized by a lack of ER, PR, and HER2. TNBC makes up about 10-20% of cancer cases and involves high-grade tumors [34].

Treatment and outcomes of the different subtypes of breast cancer largely depends on the stage of the cancer and the molecular characteristics described above. Breast cancer is treated with a combination of surgery, radiation, chemotherapy, and targeted chemotherapy. Surgery removes the bulk of the primary tumor and nearby lymph nodes. Some patients will receive neoadjuvant chemotherapy, or chemotherapy prior to surgery, to shrink the tumor and to help prevent micro-metastasis while others will not require this treatment. Standard chemotherapy is usually administered intravenously, to ensure systemic drug delivery, and affects the entire body. Commonly used chemotherapeutic drugs include: alkylating agents, plant alkaloids, antitumor antibiotics, antimetabolites, and topoisomerase inhibitors. Many chemotherapies aim to cause DNA damage, or cell cycle arrest, ultimately leading to cancer cell death. Chemotherapies are very toxic to the body and come with many adverse side effects such as nausea, vomiting, appetite change, hair loss, fatigue, and increased risk of

infection. Targeted chemotherapies aim to identify ways in which cancer cells are different from benign healthy cells. These therapies utilize these differences to treat cancer. While targeted therapies still have side effects, they tend to be less severe than those observed with traditional chemotherapy [35, 36].

Luminal A breast cancer has a very good prognosis. The rate of relapse in patients with luminal A breast cancer is lower than in all other subtypes of breast cancer [34]. Due to the high expression of the ER, these types of tumors can be treated with hormone therapy. Activation of ER in luminal A tumors leads to expression of genes involved in proliferation as well as cell survival [37]. Blocking this pathway, by blocking the ER itself or inhibiting estrogen production, has shown to be an effective treatment strategy for luminal A cancers. While luminal A breast cancer generally has a good prognosis and responds to hormone therapy, luminal B breast cancers are less responsive to hormone therapy. It has been suggested that luminal B cancer is estrogen independent due to a switch to different growth factor receptor pathways such as EGFR, IGF, or PIK [38]. Activation of these other pathways provides luminal B cancers with survival and growth advantages that are not affected by hormone therapy. Luminal B cancers have a slightly worse prognosis, and an increased recurrence rate as compared to luminal A breast cancers. This increase in relapse over luminal A is observed only in the first 5 years. Treatment for luminal B cancers differs from luminal A in that these tumors have a better response when given neoadjuvant chemotherapy, while there is no added benefit of neoadjuvant chemotherapy in luminal A breast cancer [34, 39].

HER2-positive breast cancers are so-named due to the overexpression of HER2. HER2 is a member of a family of four proteins that belong to the ErbB lineage of proteins. These proteins are a family of receptor tyrosine kinases which play a role in cell growth, survival, and proliferation [40]. The four members of this family are EGFR/ERBB1/HER1, HER2/ERBB2, HER3/ERBB3, and HER4/ERBB4 depicted in Figure 1. Typically, these four family members bind their ligand forming homo- and heterodimers, leading to activation of downstream signaling pathways including PI3K, JAK/STAT, and MAPK [41]. However, HER2 does not bind any known ligand and does not normally form homodimers. HER2 becomes active by binding to other family members that have been activated by ligand [40]. Overexpression of HER2 has been shown to lead to the formation of a functional HER2 homodimer [42]. HER2 gene amplification is the cause of HER2 overexpression 90% of the time in this subset [43]. This leads to a 40-100-fold increase in HER2 expression [44, 45]. HER2 type cancers without targeted treatment have a very poor outcome [34]. Luckily, trastuzumab, a monoclonal antibody targeting HER2 has been developed and has significantly improved the overall prognosis for HER2-positive tumors [46]. Adjuvant trastuzumab alone reduced recurrence by 50% [47]. HER2-positive cancers are therefore treated with anthracycline chemotherapy in combination with trastuzumab.

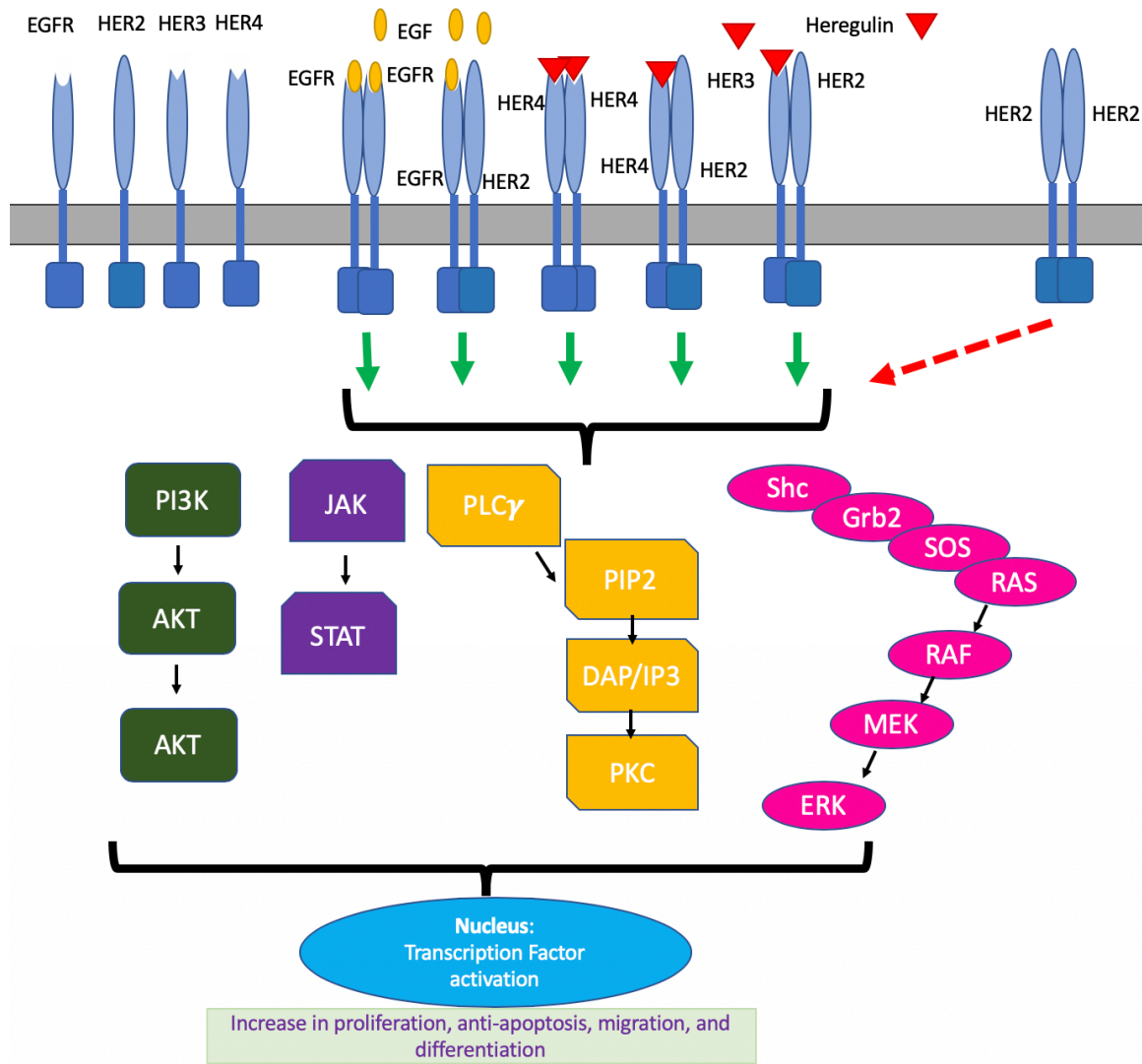


Figure 1: ErbB signaling – The ErbB receptor family signals by binding their respective ligands and forming homo- and heterodimers. HER2 does not bind any ligand and becomes active by binding to other family members that have bound ligand. Typically, HER2 does not form an active homodimer but it has been shown that overexpression of HER in cancer can lead to signaling. The ErbB family of receptors, upon dimerization, leads to activation of several signaling pathways including PI3K, MAPK, and JAK/STAT increasing proliferation, survival, differentiation, and migration [41, 48, 49].

In contrast, TNBC does not express ER, PR, or HER2, making targeted treatment difficult at present. It does not respond to hormone therapy or HER2 targeted therapies. Additionally, very few mutations occur across TNBC. Two common mutations are p53

and PI3KCA [50]. TNBC has also been associated with an increase in EGFR, however, clinical trials using EGFR inhibitors in the treatment of TNBC have shown that only a very small percentage (0-3%) of patients responded to gefitinib and erlotinib treatment [51, 52]. TNBC has the worst prognosis of all cancer subtypes and has the highest mortality rate within the first 3-5 years of diagnosis. The mainstay treatment for TNBC is currently a mix of chemotherapies with varying responses. A subset of TNBC patients are those with BRCA mutations. Patients harboring a BRCA1/2 mutation will have a TNBC phenotype 75% of the time [53]. There are two main pathways utilized by cancer cells to overcome DNA DSBs. The first, homologous recombination, occurs during DNA synthesis and is controlled by BRCA1/2 [54]. The second, NHEJ, can occur throughout the cell cycle but is an error prone method for DNA repair [55]. Due to the role of the BRCA genes in DNA repair, these patients are treated with DNA damaging agents, that ultimately lead to accumulation in DNA DSBs, leading to synthetic lethality. Studies have shown that neoadjuvant administration of cisplatin, a DNA damaging drug, leads to complete pathological response in a high number of patients with these mutations [56]. While this subset of TNBC responds well to chemotherapy, others do not and have no other treatment options. For this reason, there is significant interest in determining new treatment strategies for TNBC to improve patient health and prognosis.

Section 1.B: Fatty Acid Synthase

In 1989, OA-519 was identified as a prognostic factor in breast cancer. Patients who expressed OA-519 were 4 times more likely to have recurrence of tumors and

metastasis [57]. There was an even greater chance of recurrence and metastasis when high expression was observed in estrogen receptor negative breast cancer. OA-519 staining in prostate cancer increased with increasing stage and grade of tumors, while no OA-519 staining was observed in benign prostate tissue [58]. Further studies showed that OA-519 was a good prognostic factor for breast, ovarian, and prostate cancers [59-61]. In 1994, OA-519 was identified as fatty acid synthase [62]. Since then, FASN overexpression has been observed in many types of cancers, including breast, prostate, ovarian, thyroid, colorectal, pancreatic, hepato-cellular carcinoma, lung, melanoma, bladder and stomach [63]. Furthermore, not only is FASN overexpressed, it has also been shown, using [^{14}C] glucose, that 93% of all esterified fatty acids in cancer cells were made by *de novo* synthesis [64]. This would indicate that FASN is playing a major role in cancer cells.

In the presence of a high carbohydrate diet, glucose derived from these carbohydrates is converted to pyruvate during glycolysis. Pyruvate is transported to the mitochondria where it is converted to acetyl-CoA by pyruvate dehydrogenase and is utilized in the citric acid cycle to produce adenosine triphosphate (ATP) and nicotinamide adenine dinucleotide (NADH) [65]. NADH then releases H^+ to the electron transport chain to produce an electrochemical proton gradient that can be utilized to drive the formation of ATP, an energy storage molecule. When there is an excess of acetyl-CoA, it can be converted to citrate and shuttled back to the cytoplasm where it may be utilized for lipogenesis [66]. Lipogenesis is the process of forming fatty acids through FASN which can be stored as triglycerides or used in making other cellular lipids

[67]. Triglycerides can later be broken down by fatty acid β -oxidation to produce energy during times of low glucose supply [68]. Figure 2 depicts how glucose is taken up and utilized by the cell to produce energy in the presence and absence of oxygen as well as how glucose can be used to form other molecules required by the cell such as ribose-5-phosphate, NADPH, and, lipids.

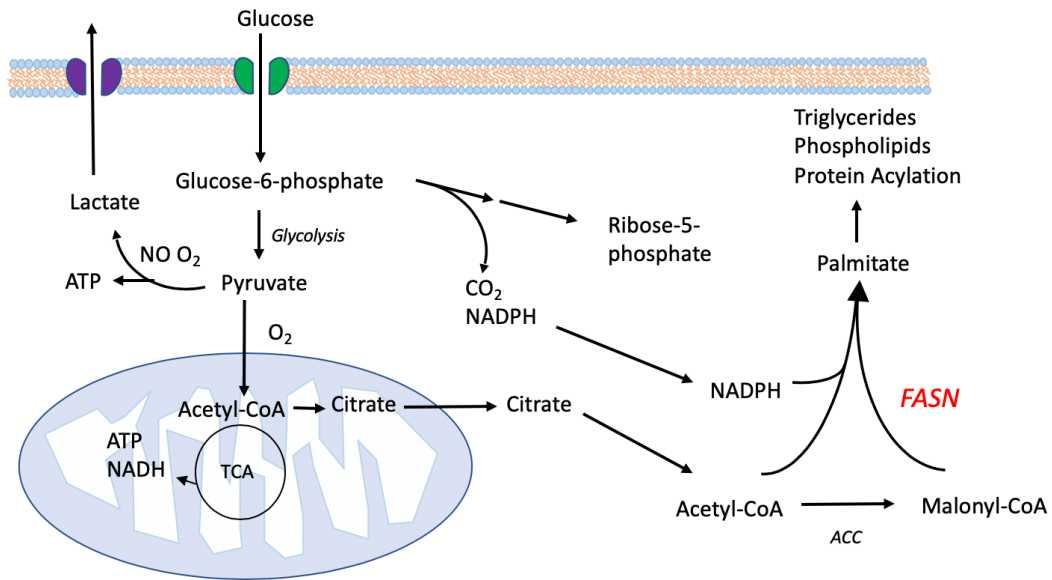
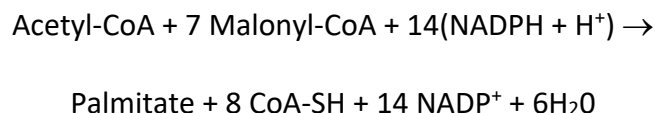
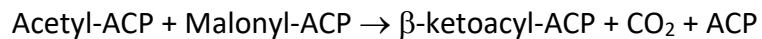


Figure 2: Overview of cellular metabolism – Cells take up glucose and shuttle it through several different pathways. In normal cells glucose is taken up by the cells and converted to pyruvate through glycolysis. The Pyruvate is then utilized in the citric acid cycle, or TCA, to produce ATP in the presence of oxygen. Normal cells can also perform lactic acid fermentation when oxygen is not available. Glucose can also move through the pentose phosphate pathway producing ribose-5-phosphate, precursor to the nucleotides, and NADPH, which can be used as a reducing agent. Excess Acetyl-CoA can be transported back to the cytoplasm in the form of citrate. Citrate is then converted back to Acetyl-CoA and can be used in the biogenesis of fatty acids by FASN. In cancer cells even in the presence of oxygen there is an increase in lactic acid fermentation, pentose phosphate pathway, and FASN [65-67, 69].

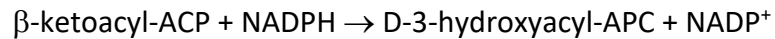
The *de novo* synthesis of 16-carbon palmitate is carried out by fatty acid synthase (FASN). In humans, FASN is a 270 kDa homodimeric enzyme made up of seven domains. FASN is the only protein in the body capable of synthesizing *de novo* fatty acids [70] from acetyl-CoA, malonyl-CoA, and NADPH. These starting molecules are used in the formation of palmitate in the following reaction [71]:



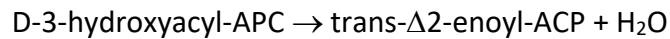
The formation of palmitate occurs as a series of reactions orchestrated by the seven domains of FASN: acyl carrier protein (ACP), β -ketoacyl synthase (KS), malonyl/acetyl transferase (MAT), β -ketoacyl reductase (KR), β -hydroxyacyl dehydratase (DH), enoyl reductase (ER), and thioesterase (TE) domain [71, 72]. Each cycle of the reaction elongates the growing carbon chain by two carbons. The first step in this process is the transfer of the acetyl group from acetyl-CoA to the ACP and malonyl from malonyl-CoA to ACP by MAT. Then, KS catalyzes the condensation of acetyl-ACP and malonyl-ACP, releasing one ACP and a CO₂ molecule.



KR then reduces the 3-keto, using NADPH, to a hydroxyl group.



A dehydration occurs by DH creating a double bond and releasing H₂O.



A second reduction occurs using NADPH and is catalyzed by ER.



This cycle will continue until the carbon chain reaches 16 carbons in length, at which point the TE domain hydrolyzes the thioester bond between the fatty acid and the ACP, releasing the free fatty acid. From there, palmitate can be used in a variety of cellular functions. The entire cycle is outlined in Figure 3.

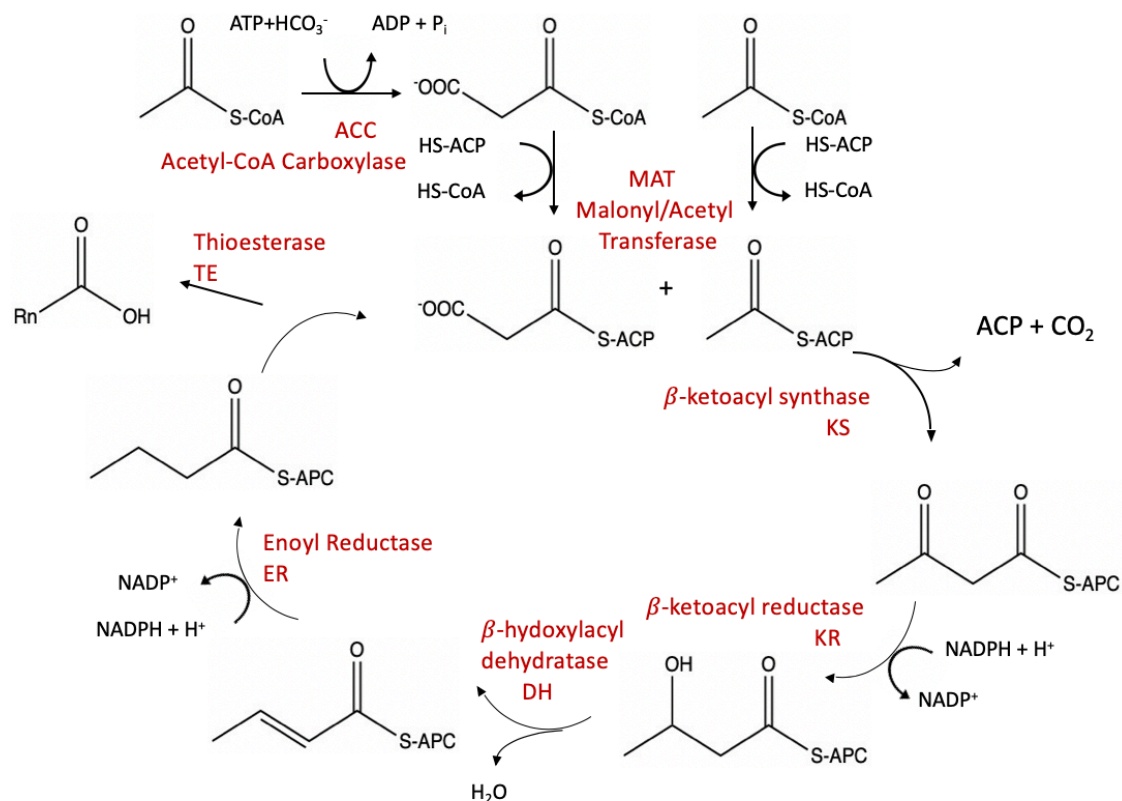


Figure 3: Reactions of Fatty Acid Synthesis – Fatty acid synthesis occurs in a series of reactions that results in the release of 16 carbon palmitate. FASN starts with the transfer of acetyl-CoA and malonyl-CoA to the APC domains in the FASN dimer, catalyzed by MAT. Malonyl-CoA is made from acetyl-CoA by ACC. KS condenses the acetyl and malonyl groups into a single chain, releasing CO₂. Then, through two reduction reactions and a dehydratase, two carbons are added to the growing chain. The new growing chain will take the place of acetyl-CoA in the beginning of the reaction, and two more carbons will be added each cycle until the chain reaches 16 carbons in length. At this point, the TE domain of FASN will cleave the new fatty acid from the enzyme, releasing it into the cytoplasm.

After palmitate is released from FASN, it can be used in a variety of ways. As discussed above (Figure 2), fatty acids can be stored in the form of triglycerides in the liver and adipose cells for use during times of low glucose [73]. Palmitate can also be used to modify different proteins. Palmitate can covalently and reversibly bind to cysteine residues within proteins in a process called palmitoylation, catalyzed by protein

palmitoyltransferases [74]. Palmitoylation of proteins increases their hydrophobicity and interaction with cellular membranes. The reversibility of this modification allows for shuttling modified proteins between cellular compartments and regions of the plasma membrane [75, 76]. Another function of palmitoylation is to target proteins to lipid rafts, where they are involved in many different types of cell signaling. Inhibition of this modification prevents localization and function of these proteins [74]. Furthermore, 16-carbon palmitate can be elongated or desaturated by other cellular enzymes. These products may then be used in cellular lipids such as phospholipids or cholesterol esters [77, 78].

In humans, fatty acid synthesis is a highly regulated pathway. Expression of FASN is controlled by the sterol regulatory element-binding protein-1c (SREBP-1c) transcription factor [79]. An increase in hormone insulin stimulated by glucose in the blood enhances transcription of SREBP-1c, leading to an increase in FASN [80, 81]. Conversely, low glucose stimulates glucagon production, suppressing SREBP-1c transcription [82]. SREBP-1c is not only regulated at the transcription level, but also post translationally. SREBP binds to SREBP-cleavage-activating protein (Scap) in the endoplasmic reticulum membrane. In the endoplasmic reticulum Scap acts as a sensor for sterol content. Cholesterol binds to Scap changing its conformation and allowing it to bind to insulin-induced gene 1 (Insig1), retaining the complex in the endoplasmic reticulum [83]. This means SREBP cannot activate transcription. When sterols are depleted in cells, Scap will not bind to Insig1, allowing the SREBP-Scap to be transported to the Golgi [84]. Here, there are two sequential proteolytic cleavage events that result

in the release of the transcription factor domain from the membrane. SREBP is now transported into the nucleus to begin transcription [84].

Another regulator of FASN is the enzyme acetyl-coenzyme A carboxylase (ACC). ACC is the rate limiting step for fatty acid synthesis because it is responsible for the conversion of 2 carbon acetyl-CoA to 3 carbon malonyl-CoA [69]. As mentioned above, malonyl-CoA is one of the starting materials required for FASN. ACC uses ATP to convert acetyl-CoA to malonyl-CoA using a carbon from CO₂ [71]. ACC activity is controlled by allosteric effectors and phosphorylation events. Citrate levels in the cytoplasm can up-regulate ACC while free CoA and fatty acyl-CoA, such as malonyl-CoA and palmitoyl-CoA, can down-regulate ACC activity [85]. AMP-activated protein kinase (AMPK), is a cellular energy sensor that tells cells to inhibit anabolic processes and conserve energy when ATP is low [86]. AMPK phosphorylates ACC, leading to its inhibition. When AMPK is turned off by low levels of AMP and high levels of ATP, ACC is dephosphorylated, becoming active again [87]. In this way, FASN is highly regulated by availability of nutrients within the cell.

Due to FASN regulation by nutrient availability, in an adult consuming a common diet today, FASN activity is not required. Today's diet high in fats reduces the need for FASN [88]. Weiss *et al.* noted that in some cases of a prolonged fat-free diet, researchers were able to observe an increase in FASN activity in human tissues; but, with the modern diet, normal cells receive enough fatty acids, with a few exceptions [88]. Expression of FASN has been observed in mostly hormone sensitive cells [89], liver cells [90, 91], and adipose cells. FASN supplies fatty acids in the breast during lactation

[92], and FASN is linked to endometrial cell proliferation during the menstrual cycle [93]. Additionally, FASN is required during embryogenesis. When mice harboring FASN^{+/}- were bred, they did not produce FASN⁻- mice. Furthermore, FASN⁻- mice produced in the lab died before implantation [94]. *De novo* FA synthesis has been shown to be active during embryogenesis and one of its known functions is in lung development, where fatty acids are used to make lung surfactant [95]. At 20 weeks gestation FASN is present in proliferative epithelial cells throughout different body systems [89].

Section 1.C: FASN and Cancer

While normal tissues do not have high expression of FASN and do not depend on *de novo* fatty acid synthesis for survival, this may not be the case for cancer cells.

Another difference in cancer cells is their preference to use lactic acid fermentation as a source of energy, even in the presence of oxygen. Normal tissues use the more efficient energy production of oxidative phosphorylation in the mitochondria when oxygen is present [96]. This phenomenon of using an inefficient method of energy production in cancer cells is known as the Warburg effect because it was first observed in the early 1920s by Otto Warburg and colleagues that cancer cells increased uptake of glucose compared to benign cells [97]. While oxidative phosphorylation is a more efficient way to produce ATP per molecule of glucose, lactic acid fermentation occurs much more rapidly and has the ability to produce comparable levels of ATP in a given time frame when glucose uptake is increased [98]. The question remains, why do cancerous cells use this method of energy production when oxidative phosphorylation is so much more

efficient? One explanation for the Warburg effect is that cells take up more glucose as an adaptation mechanism for supporting the biosynthetic requirements of proliferation. In this way, the glucose can be used as a source for anabolic processes, such as generation of nucleotides, lipids, and proteins [96]. These are building blocks which are required for rapid cellular divisions and, as stated above, 93% of esterified fatty acids in cancer cells are made by *de novo* fatty acid synthesis. This highlights the need for FASN activity. Additionally, glucose flux through the pentose phosphate pathway leads to the production of ribose-5-phosphate, a precursor for nucleotides, and NADPH, an important molecule for reduction reactions and for detoxification of reactive oxygen species (ROS) [99, 100]. These pathways are illustrated in Figure 2.

In cancer cells, a large part of the synthesized fatty acids are esterified to phospholipids in cellular membranes [62, 101]. This indicates FASN is utilized in cancer cells to produce new membranes for rapidly dividing cells. FASN overexpression and use by cancer cells may be explained by a couple different mechanisms. An increase in growth factor receptor signaling and hormones have been implicated in SREBP-1c stimulation and FASN transcription [102, 103]. Growth factor receptors such as EGFR can increase FASN transcription by activating phosphatidylinositol-3 kinase (PI3K)-Akt signaling pathway and mitogen activated protein kinase (MAPK)/extracellular signal-regulated kinase (ERK1/2) pathway [104, 105]. Additionally, commonly observed mutations in this pathway, such as the loss of phosphatase and tensin homologue (PTEN), causes activation of PI3K/Akt and correlates with FASN overexpression [106]. While this pathway has been shown to regulate FASN, FASN is also involved in

expression of receptors in this pathway. For example, FASN is responsible for regulating EGFR, HER2, and HER4 expression [107-109]. This creates a complicated coregulatory loop in which HER family members and FASN regulate each other. Steroid hormones can activate similar pathways, leading to FASN expression. Another mechanism of overexpression of FASN occurs by copy number gain of the FASN gene, which has been observed in prostate cancer [110].

FASN overexpression in cancers not only demonstrates prognosis, but also correlates with cancer stage and aggressiveness of the tumor [111]. With increasing stage, there is an increase in FASN staining within the tumor. Specifically, in terms of breast cancer, FASN is associated with clinically aggressive tumor behavior and growth [107]. In fact, there is evidence supporting the role of FASN as an early event in tumorigenesis. While FASN is not found in normal tissues, those that are pre-cancerous or early cancerous lesions have shown expression of FASN in breast, prostate, colon, esophageal, and stomach tissues [112-115]. FASN has been considered a “metabolic oncogene,” giving cells survival advantages in the hypoxic and acidic microenvironment observed in most solid tumors [116]. Overexpression of FASN in non-tumorigenic breast cells led to an increase in cell growth, HER2 expression, proliferation, and anchorage independent growth, which is indicative of tumorigenesis [111, 117]. Shutting off FASN in MCF10A transformed cells lines reversed tumorigenicity and returned cells to a more benign state [118]. Overexpression of FASN in immortalized prostate cells led to an increase in invasive tumors as compared to those lacking FASN expression [119]. FASN may be contributing to the tumorigenic phenotype in a few different ways. FASN can

affect different signaling pathways within cells. FASN overexpression leads to an increase in activation of HER1, HER2, and HER3, which has been associated with cancer [108, 117]. FASN overexpression leads to the stabilization of Wnt/ β -catenin by increasing palmitoylation of Wnt-1 [119]. Wnt/ β -catenin has been implicated in many different types of cancer by promoting tumorigenesis, proliferation, and stem cell maintenance [120, 121].

FASN has also been implicated in resistance to chemotherapeutics in cancer cells. Previously it was found in our lab that FASN was overexpressed in a doxorubicin selected breast cancer cell line and that ectopic overexpression in breast cancer cells led to an increase in resistance to doxorubicin [122]. In resistant hepatocellular carcinoma cells, FASN inhibition can sensitize cells to taxane treatment *in vitro* [123]. FASN inhibition was also capable of re-sensitizing breast cancer cells to trastuzumab treatment [62]. Furthermore, FASN is associated with resistance to gemcitabine and radiation in pancreatic cancer and radiation in nasopharyngeal carcinoma [124, 125]. These studies indicate that FASN is playing a role in resistance to a variety of anticancer agents.

There are a few proposed mechanisms as to how FASN is leading to drug resistance. One possible mechanism is FASN inhibiting apoptosis and caspase-8 activation after exposure to drug by inhibiting production of TNF- α and ceramide, upstream activators of caspase 8 [126]. Rysman *et al.* found that tumor cells that were resistant to chemotherapy had an increase in FASN. This increase correlated with an increase in saturated fatty acids in the membrane, resulting in less fluidity, as indicated

by movement of green fluorescent dye and decrease in permeability to doxorubicin. Inhibiting ACC with sorafenib or knocking down ACC or FASN returned cells to a more fluid permeable state, restoring chemo-sensitization [127]. Therefore, FASN could lead to resistance by changing cellular membrane dynamics reducing drug penetrance. A previous paper from our lab has shown that FASN increases activity of the DNA repair mechanism, non-homologous end joining (NHEJ) [128]. Repair of DNA damage by NHEJ contributes to resistance to DNA damaging agents [128]. Specifically, FASN leads to an increase in PARP expression and this increase allows for a greater recruitment of Ku proteins to sites of DNA damage and an increase in NHEJ repair [128]. This increase in repair has been shown to increase resistance to DNA damaging agents.

Section 1.D: Inhibitors of FASN

Due to the role of FASN in cancer, its association with a more aggressive form of cancer, and chemo-resistance, many studies have been conducted to identify novel inhibitors for this pathway. In breast cancer cells, silencing of FASN led to mitochondrial impairment and induction of apoptosis [129]. In colorectal cancer cells, knockdown of FASN inhibited cell proliferation, migration, and invasion [130, 131]. Proliferation and metastasis were also suppressed in gastric cancer upon suppression of FASN [132]. In prostate cancer, knockdown of FASN led to growth inhibition and induction of apoptosis while having no effect on non-malignant fibroblasts [133]. Furthermore, *Chen et al.* showed that direct injection of FASN siRNA into prostate cancer xenograft reduced tumor growth [134]. A genome-wide analysis of expression changes revealed that

silencing FASN led to a decrease in genes involved in lipid metabolism, glycolysis, the TCA cycle, and oxidative phosphorylation. Additionally, knockdown of FASN led to an upregulation of genes involved in cell cycle arrest and death receptor mediated apoptotic pathways [135]. Introduction of FASN inhibitors had synergistic effects with both docetaxel and paclitaxel in an *in vitro* model of breast cancer [136, 137]. In an *in vivo* xenograft model of non-small cell lung cancer paclitaxel and FASN inhibition had a potent synergistic effect [138]. These studies indicate that targeting FASN pharmacologically may be a way to specifically target cancers cells while having limited adverse effects on normal tissues.

Due to the number of enzymatic reactions that FASN controls, there are several ways in which FASN has been targeted. One of the first small molecule inhibitors of FASN was cerulenin. Cerulenin is a compound isolated from *Cephalosporium caerulens*, which irreversibly binds to KS domain of FASN, preventing the condensation reaction of acetyl-APC to the growing chain with malonyl-APC [139]. In breast cancer cells and promyelocytic leukemia cells, cerulenin inhibited cell growth; however, supplementing treatment with high levels of palmitate, the end product of FASN, was able to reverse this growth inhibition [62, 140]. This indicates that end product starvation has deleterious effects on cancer cells. Inhibition by cerulenin reduced growth and induced apoptosis in melanoma cells [141], breast cancer cells [142], colon cancer cells [143] and prostate cancer cells [144]. Cerulenin treatment in a xenograft model of ovarian cancer led to regression of established tumors. Furthermore, cerulenin prevented liver metastasis in a murine model of colon cancer [143]. Unfortunately, the highly reactive

cysteine epoxide group prevents cerulenin from being clinically developed. Several analogs of cerulenin have been made, including C75, C93, C247, and, FAS31 to increase potency and limit adverse side effects [145]. C75 has been shown to interact with several different FASN domains, including KS, KR, ER, and TE. While this promiscuity does not make C75 good for clinical trials, it has shown to have antitumor activity in xenograft models of breast, prostate, ovarian and mesothelioma cancers [146].

Epigallocatechin-3-gallate (EGCG), a compound found in green tea, inhibits the KR domain of FASN [147]. EGCG not only inhibits FASN but has inhibitory effects on HIF-1-alpha and PI3K/Akt [148]. EGCG showed activity against prostate cancer cells [149]; however, a randomized phase II study of the protective effect of EGCG at 600 mg/day showed no significant difference of FASN or Ki-67 levels in prostate tissue [150]. GSK2194096 is another inhibitor of the KR domain [151] which was shown to have activity against non-small cell lung cancer [152]. Fasnall, a recently developed FASN inhibitor targets the co-factor binding site [153]. This inhibitor had anti-proliferative activity and induced apoptosis in breast cancer cells.

FDA-approved orlistat, a pancreatic lipase inhibitor, was discovered to also inhibit the TE domain of FASN [154]. Orlistat has been shown to inhibit proliferation and to induce apoptosis in prostate cancer and melanoma *in vitro* and *in vivo* [154, 155]. Orlistat also led to regression of tumors in gastric cancer xenograft model and extended survival times [156]. Due to poor bioavailability, low solubility, weight loss as a side effect, and low stability, orlistat cannot be used as a cancer treatment [157, 158]. Weight loss in these mice is a side effect due to lack of specificity of orlistat which can

inhibit the breakdown, and, therefore, the absorption of fats after eating [159]. Many analogs have been synthesized but to date none have been proven effective [160-163]. Other FASN inhibitors have been reported, including triclosan [164], which inhibits ER of FASN, and a variety of natural products [165-173]. Thus far, of these novel inhibitors, only TVB2640 has made it into clinical trials. Currently, TVB2640 is in a variety of phase I and phase II clinical trials for the treatment of many different cancers by itself and in combination with other agents [174-177].

Recently, our lab has taken an interest in identifying previously FDA-approved drugs that have inhibitory activity against FASN. Many drugs fail to make it into clinical trials due to poor pharmacokinetic properties. Using currently approved FDA drugs allows for the evaluation of compounds that have known favorable pharmacokinetic properties. *In-silico* screening was used to identify possible inhibitors of FASN and proton pump inhibitors (PPIs) were shown to have inhibitory effects on the TE domain of FASN [178]. PPIs are used as the standard of care for treating acid-related diseases like esophagitis, nonerosive reflux disease, and peptic ulcer disease; they are even used in combination with antibiotics in the treatment of *Helicobacter pylori* [179]. PPIs are prodrugs that are membrane permeable, and, once they are absorbed into gastric parietal cells, the PPI undergoes acid-base reactions, producing a sulfenic acid and/or sulfonamide. This compound can then bind irreversibly to the cysteine residues on the H⁺/K⁺ ATPase proton pumps [180]. This prevents the secretion of acid into the gastric lumen until new pumps can be made by cells [181]. The current FDA approved proton pump inhibitors include lansoprazole (Prevacid), omeprazole (Prilosec), pantoprazole

(Protonix), rabeprazole (Aciphex), esomeprazole (Nexium), and dexlansoprazole (Kapidex). Studies on the safety of long-term use of PPIs have shown that they are well tolerated and safe with very few adverse side effects [182].

While our lab was the first to identify PPIs as FASN inhibitors, there have been many observations on PPI's use in cancer treatment. Early studies of solid tumors in *in vivo* mouse models of melanoma, colon, breast, and ovarian cancer cells, showed that combining chemotherapy (cisplatin, 5-FU, and vinblastine) with pretreatment of omeprazole, esomeprazole or pantoprazole, increased sensitivity to treatment [183]. Treatment of osteosarcoma cells with lansoprazole decreased invasiveness and migration abilities of these cells [184]. While the mechanism of action for decreased invasion and migration is unknown this could be due to FASN inhibition. Lansoprazole treatment, in combination with reverse transcriptase inhibitor Efavirenz, decreased proliferation and increased cellular apoptosis in metastatic melanoma [185]. Additionally, treatment of melanoma with suboptimal doses of paclitaxel and lansoprazole induced sensitivity to treatment [186]. The use of omeprazole in human B-cell tumors led to a decrease in growth and a caspase independent apoptotic event [187]. This event was mediated by early reactive oxygen species (ROS), alkalization of lysosomal pH and increased cytosolic acidification, and membrane permeabilization of cellular organelles [187]. Esomeprazole inhibited proliferation of melanoma cells and increased survival of a xenograft melanoma mouse model [188]. Treatment of xenograft models of breast and prostate cancer with pantoprazole alone did not affect tumor growth rate but combined treatment with docetaxel caused growth delay more than

single agent docetaxel alone [189]. Furthermore, treatment of mouse mammary carcinoma cell line, EMT6, and human adenocarcinoma cell line, MCF7, with lansoprazole caused an increase in cellular penetrance of chemotherapeutic doxorubicin in multilayered cell culture and improved spatial distribution in *in vivo* models of tumor growth as indicated by biomarkers of drug toxicity in all areas of the tumor [190].

Some of these observed effects of PPIs on cancer cells may be attributed to FASN inhibition, which causes changes in membrane structure and DNA repair, while others may be due to alternate effects caused by PPIs. A common occurrence in solid tumors is the acidification of the extracellular space resulting from the change in metabolic activity of cancer cells [191]. This acidic environment can lead to drug resistance by drug inactivation through protonation of the chemotherapeutic drug [192, 193]. The cells selected to survive in this acidic environment have activation of pH-regulating systems to prevent intracellular decreases in pH. Vacuolar-type H⁺ ATPase (vATPase) is a pH-regulator that prevents acidification of the cytosol by pumping H⁺ out of the cell or into lysosomes within the cell [194]. Increased expression of vATPase has been shown to provide growth advantages and improve survival of cancer cells [195-197]. Inhibition of vATPase has become an attractive target, and PPIs not only inhibit H⁺/K⁺ ATPases, but also vATPase [198]. Inhibition of vATPase by PPI may lead to cancer cell acidification and cell death. Additionally, PPIs have been shown to be substrates of ABC efflux transporter P-glycoprotein and have the ability to inhibit its activity [199]. P-glycoprotein is known to efflux a variety of anticancer agents out of the cell, leading to multi-drug resistance [200]. Inhibition of P-glycoprotein by PPIs could be having an effect on cancer cells.

Based on all these observations clinical trials have been performed to evaluate the use of PPIs in cancer.

A clinical study in companion animals showed that PPI treatment reversed chemo-resistance in lymphoma and solid tumors [201, 202]. There is currently a phase II clinical trial ongoing to evaluate the use of pantoprazole with docetaxel in men with prostate cancer [203, 204]. A completed phase II trial concluded that intermittent high doses of esomeprazole enhanced the effects of docetaxel and cisplatin in metastatic breast cancer patients [205]. There is also a phase II trial ongoing in TNBC to assess the use of omeprazole as a neoadjuvant therapy [206].

Studies in our lab as well as others have shown that not all proton pumps are equal when it comes to the treatment of cancer. Lugini *et al.* found that lansoprazole showed the highest antitumor effect when compared to other PPIs [207]. Due to the short half-life of PPIs in the body we hypothesized that not only parent compound but also the metabolites of certain PPIs have activity against FASN increasing antitumor effect.

Section 1.E: CC-115 and NHEJ

The PI3K-related kinase family (PIKK) includes ataxia-telangiectasia mutated (ATM), ataxia-telangiectasia mutated related (ATR), hSMG1, DNA-dependent protein kinase (DNA-PK), and mammalian target of rapamycin (mTOR) [208]. This family of serine/threonine kinases regulates response to DNA damage and response to nutrients, regulating cell growth [208]. Specifically, as shown in Figure 4, DNA-PK plays an

important role in non-homologous end joining (NHEJ), a repair mechanism for DNA double strand breaks (DSBs) [209]. mTOR functions in the regulation of translation, cell proliferation, and cell survival (Figure 4) [210].

DNA-PK catalytic subunit (DNA-PKcs) is required for repairing lethal DNA DSBs caused by oxidative and replicative stress, irradiation, and those caused by chemotherapeutics [216]. Ultimately, DNA repair mechanisms are utilized to allow cancer cells to overcome DNA DSBs associated with stress brought on by rapid proliferation as well as allow these cells to repair damage created by anticancer treatments leading to survival and resistance [217]. Studies have shown that knock down and pharmacologic inhibition of DNA-PK enhances chemo- and radio-sensitivity [218-220]. For this reason, efforts are currently being made to produce a drug that targets DNA-PK for use in the clinic.

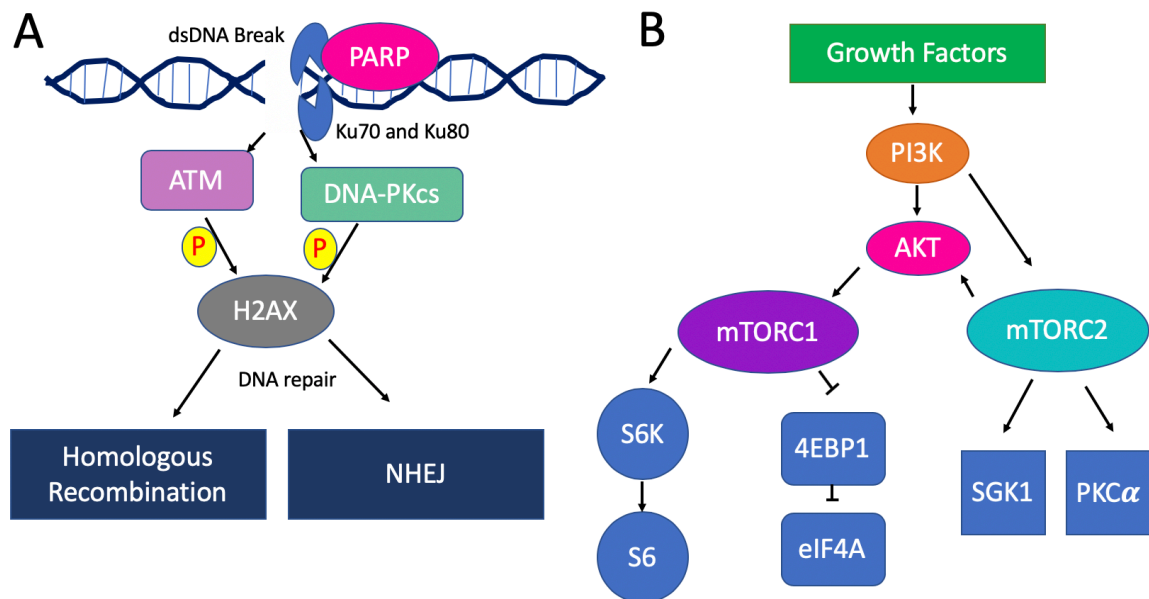


Figure 4: Schematic of the DNA-PK pathway (A) and mTOR pathway (B) A) After sensing DNA DSBs ATM and DNA-PKcs phosphorylate H2AX signaling to the cell to repair the damaged DNA. This can occur in two ways: homologous recombination or NHEJ [211-213]. DNA-PK is a trimeric protein made up of Ku70, Ku80, and catalytic subunit DNA-PKcs. B) mTORC1/2 are activated downstream of growth factor receptor signals. Upon activation mTORC1 phosphorylates S6K, leading to its activation, and 4EBP1, leading to its suppression. mTORC2 leads to the activation of AKT, SGK-1, and PKC α [214, 215].

mTOR is activated downstream of the PI3K/AKT pathway and is involved in the regulation of cell growth, proliferation, and survival [210]. mTOR is activated by signals from growth factor receptors, nutrients, and stress signals. Two functionally different complexes, mTORC1 and mTORC2, make up mTOR. mTORC1 made up of raptor, PRAS40, Deptor and LST8, regulates the level of mRNA translation by modulating the activity of several translational components including 4EPB1 and p70S6 Kinase [215]. mTORC2 consists of rictor, SIN1, Deptor, Protor and LST8. mTORC2 activates AKT, Paxillin, and PKC- α through phosphorylation and regulates the actin cytoskeleton

through small GTPase Rac and Rho, which enhances cell survival and migratory ability [215]. Dysfunction of multiple points in the mTOR pathway has been associated with many types of cancer. For example, PI3K amplification and mutations, PTEN loss of function, RTK amplifications, and AKT mutations have all been implicated in promoting tumorigenesis through upregulation of this pathway [221]. Notably, mTOR is downstream of PI3K/AKT and has also been implicated in cancer. Therefore, mTOR is a good target for the development of anticancer drugs. Currently, there are a few drugs, VX-984, CC-115, and nedisertib, that are in clinical trials for use as a single agent and in combination with other therapies.

Specifically, CC-115, which is a dual mTOR/DNA-PK inhibitor, is a triazole containing compound that was identified through structure-activity relationship studies [222]. Early studies showed that CC-115 binds to the ATP binding site with extensions into the catalytic pocket allowing for some specificity [222]. CC-115 is selective for mTOR and DNA-PK over closely related PIKK family members [223]. There are several ongoing clinical trials to test the efficacy of CC-115 in an array of different cancer types. Currently, there are phase I trials in squamous cell carcinoma of head and neck, Ewing's osteosarcoma, chronic lymphocytic leukemia (CLL), neoplasm metastasis, and prostate cancer [224]. There is also a phase II trial in glioblastoma. Early findings in clinical efficacy of CC-115 in CLL patients showed that 7 of 8 patients had a decrease in lymphadenopathy, with 1 partial response and 3 partial responses with lymphocytosis [225]. Lymphocytosis, or a prolonged state of increased lymphocyte count, is a common occurrence after treatment with BCR/ABL inhibitors [226-228]. Lymphocytosis after

treatment does not affect progression free survival. In fact, CML patients with lymphocytosis had an increase in overall survival [226].

While these early results in CLL show promise for further development of CC-115, there is an observed variability in sensitivity to drug. In this study, 1 of the 8 patients showed no decrease in lymphadenopathy and may be considered resistant to CC-115. Determining mechanisms of resistance to CC-115 will help to stratify patients into treatment groups for a more personalized approach to treating cancer and identifying new targets for cancer treatment.

Recently, it has also been shown that fatty acid synthase (FASN) contributes to drug resistance by increasing NHEJ repair of DNA damage via facilitating recruitment of Ku proteins and increasing DNA-PK activity [229]. Thus, it is possible that FASN may contribute to CC-115 resistance by increasing DNA-PK activity. In this study, we tested this hypothesis using breast cancer cell models. However, resistance to CC-115 was not mediated through FASN but through ABCG2. ABCG2 contributes to CC-115 resistance by reducing CC-115 accumulation. Inhibiting ABCG2 using small molecule inhibitors was able to reverse CC-115 resistance. These findings suggest that CC-115 is a substrate of ABCG2 and ABCG2 expression could play a role resistance to CC-115.

Section 1.F: ATP-binding cassette transporters and drug resistance

There are many known molecular mechanisms of drug resistance. In particular, ATP binding cassette (ABC) transporters such as ABCB1, ABCC1, and ABCG2 are well known transporters that contribute to multidrug resistance by actively transporting drug

substrates out of cells using ATP [230]. Transport across a membrane requires a membrane transport protein. While some molecules, such as water, can diffuse through the phospholipid bilayer, this process can be accelerated by using membrane proteins. There are four main types of membrane transport proteins: ion channels, aquaporins, transporters, and ATP powered pumps. Transporters can be either passive or active. Passive transports move a molecule down its concentration gradient, from high to low. Active transporters move a molecule against the concentration gradient by coupling this movement to the movement of a molecule down its gradient. Active transporters can move both molecules in the same direction, symporter, or in opposite directions, antiporter. Ion transporters help to maintain gradients across cell membranes that lead to voltage gradients. The regulation of these gradients is important for signaling and allowing for activation of membrane proteins [231]. Aquaporins are bidirectional channels that transport water across the membrane due to osmotic pressure [232]. Lastly, ATP powered pumps utilize the energy released by ATP hydrolysis to move substrates across cellular membranes. ATP powered pumps can move substrates into, influx, or out, efflux, of cell as well as transporting into vesicles.

ATP-binding cassette pumps (ABC) are a family of ATP powered pumps that are exclusively exporters in humans [233]. The ABC family is broken up into 7 subfamilies, A to G. This family transports a variety of substrates, including metal ions, peptides, amino acids, sugars, and large hydrophobic compounds [234]. In normal physiology the efflux of these and other endogenous and exogenous toxins acts to protect cells. ABC family members are expressed in many different tissues where they can influence elimination

of substrates and limit drug absorption [235]. This is useful in eliminating drugs and their metabolites from the body and preventing negative effects caused by these compounds. ABC family members are expressed at the BBB where they help minimize the neurotoxic effects of toxins and drugs on the brain [236]. Unfortunately, these compounds can also work against given drugs by preventing their absorption into target tissues, as in the case of treating different types of cancer with chemotherapeutics.

P-glycoprotein, or MDR1/ABCB1, was the first ABC transporter to be identified in multi-drug resistance in cancer [237]. Early studies indicated that P-glycoprotein reduced drug accumulation within cancer cells and led to their resistance to several types of drugs. After the identification of P-glycoprotein, other family members began to emerge. One of these family members is ABCG2. ABCG2, also known as BCRP, was discovered in drug resistant breast cancer cells. ABCG2 was responsible for resistance to doxorubicin, daunorubicin, and mitoxantrone by reducing cellular accumulation of these chemotherapeutics [238]. While ABCG2 was identified in breast cancer cells, it plays major roles throughout the body.

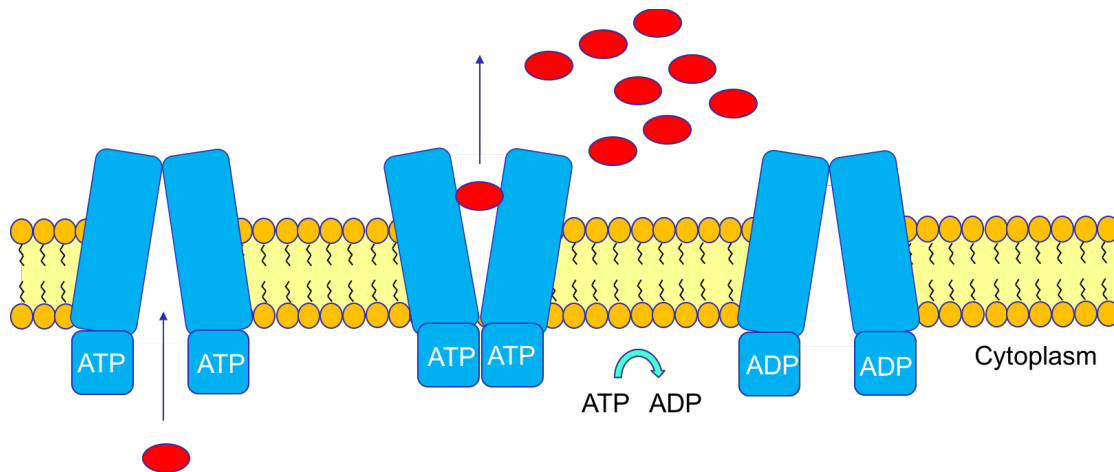


Figure 5: ABCG2 dimerization and oligomerization allows for active transport of substrates across the membrane - ABCG2 utilizes the energy from ATP hydrolysis to move substrates across the phospholipid bilayer.

ABCG2 is a “half-transporter” in that it contains only one transmembrane domain and one NBD. Therefore, ABCG2 requires dimerization or oligomerization to form a complete complex [239]. Once the functional transporter is formed, it will bind ATP at the NBD and use the energy from ATP hydrolysis to efflux its substrates as shown in Figure 5. The efflux of materials by ABCG2 happens in many different areas of the body. ABCG2 is expressed in the kidneys, intestines, placenta, BBB, and in stem cells. In the kidneys, ABCG2 mediates urate secretion, and 10% of gout cases can be attributed to a mutation in ABCG2 [240]. The intestine’s job is to absorb nutrients and water from what we eat and drink. ABCG2 expression in the intestines plays a role in xenobiotic detoxification [241]. ABCG2 is highly expressed in the placenta and is believed to protect the fetus from harmful agents [238]. Expression of ABCG2 on the luminal surface of the CNS vasculature allows the endothelial cells to limit the permeability of toxins and drugs to the brain [242, 243]. ABCG2 also plays a role in maintaining progenitor cells and is considered a marker for these cells [243]. Expression of ABCG2 in progenitor cells allows

them to survive in hypoxic conditions by reducing heme and porphyrin accumulation [244]. A change in expression of ABCG2 can have effects on the pharmacokinetics of substrate drugs. For instance, a decrease in ABCG2 expression, caused by a SNP, Q141K, carries an increased risk of adverse effects to a variety of drugs possibly due to an increase in absorption [245]. For this reason, expression of ABCG2, not only at a target tissue, but also in the intestines, endothelium, and BBB can affect the uptake of drug by tissues.

ABCG2 expression has been observed in many different types of cancer. ABCG2 has been extensively studied in acute myelogenous leukemia (AML). About 30% of all AML patients have high levels of ABCG2 [246]. Although several studies have looked at correlation between ABCG2 and clinical outcome, there have been conflicting reports. One study found no correlation between expression levels of ABCG2 and clinical outcome in 40 newly diagnosed patients [247]. However, Suvannasankha *et al.* demonstrated that ABCG2 mRNA expression correlated very poorly with ABCG2 protein expression [248]. In the above study on correlation, the researchers did note that only a small percentage of cells had a functional level of ABCG2. This may mean treatment selects for cells with high expression at the protein level. It was found in a paired study, taking AML cell samples pre-treatment and at the time of relapse, that ABCG2 was higher in relapsed samples [249]. Pretreatment mRNA levels of ABCG2 showed that fewer patients with high expression obtained complete remission compared to patients with low expression, and they also had lower disease-free survival times [250]. CML patients have also shown a population of premature CML expressing high levels of

ABCG2 [251]. Expression was detected in 25% of cells in 5 out of 7 patients [251]. While the importance of ABCG2 in clinical outcome is still to be determined, one recent study found that patients with high expression of ABCG2 had a decrease in overall treatment-free remission times after discontinuation of tyrosine kinase inhibitors [252].

Furthermore, ABCG2 has been observed in solid tumors. In a study of 150 untreated tumors comprising 21 different tumor types, immunohistochemical staining for ABCG2 frequently was positive [253]. This study revealed that ABCG2 expression was most frequently observed in adenocarcinomas of the digestive tract, endometrium, lung, and melanoma. Later studies have found that ABCG2 expression is a prognostic factor for both drug response and progression free survival in small-cell lung cancer [254]. It was also associated with shorter survival in patients with non-small-cell lung cancer [255]. Targeting ABCG2 has been considered in the treatment of cancers with overexpression of this protein. The first identified inhibitor of ABCG2 was fumitremorgin C (FTC). FTC was identified as a chemo-sensitizing agent to mitoxantrone before it was shown to specifically bind to ABCG2 [256, 257]. Unfortunately, FTC cannot be used in the clinic due to neurotoxicity. Many other inhibitors of ABCG2 have been discovered or developed since identification of FTC. Some of these include Ko143 [258], PZ-39 [259], and tryprostatin A [260]. While there have been numerous reports of ABCG2 inhibitors, few have made it into clinical trials and none have been approved for clinical use. Identifying substrates of ABCG2 will help to predict response to treatment with certain drugs and knowing ABCG2 status can help to inform on which treatment options will not be effective

CHAPTER 2: MATERIALS AND METHODS

Section 2.A: Reagents

Table 1: Buffers

Buffer	Formula
PBS	137 mM NaCl, 2.7 mM KCl, 10 mM Na ₂ HPO ₄ , 1.8 mM KH ₂ PO ₄
TBS	50 mM Tris, 150mM NaCl, pH 7.4
PBST	137 mM NaCl, 2.7 mM KCl, 10 mM Na ₂ HPO ₄ , 1.8 mM KH ₂ PO ₄ , 0.05% Tween
TBST	50 mM Tris, 150mM NaCl, pH 7.4, 0.05% Tween
TNN	50mM Tris-HCl (pH7.4), 150 mM NaCl, 20 mM EDTA (pH 8.0), 50 mM NaF, 0.5% NP-40, 1mM Na ₃ VO ₄ , before each use add 20 µl 10% SDS, 10 µl 0.2M PMSF, and 140 µl 1M DTT to every 2 ml buffer.
2X SDS loading	100 mM Tris-Cl, pH 6.8, 4% (w/v) SDS, 0.2% (w/v) bromophenol blue, 20% (v/v) glycerol, 200 mM β-mercaptoethanol

Table 2: Reagent list

Reagents	Company	Cat #
1-Kb Quick load ladder	New England Biolabs	N0552G
2-Mercaptoethanol	Sigma	M3148
5-Hydroxy Lansoprazole Potassium Salt	Toronto Research Chemicals	H943711
5-Hydroxy Lansoprazole Sulfide	Toronto Research Chemicals	131926-96-0
5-mL polystyrene round-bottom tube with cell-strainer Cap	Fisher	352235
Acetyl-CoA	Sigma	A2181
Acrylamide/bis- 37.5:1	RPI	7732-18-5
Adenine	Sigma	73-24-5
Ammonium Persulfate (APS)	Fisher	7727-54-0
Apoptosis Detection Kit	Calbiochem	PF032-1EA
Bovine Serum Albumin (BSA)	Fisher	BP1600-100
carboxy-H2DCFDA	Invitrogen	C400
CC-115	Selleckchem	S7891
CellRox Green	Fisher	C10444
Crystal Violet	Fisher	C581-25
DMEM	Fisher	10-013-CV
DMEM:F12 (1:1)	Fisher	11330-032

Donkey Serum	Sigma	D9663
Doxorubicin	Sigma	D1515
Dual-Luciferase Reporter Assay	Promega	E1960
ECL Western Blot detection reagent	GE Healthcare	RPN2106
EGF	Fisher	PHG0313
FBS	Fisher	A3160601
Free Fatty Acid Quantification Kit	Abcam	ab65341
FTC	Millipore	344847
G418	TEKnova	G5005
Gel Loading Dye (6X)	New England Biolabs	B7025S
High capacity cDNA	Fisher	4368814
Hoescht	Fisher	62249
Horse Serum	Fisher	26050088
Hydrocortisone	Sigma	50-23-7
Instant Milk	Walmart	
Insulin	Santa Cruz	sc-360248
Lansoprazole	Toronto Research Chemicals	L175000
Lansoprazole Sulfide	Toronto Research Chemicals	L175020
Lansoprazole Sulfone	Toronto Research Chemicals	L175026
Lipofectamine 3000	Invitrogen	L3000-015
Malonyl-CoA	Sigma	M4263
MEM	Fisher	10-010-CV
Menadione	Sigma	M5625
Methylene Blue Hydrate	Sigma	M4159
Mitoxantrone	Abcam	ab145668
MnTBAP	Fisher	55266-18-7
NAC	Sigma	A7250
NADPH	Roche	10107824001
Nu7441	Selleckchem	S2638
Paraformaldehyde	Fisher	4042
Pencillin/Streptomycin	Fisher	17-602E
Plasmid Prep	Invitrogen	K210014
Prestained Protein Ladder	Fisher	26616
Protein Assay Kit	Thermo Fisher	23200
PureLink mRNA extraction kit	Invitrogen	12183018A
Puromycin	Sigma	58-58-2

PVDF	Fisher	162-0184
Reporter Lysis 5X buffer	Promega	E397A
ROCK inhibitor	Chemdea	CD0141
TEMED	Fisher	110-18-9
Thiazolyl Blue Tetrazolium Bromide	Sigma	M5655
Toluene Mounting Media	Fisher	SP15-100
Triton X 100	Sigma	T8787
Trypsin	Fisher	17-161E
Tween20	Fisher	BP337

Section 2.B: Cell Culture

Cell lines were authenticated using short tandem repeat on August 3, 2016. All cells were maintained at 37°C with 5% CO₂. MCF7, M3K, MDA-MB-231, MDA-MB-468, HEK293, BC19, MCF7/Vec, MCF7/FASN, M3K/Scr, M3K/shFASN, HEK293/Vec, HEK293/ABCG2, MCF7/ABCG2, and HEK293/MRP1 cells were all grown in DMEM (Corning, Manassas, VA) media supplemented with 10% FBS (Life Technologies, Grand Island, NY). HCC1937 cells were cultured in RPMI (Corning, Manassas, VA) supplemented with 10% FBS. MDA-MB-436, MDA-MB-436/Vec and MDA-MB-436/FASN were cultured in MEM (Corning, Manassas, VA) supplemented with 10% FBS. KTB cells were cultured in a mix of 3:1 F12 (Gibco, Carlsbad, CA) and DMEM low glucose (Corning, Manassas, VA) with 5% FBS, 0.4 µl/ml hydrocortisone (Arcos, New Jersey), 1% penicilin/streptomycin (Lonza, Walkersville, MD), 5 µg/ml Insulin (Santa Cruz), 10 ng/ml EGF (Gibco, Carlsbad, CA), and at the time of culture add 2.4 µg/ml adenine (Sigma, Saint Louis, MO) and 5 µM ROCK inhibitor (Chemdea, Ridgewood, NJ). Additionally, M3K and BC19 cells were grown in 5 µM and 0.1 µM Doxorubicin (Sigma, Saint Louis, MO) respectively and MCF7/Vec, MCF7/FASN, M3K/Scr, MCF7/ABCG2, M3K/shFASN, HEK293/Vec, HEK294/ABCG2,

HEK293/MRP1, MDA-MB-436/Vec, MDA-MB-436/FASN, were all maintained in 600 µg/ml G418 (TEKnova, Hollister, CA).

M3K cells were a gift from Dr. Susan Bates, Bates also referred to as MCF7/AdrVp3000, and were made by incubating parental MCF7 cells in increasing concentrations of doxorubicin over an extended period, resulting in doxorubicin resistant cell line M3K [261]. BC19 cells were also a gift from Dr. Julie Horton and were created by transfection with pBCAdr as described previously [262]. Cell line culture information and catalog numbers are provided in Table 2 and 3. Cell line origins and plasmid information is provided in Tables 4 and 5.

Table 3: Cell lines and Media

Cell Line	Media	FBS/HS	Other
MCF7	DMEM	10% FBS	
M3K			5 µM Doxorubicin
MDA-MB-231			
MDA-MB-468			
HEK293			
BC19			0.1 µM Doxorubicin
MCF7/Vec			600 µg/ml G418
MCF7/FASN			
M3K/Scr			
M3K/shFASN			
HEK293/Vec (Venus)			
HEK293/ABCG2			
MCF7/ABCG2			
HEK293/Vec			
HEK293/MRP1			

HCC1937	RPMI	10% FBS	
MDA-MB-436	MEM	10% FBS	600 µg/ml G418
MDA-MB-436/Vec			
MDA-MB-436/FASN			
MCF10A	DMEM F12	5% HS	Insulin (10 µg/ml), EGF (20 ng/ml), Hydrocortisone (500 ng/ml), Cholera Toxin (100 ng/ml)
KTB22	F12 (Gibco 11765-054) - 375mL, DMEM (low glucose Gibco 12320-32) - 125ml,	5% FBS	Hydrocortisone (0.4 µl/ml), Penicilin/streptomycin (5 ml in 500 ml bottle), Insulin (5 µg/ml), EGF (10 ng/ml), add at time of culture; Adenine (2.4 µg/ml), ROCK inhibitor (5 µM)
KTB34			
KTB39			

Table 4: Breast Cancer subtype for each cell line and identification of plasmids used for stable transfection.

Cell Line	Origin
MCF7	Luminal A breast cancer
M3K	Derived from MCF7
HCC1937	TNBC
MDA-MB-231	TNBC
MDA-MB-468	TNBC
MDA-MB-436	TNBC
HEK293	Human embryonic kidney cells
BC19	MCF7 transfected with pBCAdr
MCF7/Vec	MCF7 transfected with pcDNA3.1 (+)
MCF7/FASN	MCF7 transfected with pcDNA3.1 (+) containing FASN
MDA-MB-436/Vec	MDA-MB-436 transfected with pcDNA3.1 (+)
MDA-MB-436/FASN	MDA-MB-436 transfected with pcDNA3.1 (+) containing FASN
M3K/Scr	M3K transfected with Scrambled control
M3K/shFASN	M3K transfected with shRNA targeting FASN
HEK293/Vec	HEK293 transfected with pcDNA3.1 (+)
HEK293/MRP1	HEK293 transfected with pcDNA3.1 (+) containing MRP1
HEK293/Vec (Venus)	HEK293 transfected with pCDH-Ne0-Venus/Dest
HEK293/ABCG2	HEK293 transfected with pCDH-Ne0-Venus/Dest containing ABCG2
MCF7/ABCG2	MCF7 transfected with pcDNA3.1 (+) containing ABCG2 MYC tagged

Table 5: Identification of Non-cancerous cell lines utilized and their origin. These cells were graciously given by Dr. Nakshatri and have just recently been characterized by his lab [263].

Cell Line	Origin
MCF10A	Non-cancerous Breast Cell line
KTb22	Non-cancerous Breast Cell line obtained from a Hispanic patient
KTb34	Non-cancerous Breast Cell line obtained from a Caucasian patient
KTb39	Non-cancerous Breast Cell line obtained from an African American patient

Section 2.C: Western Blot

Cells were treated with lansoprazole and its metabolites for the indicated time changing media and drug every 24 hours. At the given time points cell pellets were collected by centrifugation at 5,000 rpm for 5 min. Supernatant was aspirated and pellets were washed with PBS (refer to Table 1) 3 times followed by centrifugation at 5,000 rpm for 5 min and aspiration of supernatant each time. Cells were then resuspended in TNN buffer (refer to Table 1) and vortexed for 1 min every 10 mins for 30 min. The cell lysates were sonicated for 10 seconds at 40% 4 times with a 1 min rest on ice between sonication before centrifugation at 13,000 rpm for 20 min. Supernatants were transferred to a new microcentrifuge tube leaving behind cellular debris. Protein concentrations were then measured using the biorad protein assay dye (Pierce Biotechnology, Rockford, IL) to ensure equal loading. Samples are mixed with 2X SDS loading buffer (refer to Table 1) and boiled at 90°C for 5 min, before being separated by

8-15% SDS-PAGE gel, depending on the size of the protein, transferred overnight to a PVDF membrane (Biorad, Rockford, IL), and western blots were performed the following morning. Membranes were first blocked in 5% milk in TBST (refer to Table 1) buffer for 2 hours and then probed with the primary antibodies listed in Table 6 for 2 hours, or overnight for phosphorylated probes. Primary antibodies were diluted in 5% milk in TBST buffer and 5% BSA in TBST for phosphorylated proteins. Membranes were then washed 3 times for 15 min each time with TBST or PBST (refer to Table 1) and then placed in secondary, which was diluted in 5% milk in TBST. Membranes were washed 3 times for 15 min each time with TBST. Blots were visualized using ECL western blot detection reagent (Biorad, Chicago, IL). To test CC-115 inhibition of mTOR and its downstream targets, cells were treated for 2 hours with the indicated concentration of drug. After 2 hours cell pellets were collected, lysed, and protein concentrations were determined as described above. After visualization band density was measured by using imageJ software.

Table 6: Antibodies – list of Antibodies used in all studies with catalog number

Antibody	Company	Catalog #	Dilution
ABCG2	Millipore	MAB4146	1:1000
Actin	Sigma	JLA-20	1:2000
AKT	Cell Signaling	9272	1:1000
ALEXA FLUOR 647 Secondary	abcam	ab150107	1:200
Anti-Mouse Secondary	Sigma	A2554	1:3000
Anti-phospho-histone H2A.X	Millipore	05-636	1:1000
Anti-Rabbit Secondary	Sigma	A0545	1:3000
Anti-Rat Secondary	Sigma	A9037	1:2000
Caspase 3	Cell Signaling	9662	1:1000
Cleaved Caspase 3	Cell Signaling	9661	1:200
Cleaved PARP	Cell Signaling	9451	1:500
DNA-PKcs	Calbiochem	PC127	1:500
Fatty acid synthase	BD Transduction Laboratories	610963	1:1000
MRP1	abcam	ab3368	1:1000
mTOR	Cell Signaling	2983	1:500
P-Glycoprotein Antibody (C219)	Invitrogen	MA1-26528	1:200
PARP	Cell Signaling	9532	1:1000
Phospho-AKT (S473)	Cell Signaling	4051	1:500
Phospho-p70 S6 Kinase (Thr389)	Cell Signaling	9234	1:500
Phospho-S6	Cell Signaling	2215	1:1000
S6	Cell Signaling	2317	1:200
S6K	Cell Signaling	2708	1:1000

Section 2.D: RT-PCR

To set up for RT-PCR cells were plated in a 6 well dish at a concentration of MDA-MB-231 – 1×10^5 and MDA-MB-468 – 2.5×10^5 . Cells were treated every 12 hours for 72 hours with drug. After 72 hours, cells were collected and mRNA was extracted following the protocol outlined in the PureLink RNA Mini Kit (Invitrogen, Carlsbad, CA). Following mRNA extraction cDNA was produced using the high capacity cDNA kit (Applied

Biosystems, Waltham, MA). The thermocycler was set for, stage 1: 25°C – 10 min, stage 2: 37°C – 120 min, stage 3: 85°C – 5 min, stage 4: 4°C – hold. The cDNA was then used in the RTPCR with PARP and GAPDH primers. The primer sequence is listed in Table 7.

Table 7: RTPCR Primers

Primer	Orientation	Sequence
GAPDH	Forward	5'-TGCACCACCAACTGCTTAGC-3'
	Reverse	5'-GGCATGGACTGTGGTCATGAG-3'
PARP	Forward	5'-CCCAGGGTCTTCGGATAG-3'
	Reverse	5'-AGCGTGCTTCAGTTCATACA-3'

Section 2.E: Proliferation and Survival Assays

2.E.1 Methylene Blue

Methylene blue proliferation assay was derived from the protocol described by Oliver *et al.* [264]. Cell lines were plated in 96 well plate in 100 µl media at 500 cells/well to 4000 cells/well, depending on the cell line. After 24 hours, cells were treated with increasing concentration of drug using DMSO (0.5%) as the control treatment. Drug was added in 100 µl of media to each well. Cells were placed in 37°C incubator and allowed to grow for 72 hours in the presence of drug. At 72 hours, media was removed by aspiration and cells were fixed with 100 µl of methanol for 30 min. Cells were then stained with 1% (w/v) methylene blue in 10 mM borate buffer, pH 8.5, for 30 minutes. Excess dye was removed by aspiration and plates were then washed 3 times with ddH₂O. Dye was then released from cells by adding 100 µl of a 1:1 mixture of 100% ethanol and 0.1 M HCl. The plate can then be read in a 96 well plate reader at 650 nm. The OD correlates to the number of cells in each well. Methylene blue is a basic dye that

has a positive charge at pH 8.5. When cells are treated with methylene blue at pH 8.5 its binds to negatively charged moieties within the cells including proteins and DNA. After washing, the dye is released from cells by lowering the pH, causing protonation of acid groups and release of methylene blue into the solution, allowing for OD readings.

2.E.2 MTT

Cell lines were plated in 96 well plate in 100 μ l media at 500 cells/well to 4000 cells/well, depending on the cell. After 24 hours, cells are treated with increasing concentration of drug, using DMSO (0.5%) as the control treatment. Drug was added in 100 μ l of media to each well in triplicate. Cells were placed in 37°C incubator and allowed to grow for 72 hours in the presence of drug. At 72 hours, 20 μ l of MTT dye (5 mg/ml in PBS) was added to each well. Cells were incubated at 37°C for 4 hours. After incubations, plates were centrifuged at 2,000 rpm for 10 min, and the supernatant was carefully aspirated. Finally, 100 μ l of DMSO was added to each well to solubilize the dye, and absorbance was read at 570 nm, using 630 nm for background. MTT is a measure of cell viability by measuring the metabolic activity. When the MTT dye, 3-(4,5-dimethylthiazol-2-yl)-2,5-diphenyltetrazolium bromide, is taken up by metabolically active cells, it is converted to formazan, (E,Z)-5-(4,5-dimethylthiazol-2-yl)-1,3-diphenylformazan. MTT is yellow in color, and, after being reduced it becomes purple. The Absorbance at 570 nm is a reflection of the metabolically active cells.

2.E.4 Apoptosis Assay

Cells were plated in a 6-well dish at a concentration of: MDA-MB-231 – 1×10^5 and MDA-MB-468 – 2.5×10^5 . After plating cells were placed in the incubator overnight

at 37°C. Then cells were treated with the given concentration of drug every 24 hours for 72 hours in the case of MDA-MB-231 cells and every 12 hours for MDA-MB-468. In the presence of N-acetyl-L-cysteine (NAC) (Sigma, Saint Louis, MO) the media pH had to be corrected by adding NaOH. After 72 hour treatment cells were collected and stained for Annexin V-FITC and propidium iodide, following manufacturers protocol (Calbiochem, Temecula, CA), and then analyzed by FACs. After induction of apoptosis there is a rapid change in phospholipids causing the exposure of phosphatidylserine on the cell surface which will readily bind Annexin V-FITC. Propidium iodide stain can only enter cells when there is a disruption of cellular membranes which would indicate late apoptotic or necrotic cells. These dyes together were used to determine number of cells in apoptosis following treatment. Briefly, cells were collected and washed with PBS two times. Then 5×10^5 cells, in 500 μ l binding buffer (provided in the kit), were stained with Annexin V-FITC for 15 min at room temperature. Cells were centrifuged at 1000 X g for 5 min and the supernatant was removed. Cells were resuspended in 500 μ l binding buffer and propidium iodide. Samples were run through 5-mL polystyrene round-bottom tube with cell-strainer Cap and run on BD LSR II analyzer (excitation 488 nm FITC- emission 518nm and propidium iodide 620 nm). H_2O_2 was used at a concentration of 100 μ M for 30 min as a positive control for apoptosis.

2.E.5 Cell Cycle Analysis

Cells were plated in 10 cm dish at a concentration of 4×10^5 for MDA-MB-231 cells and 6×10^5 for MDA-MB-468 cells and incubated overnight at 37°C. Cells were then treated with the given concentration of drug for 72 hours. Cells were harvested with

trypsin and washed 3 times with PBS. 70% ice cold ethanol was used to fix cells for 30 min, making sure to separate cellular clumps. Cells were then washed 2 times with PBS and treated with 500 μ l of 20 μ g/ml RNase in PBS for 30 min at 37°C. Cells were pelleted and supernatant was aspirated. Pellets were resuspended in 500 μ l of 50 μ g/ml propidium iodide in PBS and incubated at room temperature for 30 min. Cells were filtered through 5 mL polystyrene round-bottom tube with cell-strainer cap for FACs analysis.

Section 2.F: Drug Accumulation Assay

Cells were trypsinized and pelleted by centrifugation. They were then washed twice with warm PBS. Cells were then resuspended in 1 ml of warm PBS. ABCG2 inhibitor was added at given concentrations and cells were incubated for 15 min at 37°C. Then, 10 mM CC-115 or DMSO control was added to the suspended cells, and cells were incubated at 37°C for 30 min, shaking every 10 min. After treatment cells were pelleted by centrifugation and washed with PBS 1 time. Cells were resuspended in 500 μ l PBS and filtered through 5 mL polystyrene round-bottom tube with cell-strainer cap. Accumulation was measured by FACs with an excitation at 405 nm and emission 421 nm.

Section 2.G: Confocal Microscopy

For confocal microscopy cells were grown on a sterilized coverslip to about 80% confluency. To do this first the cover slips were first autoclaved, and one coverslip was

placed in each well of a 6-well plate. Cells were plated at a concentration of 2×10^5 for MDA-MB-231 and 2.5×10^5 for MDA-MB-468. Cell concentrations will vary based on the growth rate of cells. After 24 hours, media was carefully aspirated and cells were treated with the appropriate amount of drug. Cells will be treated every 24 hours for 72 hours. At 72 hours media was aspirated and cover slips were washed with PBS twice for 5 min. Slides were fixed with 4% paraformaldehyde for 15 min at room temperature and washed 3 times with PBS for 5 min each time. Then slides were blocked and permeabilized in PBS with 5% normal donkey serum (Sigma, Saint Louis, MO), and 0.3% triton X 100 (Sigma, Saint Louis, MO) for 60 min. Permeabilization buffer was removed and slides were placed in primary antibody overnight at 4°C (PBS, 1% BSA, 0.3% Triton X 100). Slides were washed with PBS 3 times 5 min each time. Secondary antibody was diluted 1:200 in PBS, 1% BSA, and 0.3% Triton X 100 and slides incubated for 60 min at room temperature in the dark. (Negative controls should also be incubated in secondary antibody) Secondary antibody was removed and Hoescht (Pierce Biotechnology, Rockford, IL) was diluted in 25 µl in 250 ml PBST. 2 ml of diluted Hoescht was added to each well and allowed to sit in the dark for 10 min. Slides were then prepared with toluene mounting media (Fisher, Fair Lawn, NJ) and sealed using nail polish. Slides were imaged using the Olympus2 FV-1000 MPE inverted confocal imaging system and the 60X/1.2 W ∞ /0.13-0.21/FN26.5 lens.

2.G.1 Quantification of puncta staining

γH2AX puncta staining was quantified using the GDSC plugin in on Fiji imageJ software.

Section 2.H: NHEJ Activity Assay

To determine NHEJ activity a luciferase and renilla assay system was used as previously described [128]. Briefly, pGL3-luc plasmid was first cut by HINDIII, separating the promoter sequence from the luciferase gene, creating a linearized plasmid and purified using a gel extraction kit (Invitrogen, Carlsbad, CA). Linearization is verified by running a 0.8% agarose gel. Upon transfection, this linearized plasmid will be repaired to a circular plasmid that expresses luciferase, if NHEJ is active. If it is not active there will be no luciferase activity. pRL-TK, renilla plasmid is used as a transfection efficiency control and pGL3-Luc is used as 100% control. To test NHEJ after drug exposure cells were plated in 24-well plate (MDA-MB-231 – 1×10^4 MDA-MB-468 – 2×10^4). Cells were treated every 12 hours for 72 hours. After 72 hours cells were co-transfected (Lipofectamine 3000, Carlsbad, CA) with pRL-TK (400ng) and pGL3-Luc (400ng) or linearized pGL3-Luc (400ng). Cells are incubated at 37°C for 8 hours when they were collected for analysis. Briefly, media was aspirated from the 24-well plates and 100 μ l of 1X reporter lysis buffer was added to each well (Promega, Madison, WI). Plates were shaken for 10 min and then collected in microcentrifuge tubes. Tubes were then subjected to freeze thaw cycles to ensure cell lysis. This was accomplished by using dry ice/ethanol bath of 2 min and then 2 min in 37°C water bath. Lysates were centrifuged at 13,000 rpm for 2 min and supernatant was transferred to a new tube. Using first 20 μ l of firefly luciferase substrate (substrate E151A and buffer E195A, Promega, Madison, WI) and 5 μ l lysate, firefly luciferase was measured. Then 20 μ l of Stop & Glo substrate

(substrate E640A and buffer E641A, Promega, Madison WI) was added to measure Renilla. NHEJ was determined by the following formula.

$$(\text{Luciferase}/(\text{linearized})/\text{Renilla})_{(\text{treatment X})} \div (\text{Luciferase}/(\text{circularized})/\text{Renilla})_{(\text{treatment X})} = \% \text{ NHEJ}$$

2.H.1 Plasmid Prep

To obtain the plasmids for NHEJ DH5 ∞ cells were chemically transformed with pRL-TK and pGL3 plasmid. After growth a single colony was picked and placed in 500 ml LB media and allowed to grow overnight at 37°C with agitation. Cells were then collected by centrifugation at 4,000 g for 10 min and supernatant was removed. Following the PureLink HiPure Plasmid Filter DNA Purification Kit protocol (Invitrogen, Carlsbad, CA), plasmids were extracted from cell lysates.

Section 2.I: FASN Activity Assays

2.I.1 Free Fatty Acid Quantification Assay

Free fatty acids were quantified using the protocol provided by the Abcam free fatty acid quantification kit (Abcam, Cambridge, MA). Briefly, acyl CoA synthetase is used in acylation of coenzyme A. In this way free fatty acids are converted to CoA derivatives. Then the acyl-CoA is oxidized by an acyl CoA oxidase. Upon oxidation H₂O₂ is produced, which reacts with the colorimetric probe and can be easily quantified by microplate reader at $\lambda=570$ nm. To start this assay cells are plated in 150 mm dish, 2 dishes per condition, and treated every 24 hours with drug for 72 hours. At 72 hours cells are collected via trypsinization, counted, and washed with PBS. Cells are resuspended in 200 μ l chloroform/1% triton X-100 and homogenized using a micro-

homogenizer. Homogenate was placed on ice for 30 min and then centrifuged at 13,000 rpm for 10 min. The lower organic phase was collected into a new microcentrifuge tube and allowed to air dry in a chemical hood at 50°C to remove chloroform (about 1 hour). To ensure total removal of chloroform samples were vacuum dried for 30 min. Samples were then resuspended in fatty acid assay buffer (provided by the kit), heated at 85°C and vigorously vortexed for 5 min. Before use in the assay samples were quickly centrifuged at 7,000 rpm to remove any debris.

Section 2.J: Measurement of Reactive Oxygen Species

To measure reactive oxygen species cells were plated in a 96 well black plate with clear bottoms. MDA-MB-231 cells were plated at 20,000 cells per well and MDA-MB-468 cells were plated at 25,000 cells per well to obtain 90% confluence after incubation overnight at 37°C. Cells were then treated with indicated concentrations of drug for indicated time period in 100 µl Opti-MEM at 37°C. Menadione at a concentration of 100 µM was used as a positive control, treated for 2 hours. NAC and MnTBAP were used as reactive oxygen scavengers. After treatment 100 µl of CellROX green (Molecular Probes, Eugene, OR) is added for a final concentration of 5 µM, while being protected from light. The plate is then placed back in the incubator for 30 min at 37°C. Continue to protect the plate from light and after incubation 200 µl of 8% PFA is added to each well to fix cells for 15 mins. The plate is gently poured into a waste container tapped onto a stack of paper towel. Wells are carefully washed with 200 µl of PBS 3 times and each time the PBS is gently poured off and the plate is tapped on a

stack of paper towels. The wells are then filled with 100 μ l of PBS and are ready to be read in the microplate reader. CellROX green begins to brightly fluoresce when it becomes oxidized by reactive oxygen species and binds to DNA. Therefore, plates were read at excitation of 485 nm and emission 520 nm.

Section 2.K: Statistical Analysis

Statistical analysis for all experiments was run using Prism Graphpad. Results are presented as \pm SD unless otherwise indicated. All statistics were run on triplicate experiments unless otherwise indicated. Statistics are as follows $P < 0.05 = *$, $P < 0.01 = **$, and $P < 0.001 = ***$. Statistical tests used in this thesis were the two-tailed T-test comparing two means, ANOVA for comparing a group of mean values, and Two-Way ANOVA for comparing cell cycle analysis after treatment.

CHAPTER 3: RESULTS

Section 3.A: 5-Hydroxy Lansoprazole Sulfide

3.A.1 Lansoprazole and its metabolite 5-Hydroxy Lansoprazole Sulfide have cytotoxic effects in TNBC cell lines.

Proton pump inhibitors are FDA-approved drugs that have been on the market since 1989 [179]. They have been used in the successful treatment of many different non-cancerous acid related diseases. With the identification of PPIs as a FASN inhibitor [178] and the known role of FASN in cancer, our lab wanted to determine if inclusion of PPIs into breast cancer treatment could improve overall patient survival. To look at this possibility a retrospective study was performed on just over 6,700 patients diagnosed between January 1st, 1995 and February 27th, 2014. 840 of whom started taking a PPI during treatment. These studies to be published by other lab members, (manuscript in preparation) used log-ranked statistical analysis to show that breast cancer patients who were taking a PPI concurrently with treatment had a significant increase in overall survival. This retrospective study included patients with different treatment courses including hormone therapy, irradiation, DNA damaging chemotherapeutics, and cell cycle inhibitors. When the data was separated by the PPI utilized, it showed that lansoprazole, omeprazole, and pantoprazole, in combination with chemotherapy, had the highest overall survival. Furthermore, when the data was analyzed based on the subtype of breast cancer, TNBC patients that used a PPI during chemotherapy had a significant increase in survival over those that did not with a p-value of 0.015.

Using this information, the effect of PPI's on cells in a lab setting was analyzed. Data from our lab and others has shown that the different proton pumps have varying effects on cancer cells. Both our lab and others [207] have shown that the PPI lansoprazole has the greatest observed anti-tumor effects. PPI rabeprazole consistently was shown to have the least anti-cancer activity. Analyzing the metabolites of the four commonly used PPIs, omeprazole, lansoprazole, pantoprazole, and, rabeprazole, (Figure 6) it can be seen that omeprazole, lansoprazole, and pantoprazole are all degraded in a similar enzymatic fashion, by similar CYP450s, while rabeprazole is mostly degraded non-enzymatically. Omeprazole, Lansoprazole, and pantoprazole are degraded by CYP3A4 and CYP2C19. This led us to the hypothesis that a metabolite of these drugs may have antitumor activity. Based on our preliminary data that PPIs have inhibitory effects on FASN, we further hypothesized that a metabolite of lansoprazole also had inhibitory effects on FASN. In this thesis it is shown that inhibition of FASN by 5-hydroxy lansoprazole sulfide leads to a decrease in PARP and a decrease in the DNA repair pathway, NHEJ, causing accumulation of DNA damage and cellular apoptosis.

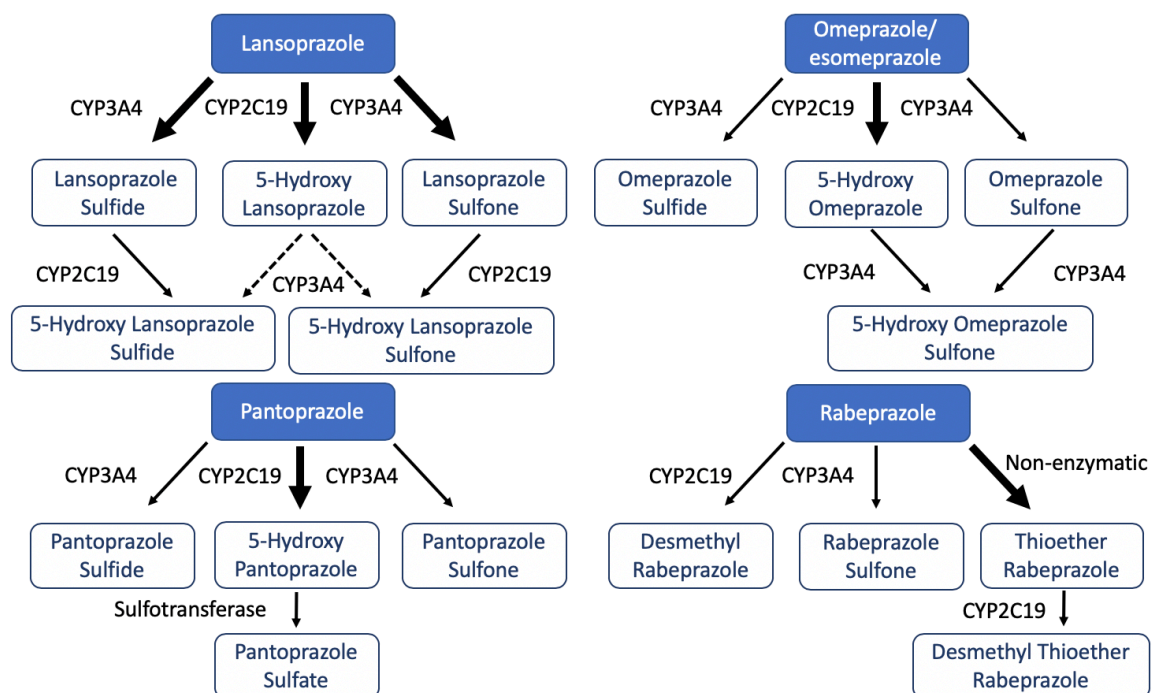


Figure 6: Metabolic Pathways for Proton Pump Inhibitors – The four commonly used proton pump inhibitors and how they are degraded in the body. Lansoprazole, omeprazole, and pantoprazole are all degraded mainly in an enzymatic fashion by CYP450s, while rabeprazole is mostly degraded non-enzymatically. Lansoprazole, omeprazole, and pantoprazole metabolism leads to formation of very similar metabolites including sulfones, 5-hydroxy, and sulfides. Thickness of the lines indicates the major and minor pathways of degradation.

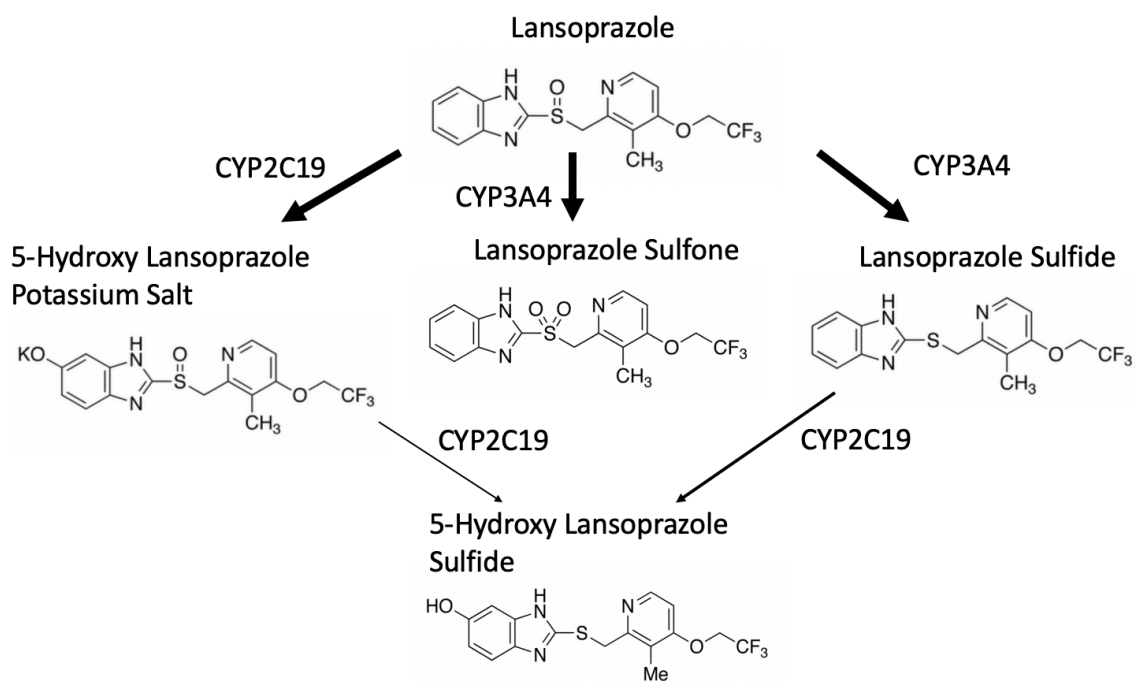


Figure 7: Lansoprazole's Metabolites – Lansoprazole and its metabolites chemical structures. Size of arrows indicates the major and minor routes of metabolism by CYP3A4 and CYP2C19.

Based on the retrospective study and cell based studies in our lab and others [207] indicating lansoprazole had the greatest anti-cancer effect, lansoprazole metabolites were used to test their effect on breast cancer cell lines. The parent compound and metabolites used in this study are shown in Figure 7. These compounds were first tested in MCF7, MDA-MB-231 and MDA-MB-468 cells. MCF7 cells are luminal A type breast cancer cells while MDA-MB-231 and MDA-MB-468 are TNBC cell lines. Using the methylene blue assay, the IC_{50} to the parent compound, lansoprazole, and each metabolite was determined. As shown in Figure 8A-C, there was a wide variety of response to different agents. All three cell lines tested had high IC_{50} values to the metabolite lansoprazole sulfone. This would indicate that this metabolite has very

minimal anti-cancer activity or it is also possible that this metabolite is not permeable to the cell membrane. Lansoprazole sulfide, while having lower IC_{50} than lansoprazole sulfone, still had an IC_{50} significantly higher than parent compound lansoprazole. 5-hydroxy lansoprazole potassium salt did not have a significantly different IC_{50} as compared to parent compound lansoprazole in both TNBC cell lines but was significantly higher in MCF7 cells. The last metabolite 5-hydroxy lansoprazole sulfide had no significant difference in IC_{50} value in MCF7 cells but IC_{50} values were significantly decreased in both MDA-MB-231 and MDA-MB-468 TNBC cells (Figure 8D-F) compared to parent compound lansoprazole. These observed differences in sensitivity in different cell lines could be attributed to differences between luminal A type cancers and TNBC or differences in expression levels of CYP enzymes in these particular cells (see discussion). The possibility that a metabolite of lansoprazole may be a more effective treatment in TNBC has been intriguing. For this reason, the IC_{50} values to lansoprazole and 5-hydroxy lansoprazole sulfide were tested in an additional two TNBC cell lines.

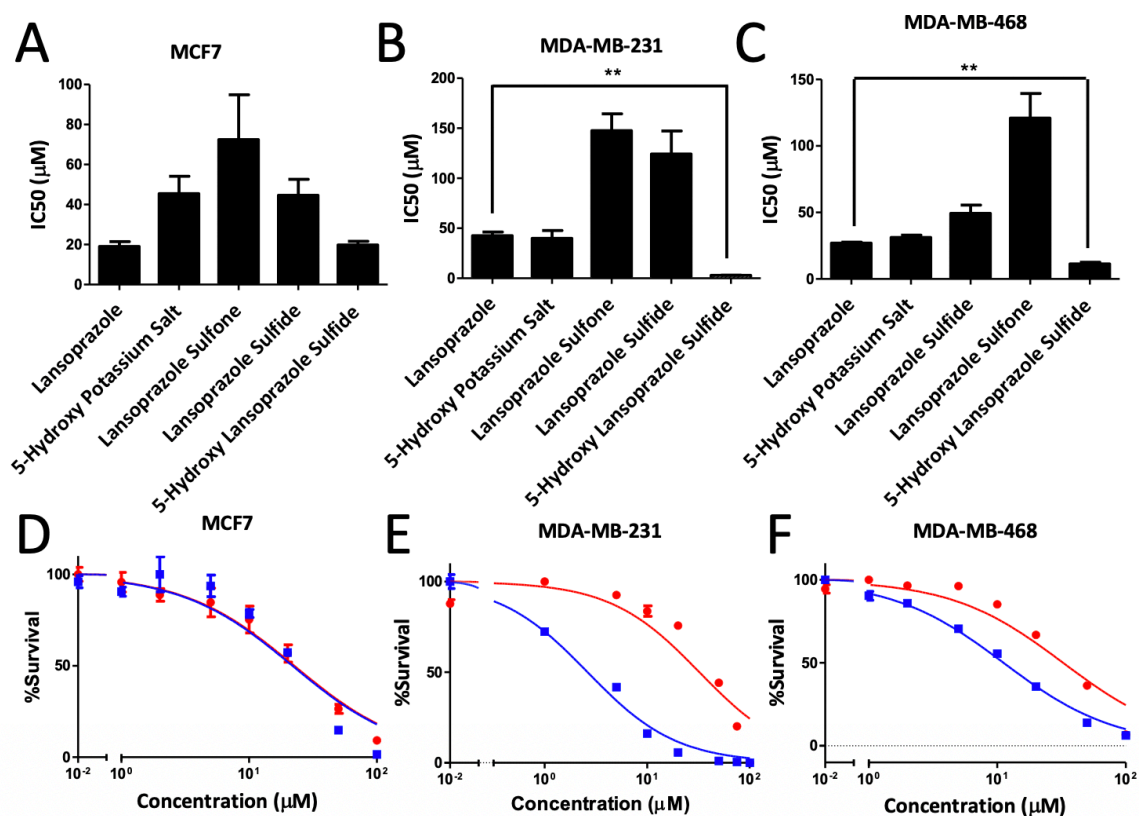


Figure 8: Effect of Lansoprazole and its Metabolites on Breast Cancer Cell lines – IC₅₀ values for lansoprazole and its metabolites in MCF7 (A), MDA-MB-231 (B), and MDA-MB-468 (C) cell lines. Survival curves for lansoprazole (red ●) and 5-hydroxy lansoprazole sulfide (Blue ■) in MCF7 (D), MDA-MB-231 (E), and MDA-MB-468 (F). (all n=3) Statistical analysis ANOVA P<0.05 = *, P<0.01 = **, and P<0.001 = ***

The additional breast cancer cell lines tested were MDA-MB-436 and HCC1937.

Figure 9A, D-E shows that all four TNBC cell lines are more sensitive to treatment with 5-hydroxy lansoprazole sulfide than parent compound lansoprazole. Interestingly, there was no significant difference in treatment with lansoprazole or 5-hydroxy lansoprazole sulfide in non-cancerous breast epithelial cell lines (Figure 9B, F-H). The non-cancerous cell lines KTB22, KTB34, and KTB39 were derived from Hispanic, Caucasian, and African American samples, respectively, and were a gift from Dr. Nakshatri [263]. They were immortalized by transfection with hTERT. Figure 9C shows the average IC₅₀ values for all

TNBC and non-cancerous cell lines tested. The IC_{50} values for TNBC cell lines treated with 5-hydroxy lansoprazole sulfide is significantly lower than all other treatment groups. This indicates an *in vitro* therapeutic window.

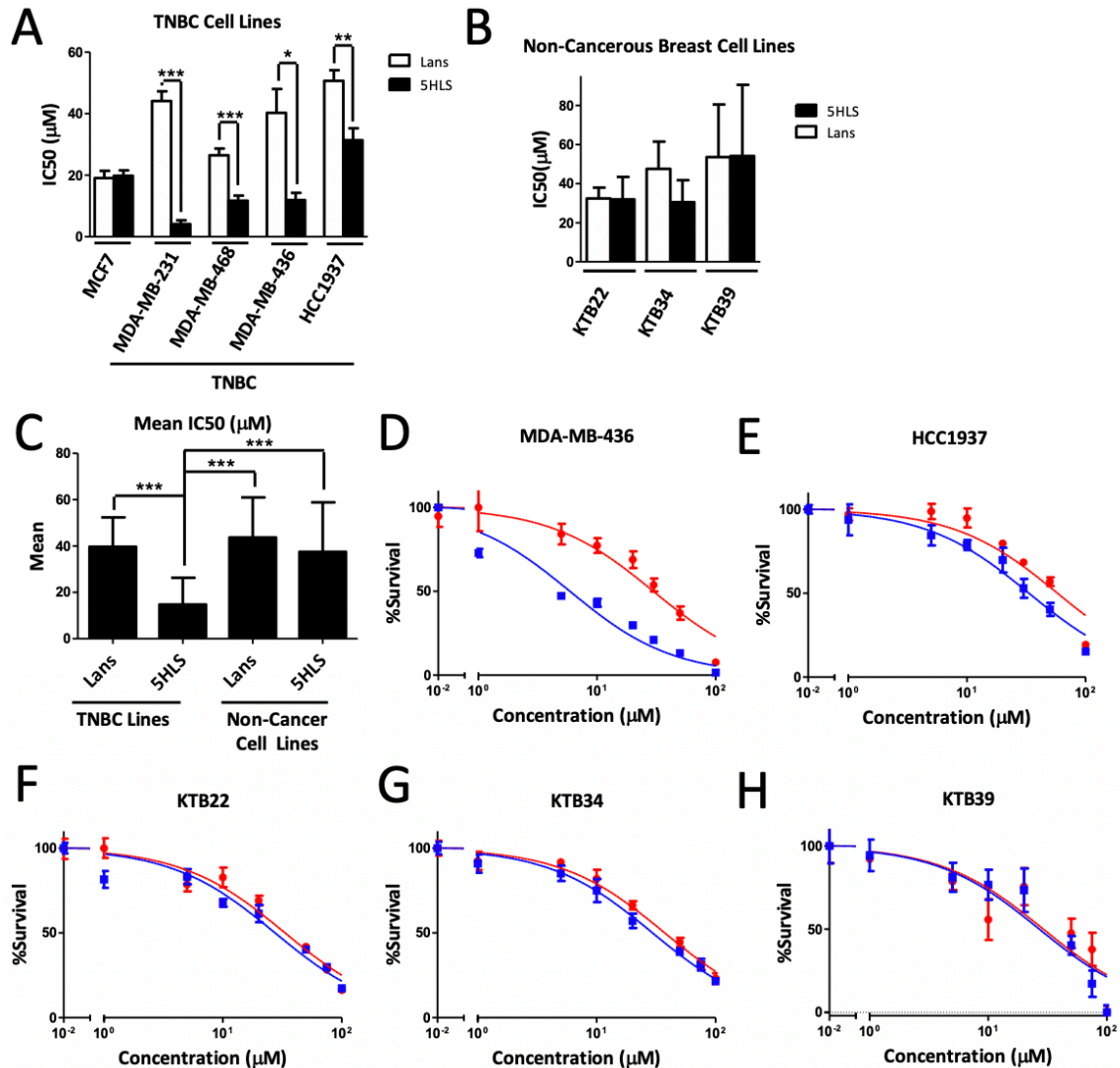


Figure 9: Lansoprazole and 5-Hydroxy Lansoprazole Sulfides effect on TNBC cell and non-cancerous breast cell lines - A) IC₅₀ values to lansoprazole and 5-hydroxy lansoprazole sulfide (5HLS) in luminal A breast cancer cell line MCF7 and TNBC cell lines MDA-MB-231, MDA-MB-468, MDA-MB-436, and HCC1937. B) Response to lansoprazole and 5-Hydroxy lansoprazole sulfide in non-cancerous breast cell lines KTB22, KTB34, and KTB39. C) Average IC₅₀ values for TNBC cell lines tested as well as non-cancerous cell lines. Survival curves for lansoprazole (red ●) and 5-hydroxy lansoprazole sulfide (Blue ■) in MDA-MB-436 (D), HCC1937 (E), and the KTB22 (F), KTB34 (G), and KTB39 (H) cell lines. (all n=3) Statistical analysis using a T-test comparing IC₅₀ of lansoprazole and 5HLS in each cell line (A) and ANOVA comparing all groups (C) was used. P<0.05 = *, P<0.01 = **, and P<0.001 = ***

3.A.2 5-Hydroxy Lansoprazole Sulfide causes apoptosis

To determine the effect 5-hydroxy lansoprazole sulfide has on TNBC cells, cell cycle analysis and apoptosis assays were performed. As shown in Figure 10A-D, while there are apoptotic/necrotic cells after treatment with 5-hydroxy lansoprazole sulfide, the distribution between phases of the cell cycle was not affected as indicated by a two-way ANOVA.

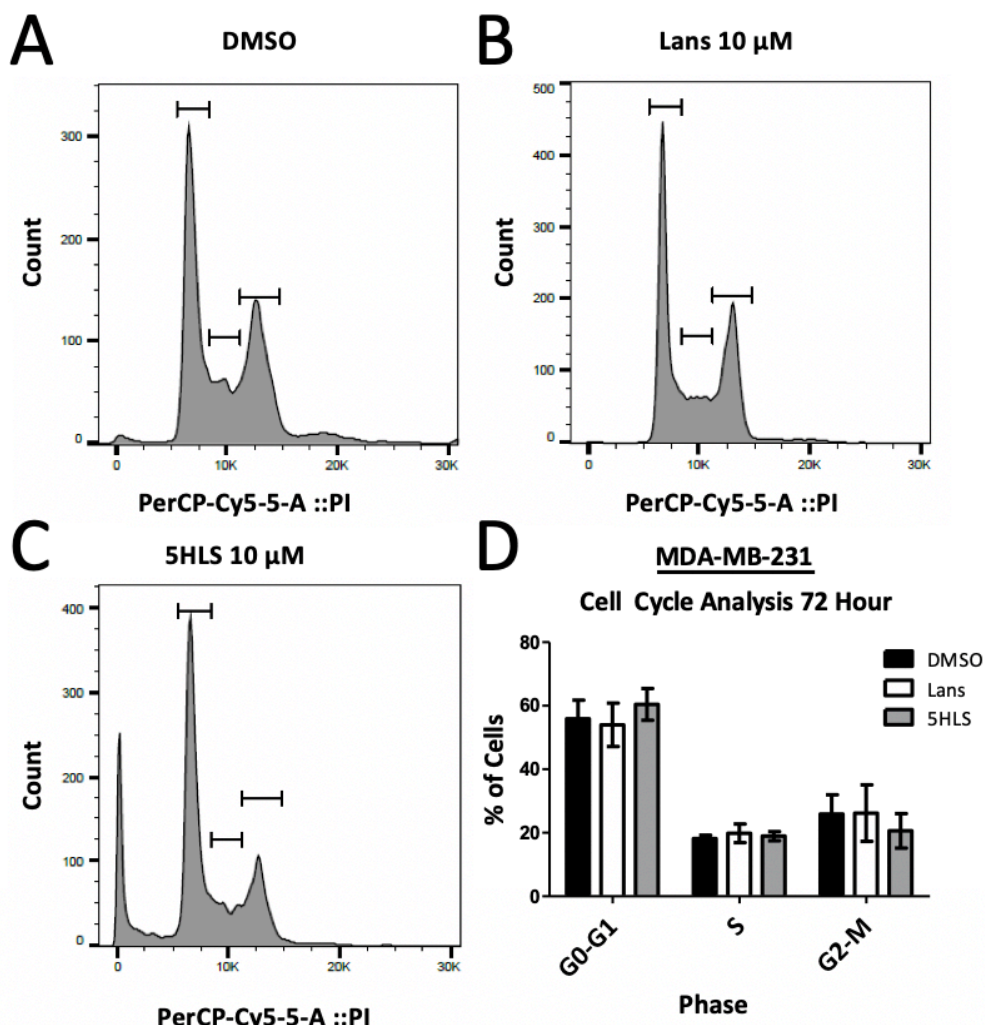


Figure 10: Treatment of TNBC cell line MDA-MB-231 with lansoprazole of 5-hydroxy lansoprazole sulfide does not affect cell cycle – MDA-MB-231 cells were treated with 10 μ M drug for 72 hours and cell cycle analysis was performed using flow cytometry. (n=3)

Due to the lack of cell cycle arrest in MDA-MB-231 cells, the amount of apoptosis was measured using annexin and propidium iodide staining. Using the kit provided by calbiochem (#PF032-1EA), apoptosis was checked at 48 and 72 hours. Figure 11 shows the scatterplots obtained using this kit and detecting PI and annexin staining. While treating the MDA-MB-231 cells with 10 μ M concentration of drug for 48 hours did not induce apoptosis (Figure 11A-C), treatment with 10 μ M concentration for 72 hours induced apoptosis in 5-hydroxy lansoprazole sulfide treated cells (Figure 11 D-F). Quantification of apoptosis in MDA-MB-231 cells after 72 hours treatment is shown in Figure 11G. MDA-MB-468 cells also showed apoptosis at 72 hours when treated with a 20 μ M concentration (Figure 12A-D). Additionally, due to the high staining of PI, which could indicate necrotic cells rather than apoptotic, and the long treatment, apoptosis was confirmed in MDA-MB-231 cells by using cleaved PARP and cleaved caspase 3 antibodies to show that apoptotic pathways are active in these cells. Figure 13A-E shows that with an increase in concentration of 5-hydroxy lansoprazole sulfide there is an increase in both cleaved PARP and cleaved caspase 3. Cleaved PARP molecular weight is 89 kDa and cleaved caspase 3 has two cleavage products one at 17 kDa and one at 19 kDa. MDA-MB-468 cells also had an increase in cleaved PARP and cleaved caspase 3 as shown in Figure 14. However, in MDA-MB-468 cells higher concentrations of drug were needed to see cleaved PARP and cleaved caspase 3. Additionally, there does not seem to be a significant difference in caspase 3 cleavage or PARP cleavage between lansoprazole and 5-hydroxy lansoprazole sulfide treated MDA-MB-468 cells. The fact that caspase cleavage in 5-hydroxy lansoprazole treated cells is not greater than

lansoprazole treated, and that 5-hydroxy lansoprazole sulfide leads to a greater increase in apoptotic/necrotic cells using annexin and propidium iodide staining, this could indicate that cells are potentially dying through another mechanism such as necroptosis which could explain why caspase 3 cleavage is not as pronounced (See Discussion). Further repeats should be performed to confirm these western blots and perform quantification.

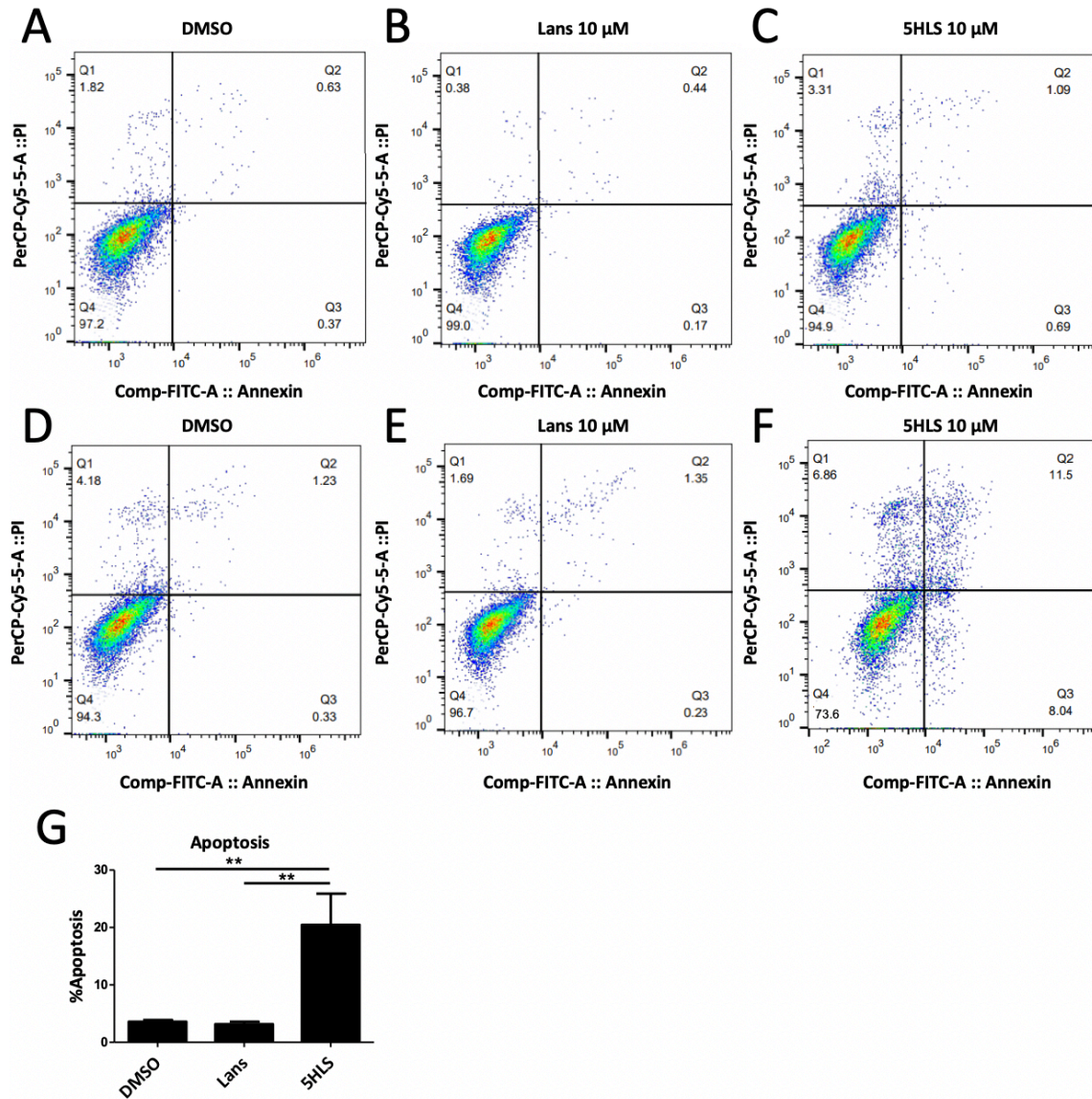


Figure 11: Treatment with 5-hydroxy lansoprazole sulfide induces apoptosis in MDA-MB-231 cells - MDA-MB-231 cells were treated for 48 hours with DMSO (A), 10 μ M lansoprazole (B), and 10 μ M 5-hydroxy lansoprazole sulfide (C). MDA-MB-231 cells were treated 72 hours with DMSO (D), 10 μ M lansoprazole (E), and 10 μ M 5-hydroxy lansoprazole sulfide (F). Quantification of apoptotic cells is given in G at 72 hour treatment and an ANOVA comparing all three groups was used for statistical analysis. $P < 0.05 = *$, $P < 0.01 = **$, and $P < 0.001 = ***$. (n=3)

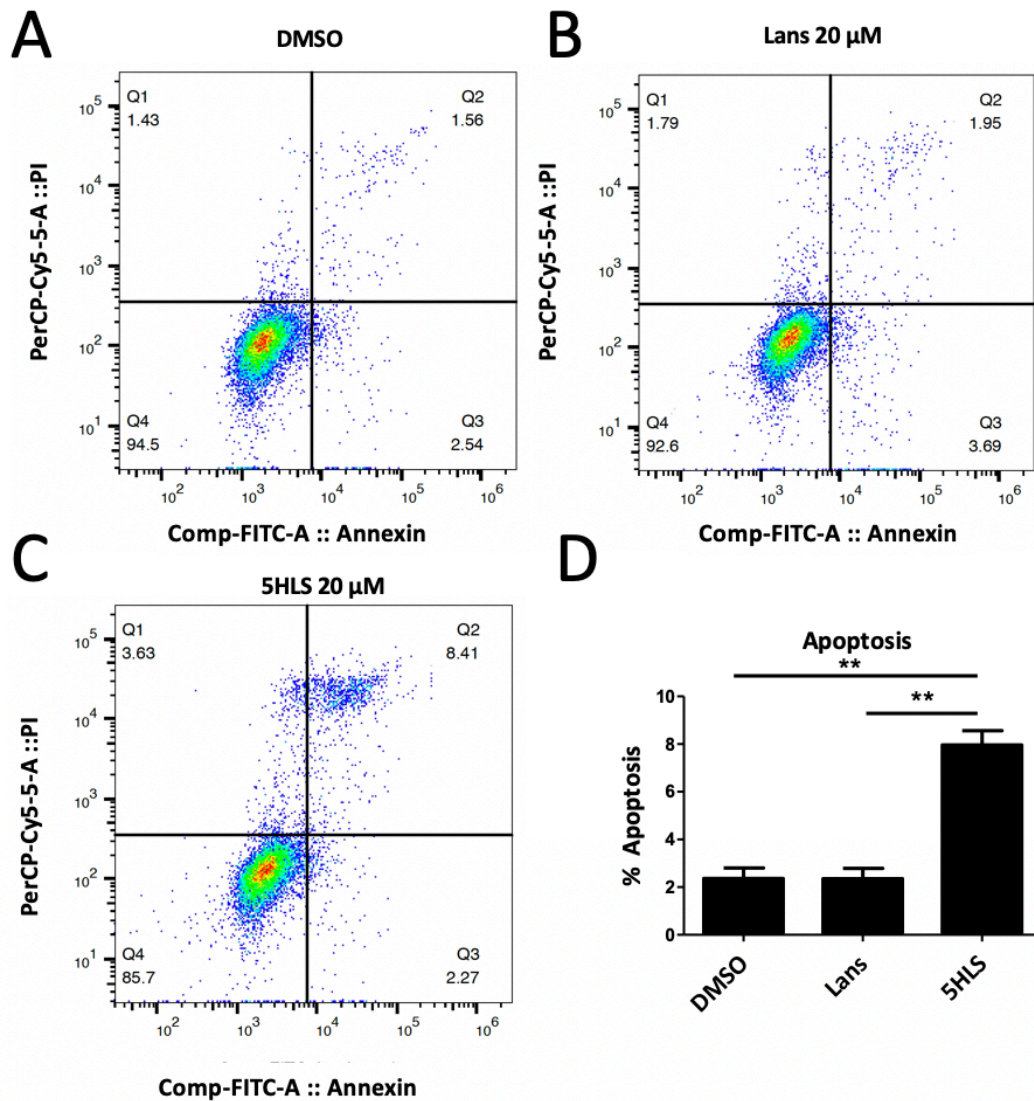


Figure 12: Treatment with 5-hydroxy lansoprazole sulfide induces apoptosis in MDA-MB-468 - MDA-MB-468 cells were treated for 72 hours with DMSO (A), 20 μ M lansoprazole (B), and 20 μ M 5-hydroxy lansoprazole sulfide (C). Quantification of apoptotic cells is given in D and an ANOVA comparing all three groups was used for statistical analysis. $P < 0.05 = *$, $P < 0.01 = **$, and $P < 0.001 = ***$. (n=3)

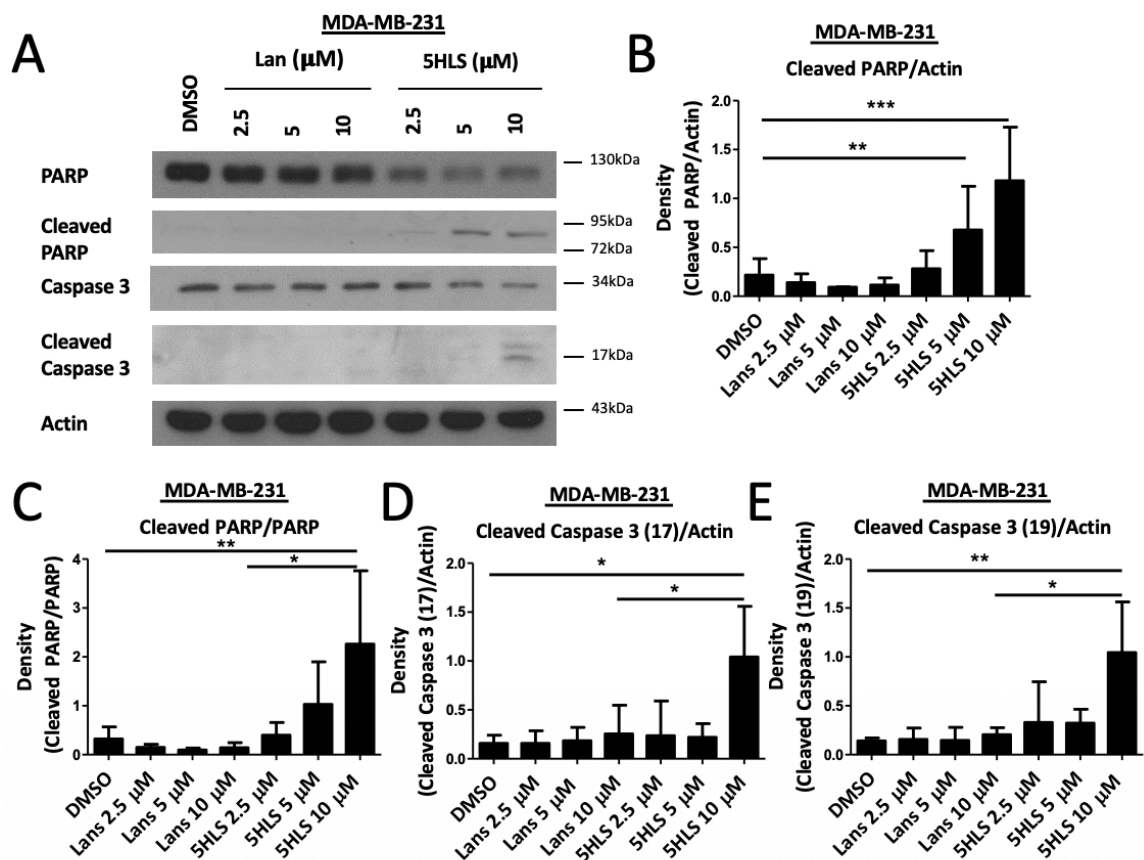


Figure 13: Treatment with MDA-MB-231 induces cleavage of PARP and caspase 3 - MDA-MB-231 cells treated with increasing concentrations of lansoprazole and 5-hydroxy lansoprazole sulfide were analyzed to determine the amount of cleaved PARP and cleaved caspase 3 (A). Quantification of cleaved PARP/Actin (B), cleaved PARP/PARP (C), and the two cleavage products of caspase 3: 17 kDa (D) and 19 kDa (E). (n=3) ANOVA comparing all groups was used for statistical analysis. $P < 0.05 = *$, $P < 0.01 = **$, and $P < 0.001 = ***$

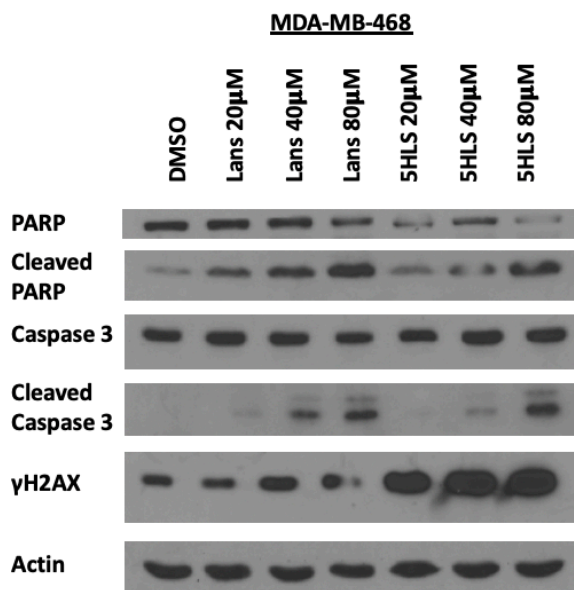


Figure 14: Treatment of MDA-MB-468 with lansoprazole and 5-hydroxy lansoprazole sulfide induces cleaved PARP and cleaved caspase 3 – Cleaved PARP and Cleaved Caspase 3 in MDA-MB-468 cells. (n=2)

3.A.3 Treatment with 5-Hydroxy Lansoprazole Sulfide increases DNA double strand breaks

FASN expression has been shown to be associated with resistance to DNA damaging agents [128] by increasing DNA repair pathway NHEJ. When FASN was overexpressed or knocked down, NHEJ repair increased and decreased, respectively, affecting resistance to DNA damaging agents. To test the possibility that 5-hydroxy lansoprazole sulfide is inhibiting FASN which would thereby increase DNA damage, the amount of γH2AX was determined by western blot analysis and puncta staining using confocal imaging. γH2AX can be used as an indicator of DNA DSBs [265, 266]. H2AX is a histone that becomes phosphorylated by ATM or DNA-PKcs in response to DNA DSBs [267]. Phosphorylation of H2AX leads to the recruitment of repair proteins and will

persist until the damage is repaired at which point the phosphate is removed by a three-protein complex known as HTP-C [268]. Treatment with lansoprazole and 5-hydroxy lansoprazole sulfide increases γ H2AX staining with increasing concentrations in both MDA-MB-231 (Figure 15A and C) and MDA-MB-468 (Figure 15D and F) cells. At the same concentration of drug, 5-hydroxy lansoprazole sulfide produces significantly more DNA DSBs than lansoprazole. We also observed a significant decrease in PARP expression in both MDA-MB-231 (Figure 15B) and MDA-MB-468 (Figure 15E) cells which will be discussed later. To confirm γ H2AX puncta staining is within the nucleus, confocal imaging was used. As shown in Figure 16A-C, 5-hydroxy lansoprazole sulfide significantly increased γ H2AX in treated cells as compared to lansoprazole. Quantification of the number of γ H2AX foci in the nucleus (Figure 16C) shows that at the same concentration 5-hydroxy lansoprazole sulfide creates significantly more foci/nucleus than parent compound lansoprazole. Interestingly, when treating the non-cancerous cell lines KTB22, KTB34, and KTB39 neither lansoprazole nor 5-hydroxy lansoprazole sulfide produced γ H2AX staining at IC_{50} values (Figure 17). While it is not clear why non-cancerous cells are not affected in the same way this could be due to differences in cellular metabolism, differences in cellular growth rate, or potentially that FASN/PARP/NHEJ axis may only apply to cancer cells as FASN is not required for benign cell survival. Further study is required to determine the differences.

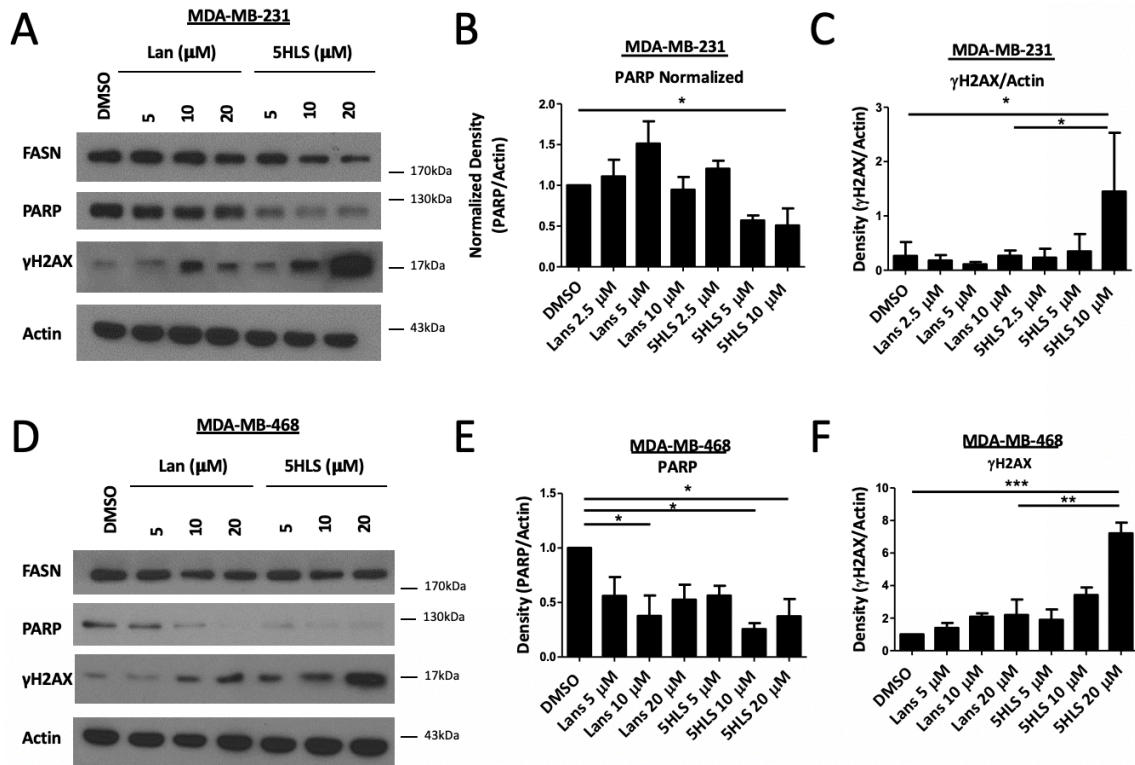


Figure 15: 5-hydroxy lansoprazole sulfide reduces PARP expression and increases γH2AX - A) MDA-MB-231 cells treated with increasing concentrations of parent compound, lansoprazole, and metabolite 5-hydroxy lansoprazole sulfide with quantification for PARP expression (B) and γH2AX (C). D) MDA-MB-468 cells treated with increasing concentrations of lansoprazole and 5-hydroxy lansoprazole sulfide with quantification for PARP expression (E) and γH2AX (F). (n=3) ANOVA comparing all groups was used for statistical analysis. $P < 0.05 = *$, $P < 0.01 = **$, and $P < 0.001 = ***$ FASN was also quantified but showed no significant difference in any treatment group.

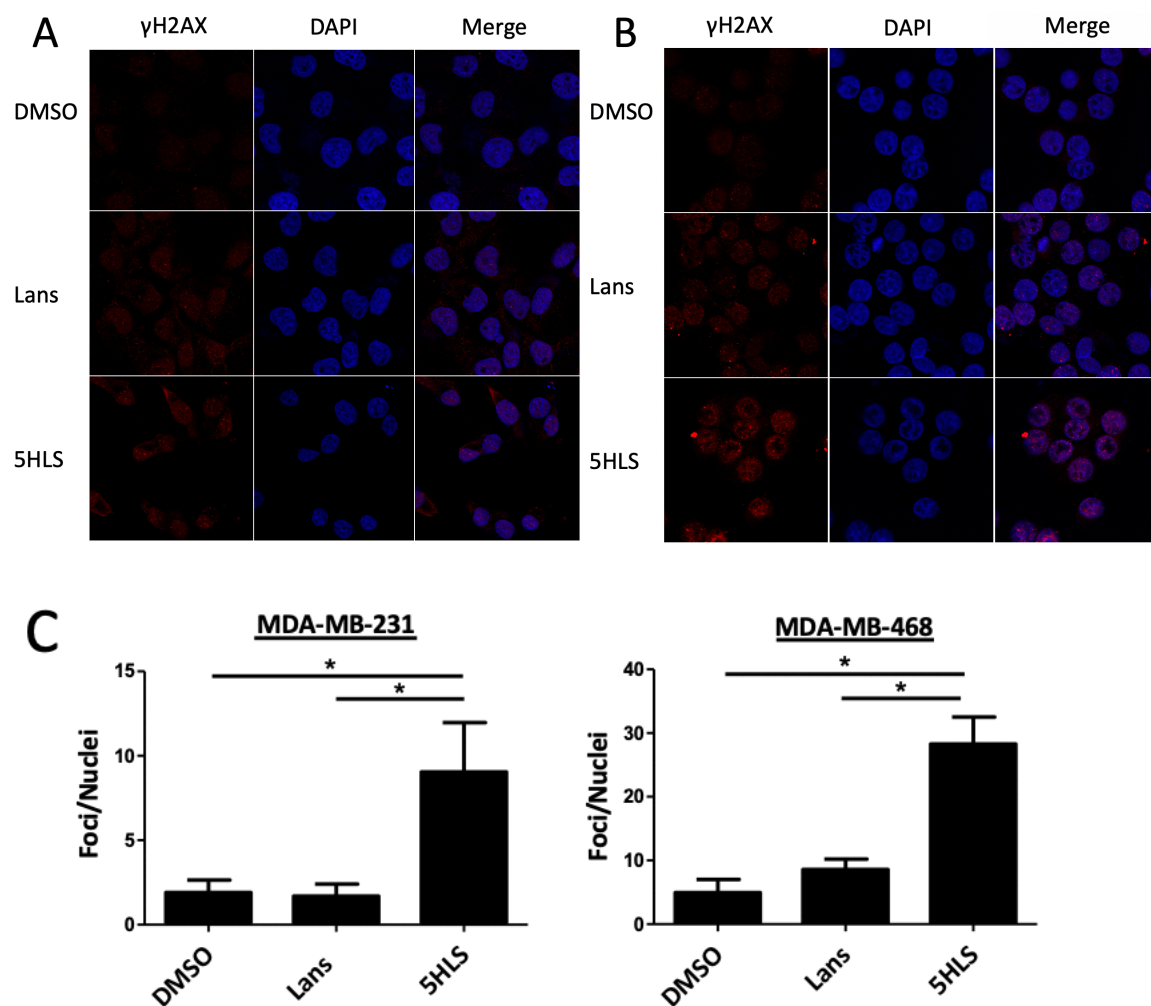


Figure 16: 5-hydroxy lansoprazole sulfide treatments leads to DNA double strand breaks as indicated by γ H2AX puncta staining - MDA-MB-231 cells treated with 10 μ M lansoprazole and 5-hydroxy lansoprazole sulfide (A) and (B) MDA-MB-468 cells treated with 20 μ M lansoprazole and 5-hydroxy lansoprazole sulfide. C) Quantification of number of γ H2AX foci within the nucleus compared using an ANOVA for statistical analysis. (n=3) $P < 0.05 = *$, $P < 0.01 = **$, and $P < 0.001 = ***$

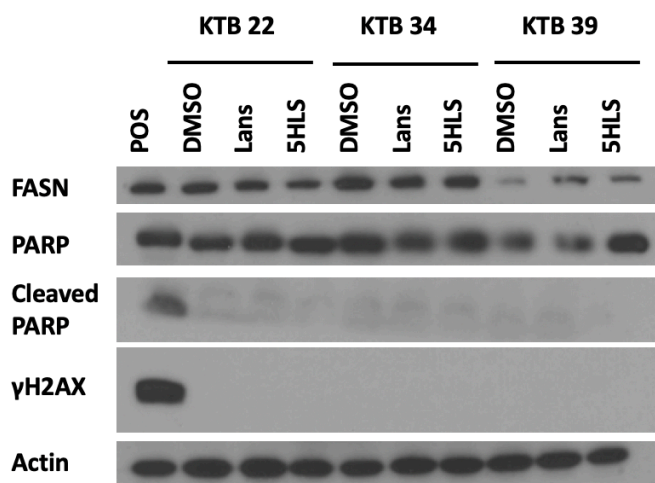


Figure 17: Lansoprazole and 5-hydroxy lansoprazole sulfide does not create DNA double strand breaks, as indicated by γH2AX, or induce cleavage of PARP in non-cancerous breast epithelial cells lines – 5-hydroxy lansoprazole sulfide nor parent compound lansoprazole causes DNA damage in non-cancerous breast epithelial cells at IC₅₀ concentrations. (n=2)

3.A.4 Reactive oxygen species scavenger NAC reverses DNA damage and apoptosis

One way in which cells acquire DNA damage is through exposure to reactive oxygen species. While ROS typically cause DNA base damage leading to single strand DNA breaks, if these breaks are not repaired before replication, they will be converted to DNA DSBs [269]. ROS can occur in cells due to normal metabolic activities. Thiols, hydroquinones, and flavins can all contribute to ROS due to their ability to undergo redox reactions. The mitochondria is another source of ROS production within cells as it performs oxidative phosphorylation [270]. Additionally, exposure to environmental factors such as chemotherapeutics and radiation can also create ROS. We tested if reactive oxygen scavenger NAC could prevent apoptosis. When MDA-MB-231 cells were treated with 5 mM NAC, in addition to 5-hydroxy lansoprazole sulfide, there was a reduction in the overall amount of apoptosis. This was tested using annexin and

propidium iodide staining (Figure 18 A-D) as well as by cleaved PARP and cleaved caspase 3 (Figure 19A, C-E). Additionally, 5 mM NAC reduced the amount of γ H2AX indicating it has a protective effect against DNA DSBs (Figure 19B). Possibly, 5-hydroxy lansoprazole sulfide is producing reactive oxygen species causing DNA DSBs.

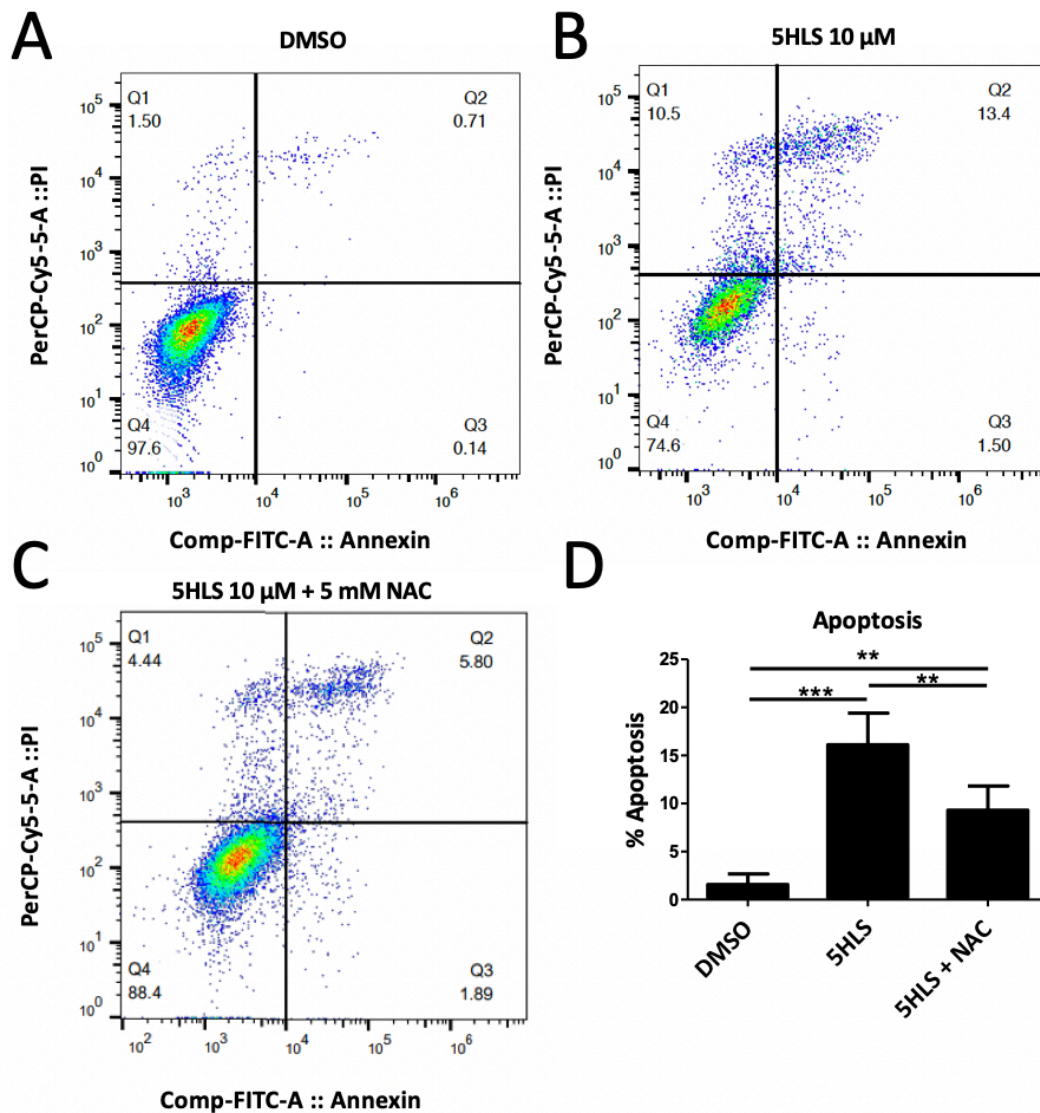


Figure 18: ROS scavenger NAC abrogates apoptosis in MDA-MB-231 cells treated with 5-hydroxy lansoprazole sulfide - MDA-MB-231 cells were treated for 72 hours with DMSO (A), 10 μ M 5-hydroxy lansoprazole sulfide alone (B), and 10 μ M 5-hydroxy lansoprazole sulfide plus 5 mM NAC (C). Quantification of apoptotic cells is given in D using an ANOVA for statistical analysis. (n=3) P<0.05 = *, P<0.01 = **, and P<0.001 = ***

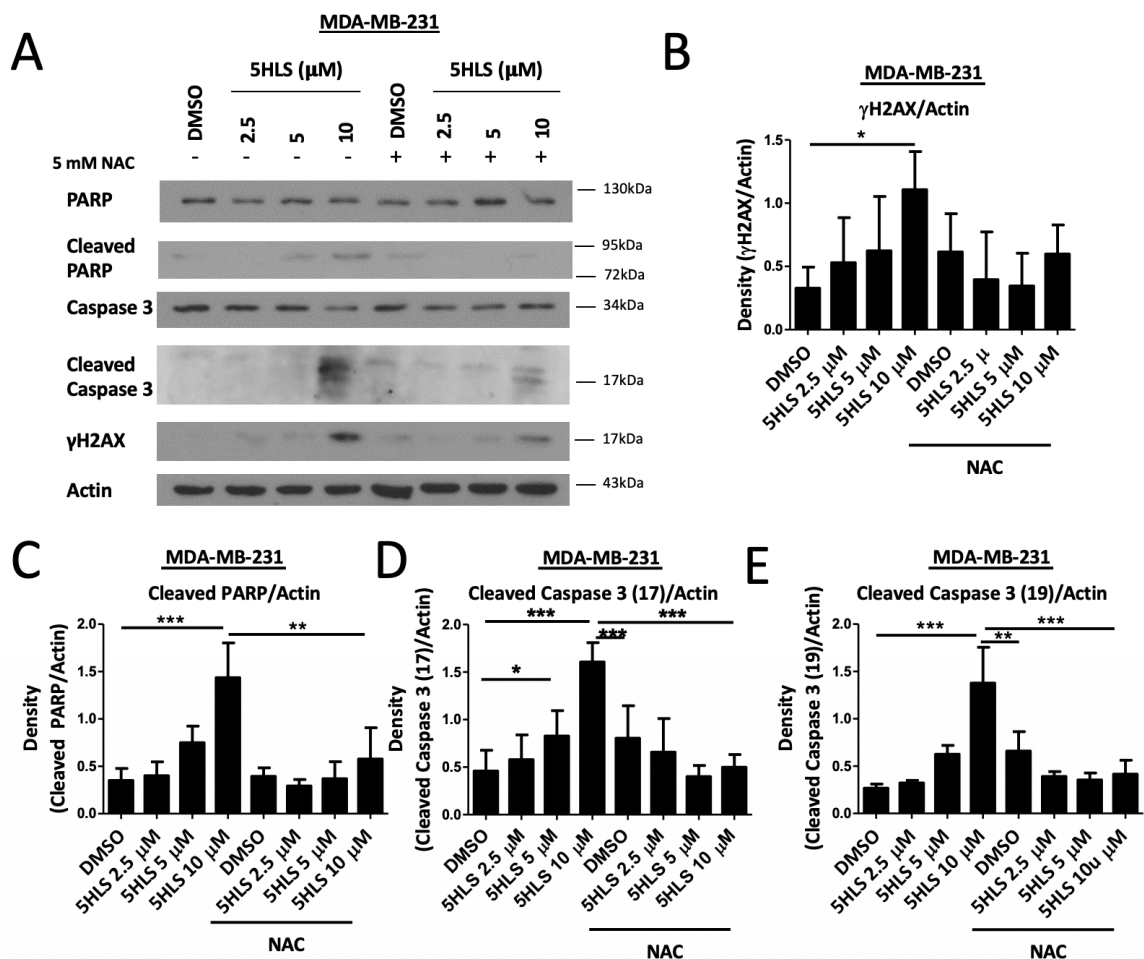


Figure 19: ROS scavenger NAC reduces cleavage of PARP and caspase 3 - MDA-MB-231 cells treated with increasing concentrations of 5-hydroxy lansoprazole sulfide in the presence or absence of 5 mM NAC (A). Quantification of γ H2AX (B), cleaved PARP (C), cleaved caspase 3 (17) (D), and cleaved caspase 3 (19) (E). (n=3) An ANOVA was used to compare all groups. $P < 0.05 = *$, $P < 0.01 = **$, and $P < 0.001 = ***$

3.A.5 5-Hydroxy Lansoprazole Sulfide does not produce reactive oxygen species

The previous data in Figures 18 and 19, would indicate that 5-hydroxy lansoprazole sulfide is producing reactive oxygen species that are leading to DNA damage and cell death. To confirm that 5-hydroxy lansoprazole sulfide creates reactive oxygen species, a 96-well format with CellROX green, to visualize ROS, was used. CellROX green is a cell permeable dye that becomes fluorescent once oxidized by ROS

and binds to DNA. Menadione, a superoxide generator, was used as a positive control and the reactive oxygen scavenger NAC, an L-cysteine source for the biosynthesis of glutathione, were also used. As shown in Figure 20A, CellROX is able to detect a significant difference between basal treated cells, positive control menadione treated cells, and menadione + 5 mM NAC treated cells in both MDA-MB-468 and MDA-MB-231 using an ANOVA to compare the three treatment groups. Figures 20B and C show that lansoprazole at low concentrations did not significantly increase reactive oxygen species in MDA-MB-231 cells but did at 4 hours and 6 hours in MDA-MB-468 cells. However, at high concentrations, of 200 μ M, for a short 2-hour treatment, lansoprazole significantly increased reactive oxygen species in both cell lines. Figure 20B and C also show that 5-hydroxy lansoprazole sulfide does not create reactive oxygen species even at very high concentrations of 100 and 200 μ M in MDA-MB-468 cells. In fact, high concentrations of 5-hydroxy lansoprazole sulfide significantly decrease ROS compared to basal cells in MDA-MB-468. In MDA-MB-231 cells there was only a significant difference between 5-hydroxy lansoprazole sulfide and basal at 24 hours, and, while not significant in MDA-MB-231 cells there is a trend towards a decrease at the higher concentrations of 5-hydroxy lansoprazole sulfide treatment. This could indicate at high concentrations 5-hydroxy lansoprazole sulfide is acting as a reactive oxygen scavenger. Further testing would need to be performed to confirm this. However, at the lower doses, used in the *in vitro* studies, except for 24 hours in MDA-MB-231 cells, 5-hydroxy lansoprazole does not change reactive oxygen species compared basal levels. While MDA-MB-231 cells show a significant difference in positive and negative controls there are few treatments that

cause a significantly different change in ROS. There are, however, visible trends within the data that may indicate a need to further optimize this experiment for MDA-MB-231 cells or perform repeated experiments. In any case, we can conclude that 5-hydroxy lansoprazole sulfide is not causing DNA damage through reactive oxygen species. While 5-hydroxy lansoprazole sulfide is not causing DNA damage through ROS the use of 5 mM NAC reduces the amount of DNA damage after 72 hours as shown in Figure 19A-B. This indicates that NAC is having a protective effect. While it is not clear how this may be occurring, previous studies in our lab concluded that an increase in γ H2AX phosphorylation can be caused by a decrease in DNA damage repair pathways alone. Potentially, 5-hydroxy lansoprazole sulfide is preventing the repair of DNA damage caused by normal cellular processes leading to a build-up of damage and apoptosis.

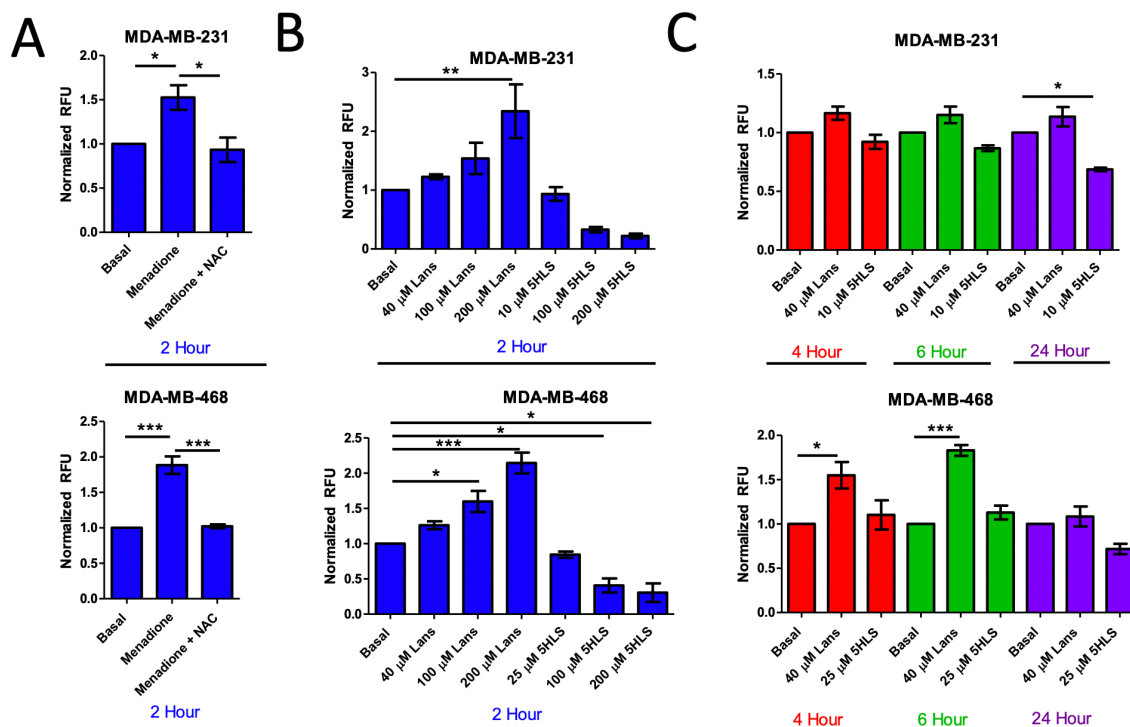


Figure 20: 5-hydroxy lansoprazole sulfide does not produce ROS - (A) Positive and negative controls in MDA-MB-231 and MDA-MB-468 cells using CellROX ROS detection assay at 2 hours. NAC was used at a concentration of 5 mM. (B) ROS detection in MDA-MB-231 and MDA-MB-468 cells treated for 2 hours with given concentrations of drugs. (C) ROS detection in MDA-MB-231 and MDA-MB-468 cells at 4 hours (red), 6 hours (green), and 24 hours (purple). (n=3, each value is the mean \pm SEM) An ANOVA was used to compare all groups in each graph. $P < 0.05 = *$, $P < 0.01 = **$, and $P < 0.001 = ***$

3.A.6 5-Hydroxy Lansoprazole Sulfide treatment decreases NHEJ repair activity

One way in which cells overcome DNA DSBs is through NHEJ repair [55, 271].

NHEJ is an error prone method in which cells can ligate broken ends of DNA. NHEJ is initiated by Ku 70 and Ku 80 binding to the broken ends of DNA. This leads to recruitment of DNA-PKcs and initiation of DNA damage repair. NHEJ is also controlled by PARP expression. One study found that PARP regulates NHEJ by promoting Ku retention at sites of DNA DSBs [272]. Furthermore, our lab has shown that PARP expression is controlled by FASN [128]. When FASN is inhibited or knockdown there is a decrease in

PARP expression. For these reasons, the expression of levels of PARP after treatment with lansoprazole and 5-hydroxy lansoprazole sulfide was determined. Both lansoprazole and 5-hydroxy lansoprazole sulfide led to a decrease in total PARP expression as shown in Figure 15A-B and 15D-E. Additionally, treatment of both MDA-MB-231 and MDA-MB-468 led to a decrease in the mRNA levels of PARP as shown in Figure 21A-B. Our lab has shown that an increase in FASN leads to an increase in PARP mRNA and a decrease in FASN leads to a decrease in PARP mRNA [128]. The mechanism of this is still unclear and should be further researched in the future. It is possible that 5-hydroxy lansoprazole sulfide is leading to a reduction in NHEJ via downregulation of PARP through inhibition of FASN.

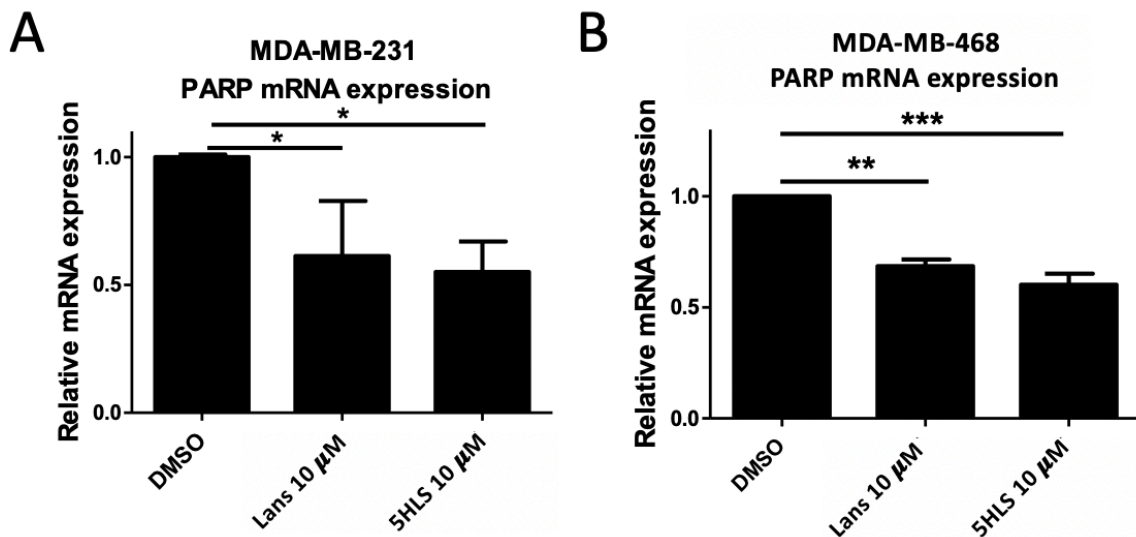


Figure 21: Treatment of MDA-MB-231 and MDA-MB-468 cells with lansoprazole and 5-hydroxy lansoprazole sulfide reduces mRNA levels of PARP – MDA-MB-231 (A) and MDA-MB-468 (B) cells were treated with 10 μ M lansoprazole or 5-hydroxy lansoprazole sulfide for 72 hours before samples were collected and PARP mRNA levels were measured. (n=3) An ANOVA was used for statistical analysis. (n=3) $P < 0.05 = *$, $P < 0.01 = **$, and $P < 0.001 = ***$

Due to the increase in γ H2AX, indicative of DNA DSB, and the decrease in PARP the ability of these cells to repair damaged DNA by NHEJ may be impaired after treatment with lansoprazole and 5-hydroxy lansoprazole sulfide. While PARP can also affect other modes of DNA damage repair (SSB, BER, and NER) which would affect DNA damage it was decided to analyze NHEJ due to the presence of DNA DSB and the fact that many anti-cancer treatments mediated their effects by causing DNA DSB. Effecting the ability of cells to repair DNA through NHEJ may have a significant impact in the clinical treatment of cancer.

Our NHEJ activity assay protocol was adapted from those described in previous papers [128, 273]. Figure 22 gives a brief summary of how this assay works. In this assay the pGL3 plasmid containing a SV40T promoter is utilized. The plasmid is cut using HindIII which produces a linear strand of DNA. The linear strand of DNA separates the SV40 promoter from the luciferase gene. In this way the linear plasmid cannot produce luciferase. After NHEJ repair, the plasmid will be re-circularized joining the promoter with the luciferase gene allowing for signal. In this way we can monitor NHEJ by determining the amount of luciferase using an intact pRL-TK, the Renilla plasmid, as a transfection efficiency control. Treatment of MDA-MB-231 cells with lansoprazole at 10 μ M concentration did not significantly decrease NHEJ activity while 10 μ M 5-hydroxy lansoprazole sulfide significantly decreased NHEJ repair (Figure 23A). In MDA-MB-468 cells both lansoprazole and 5-hydroxy lansoprazole sulfide significantly decreased NHEJ repair (Figure 23B). It is not surprising that lansoprazole at 10 μ M concentration does

not inhibit NHEJ repair in MDA-MB-231 cells due to the high IC₅₀ value to lansoprazole in these cells.

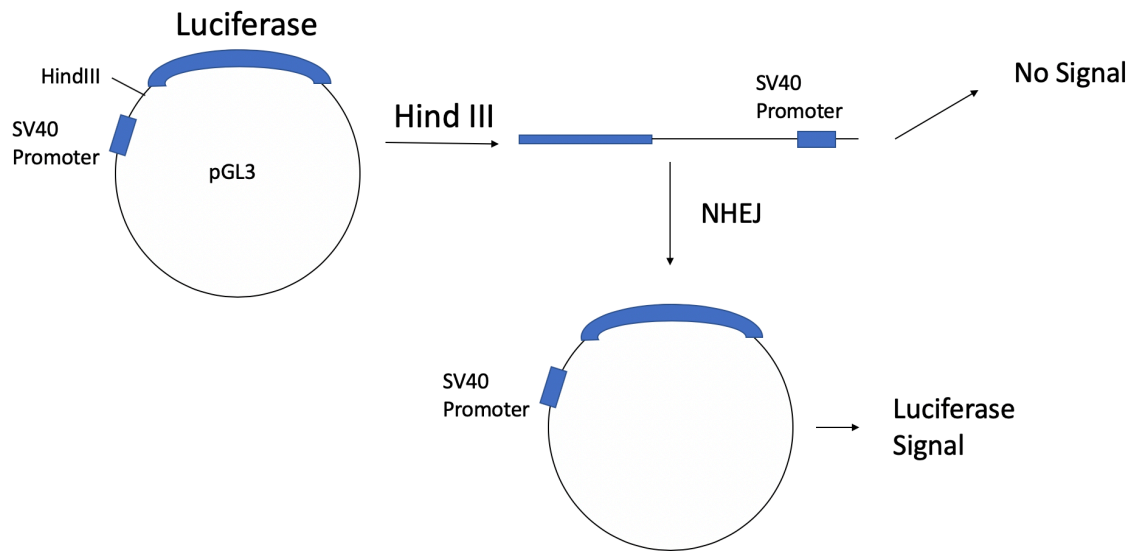


Figure 22: Depiction of the NHEJ assay – The pGL3 plasmid is cut between the promoter and the luciferase gene using HindIII creating blunt ends. In this linearized form, the plasmid is unable to produce luciferase. When the plasmid is repaired and re-circularized by NHEJ that plasmid will again produce luciferase.

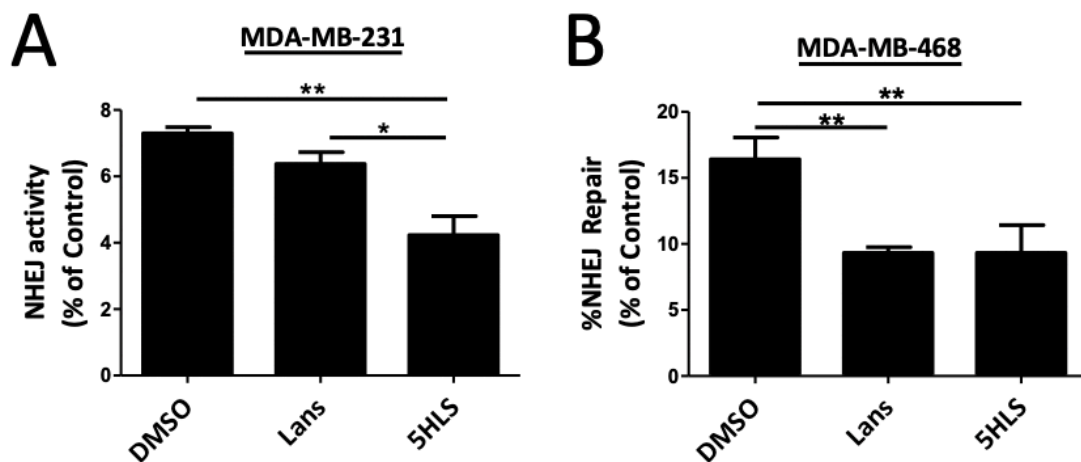


Figure 23: 5-Hydroxy Lansoprazole Sulfide decreases NHEJ activity– MDA-MB-231 (A) cells and MDA-MB-468 (B) cells treated with 10 μM for 72 hours. (n=3) Statistical analysis was performed using an ANOVA. P<0.05 = *, P<0.01 = **, and P<0.001 = ***

3.A.7 5-Hydroxy Lansoprazole Sulfide inhibits Fatty Acid Synthesis

Previous experiments in our lab have shown that lansoprazole inhibits FASN through binding to the TE domain [178]. Upon binding of lansoprazole, activity of FASN was decreased as determined by incorporation of radiolabeled acetate into fatty acid chains during a 2-hour pulse experiment [178]. All of the above evidence would indicate that 5-hydroxy lansoprazole sulfide is working through inhibition of FASN to decrease PARP expression, decrease NHEJ repair, and increase DNA damage. To determine if 5-hydroxy lansoprazole sulfide inhibits FASN activity the end product, free fatty acid content, was measured using the free fatty acid quantification kit from Abcam (ab65341). To test the ability of the assay to detect differences in fatty acid content MDA-MB-436 cells which had vector control or FASN overexpression were utilized. As shown in Figure 24A, MDA-MB-436/FASN cells had a significant increase in free fatty acids as compared to control MDA-MB-436/Vec cells.

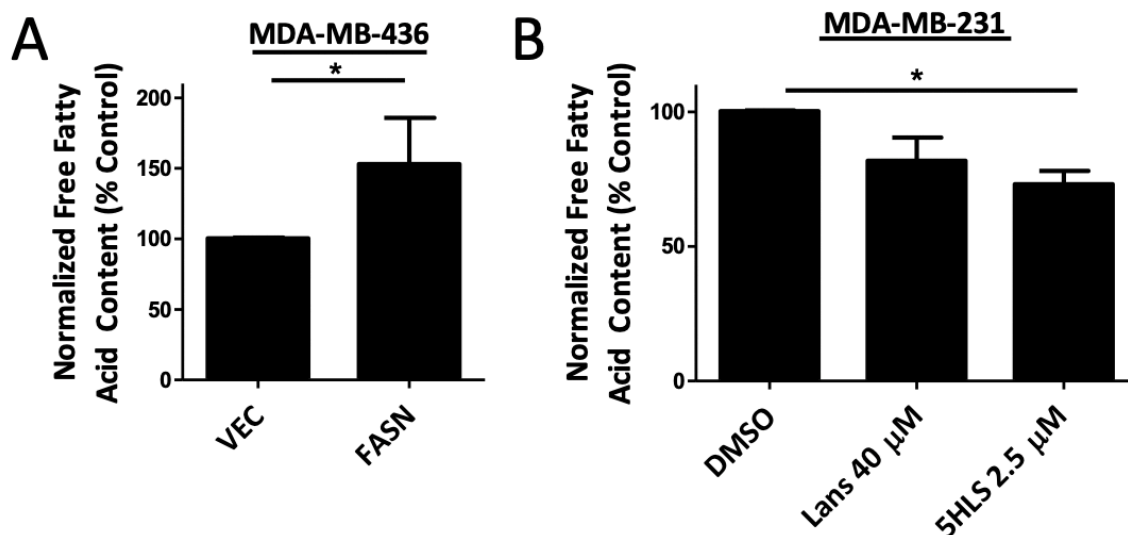


Figure 24: 5-hydroxy lansoprazole sulfide treatment reduces the free fatty acid content in MDA-MB-231 cells - A) Free fatty acids in MDA-MB-436/Vec vs. MDA-MB-436/FASN cells (n=3) B) Effect of lansoprazole and 5-hydroxy lansoprazole sulfide on free fatty acid content after 72-hour treatment using the IC₅₀ concentrations (n=4). T-test was used in (A) for statistical analysis and an ANOVA was used in (B). P<0.05 = *, P<0.01 = **, and P<0.001 = ***

To test the effect of lansoprazole and 5-hydroxy lansoprazole sulfide on free fatty acids, MDA-MB-231 cells were treated with IC₅₀ concentrations of drug for 72 hours. Cells were collected and counted to normalize to cell number and then the amount of free fatty acid was determined. 5-hydroxy lansoprazole sulfide treated cells had a significant reduction in free fatty acids (Figure 24B) compared to DMSO control. This indicates that 5-hydroxy lansoprazole sulfide is causing a decrease in free fatty acids by inhibiting FASN.

3.B.8 Summary

The data indicates that using the metabolite 5-hydroxy lansoprazole sulfide may be an effective method for improving the treatment of TNBC. Here, it is shown that 5-hydroxy-lansoprazole sulfide treatment leads to cellular apoptosis in TNBC. Figure 25 shows a hypothetical schematic summary of how this is might be occurring. 5-hydroxy lansoprazole sulfide inhibits FASN, thereby reducing cellular free fatty acids. This inhibition leads to a decrease in PARP and ultimately to a decrease in NHEJ activity. While it is not clear what the mechanism is for reduction of PARP, it is possible that end product starvation, palmitate, or FASN enzyme itself is playing a role in reduced transcription of PARP. While it is not clear how DNA damage is occurring, it is possible that DNA damage is occurring due to a decrease in NHEJ repair and the cells failing to repair damage that occurs due to normal cellular activity and DNA decay. Additionally, 5-hydroxy lansoprazole sulfide causes apoptosis through activation of caspase 3 and potentially necroptosis. Use of the reactive oxygen species scavenger NAC leads to a reduction in DNA damage and apoptosis. While this could suggest that the DNA damage is leading to apoptosis it is also possible that ROS scavenging is playing another role in the prevention of apoptosis (see discussion).

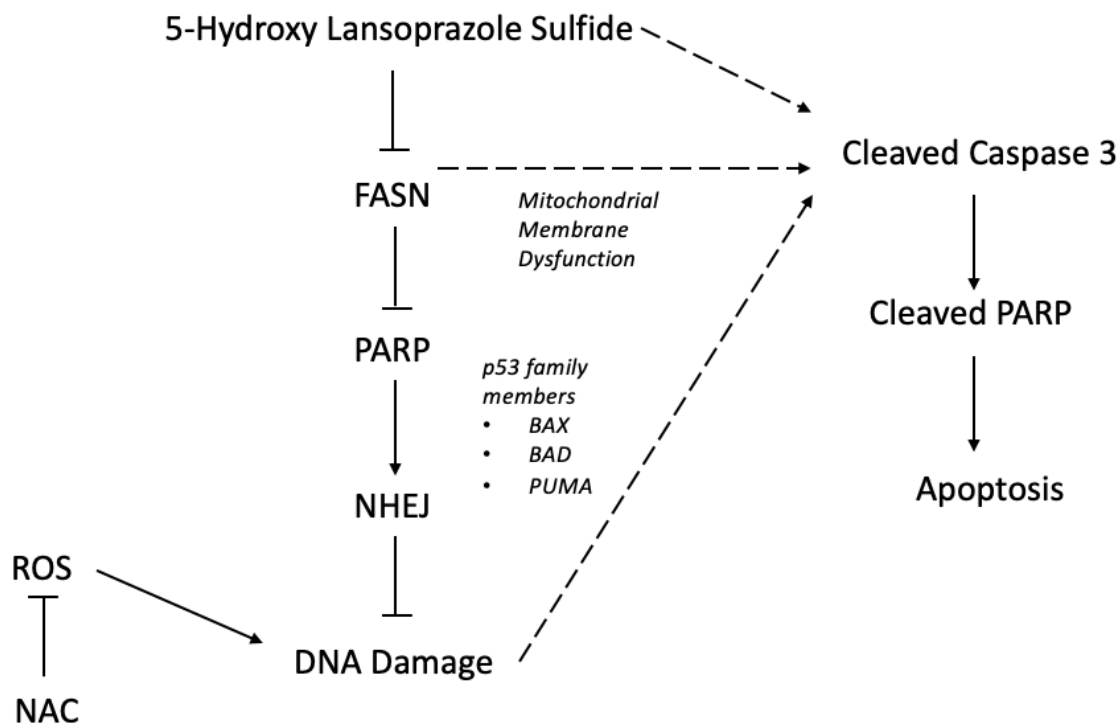


Figure 25: Hypothetical schematic of pathway – 5-hydroxy lansoprazole sulfide inhibits FASN causing a reduction in PARP and NHEJ repair. Reduction in NHEJ leads to an increase in DNA damage. Treatment with 5-hydroxy lansoprazole sulfide leads to apoptosis. The exact mechanism of how caspase 3 is activated by 5-hydroxy lansoprazole sulfide remains to be elucidated. Potentially, mitochondrial membrane dysfunction or activation of p53 family members may be playing a role as has been observed in the literature (see discussion). Further studies are required to confirm the mechanism.

Section 3.B CC-115

3.B.1 FASN does not play a role in resistance to DNA-PK inhibitor Nu7441 or CC-115

This thesis has shown that FASN affects NHEJ repair. Previous studies in our lab have shown that FASN increases NHEJ repair by increasing recruitment of Ku proteins to the site of DNA damage and increasing DNA-PK activity [229]. It is estimated that there are about 10 DNA DSB per day in dividing mammalian cells caused by cleavage of nuclear enzymes, DNA replication errors, ROS, and ionizing radiation [55]. Additionally, many chemotherapeutics aim to produce DNA DSBs as a way to target cancer cells [274]. Inhibition of DNA-PK is an emerging field with inhibitors in clinical trials to improve patient outcomes. With any treatment, the development of resistance will hinder efficacy of a drug. If FASN effects the activity of DNA-PK, it could therefore lead to resistance in DNA-PK inhibitors. For these reasons, we hypothesized that FASN contributed to resistance to CC-115 by increasing DNA-PK activity.

To investigate the potential mechanism of CC-115 resistance, I first took advantage of MCF7/AdVp3000 (M3K) cell line, which was selected for Adriamycin resistance. M3K cells harbor multiple mechanisms of drug resistance, including overexpression of FASN [122], and we tested their response to CC-115 in comparison with its parental MCF7 cells. As shown in Figure 26A and B, M3K cells are about 44 times more resistant than parental MCF7 cells to CC-115 with IC_{50} of $\sim 2.2 \mu M$ and $\sim 50 nM$, respectively.

Due to the fact that CC-115 inhibits DNA-PK and FASN increases DNA-PK activity in M3K cells [128], it is possible that FASN overexpression in M3K cells contributes to CC-

115 resistance. To test this possibility, we took advantage of MCF7 cells with stable overexpression of FASN (MCF7/FASN) and M3K cells with stable FASN knockdown (M3K/shFASN) (see Figure 26C) and tested their response to CC-115 in comparison with their respective control cells (MCF7/Vec and M3K/Scr). As shown in Figure 26A, D and E, ectopic FASN overexpression or FASN knockdown did not influence cellular response to CC-115. Thus, FASN may not contribute to CC-115 resistance via its DNA-PK inhibitory activity. Additional cell lines tested, while having slightly higher resistance than MCF7 cells, did not have a significant resistance. (Figure 26A)

CC-115 is a dual mTOR/DNA-PK inhibitor, therefore, to confirm that DNA-PK inhibition is not part of the resistance due to FASN expression, we also tested a DNA-PK selective inhibitor, NU7441. As shown in Figure 27A-D, alteration of FASN expression did not change cellular response to NU7441 albeit M3K cells are slightly more resistant to NU7441 than the parental MCF7 cells, this was not significant and could be due to other difference between MCF7 and M3K and not FASN. There was also no difference in sensitivity between all additional cell lines tested (Figure 27A).

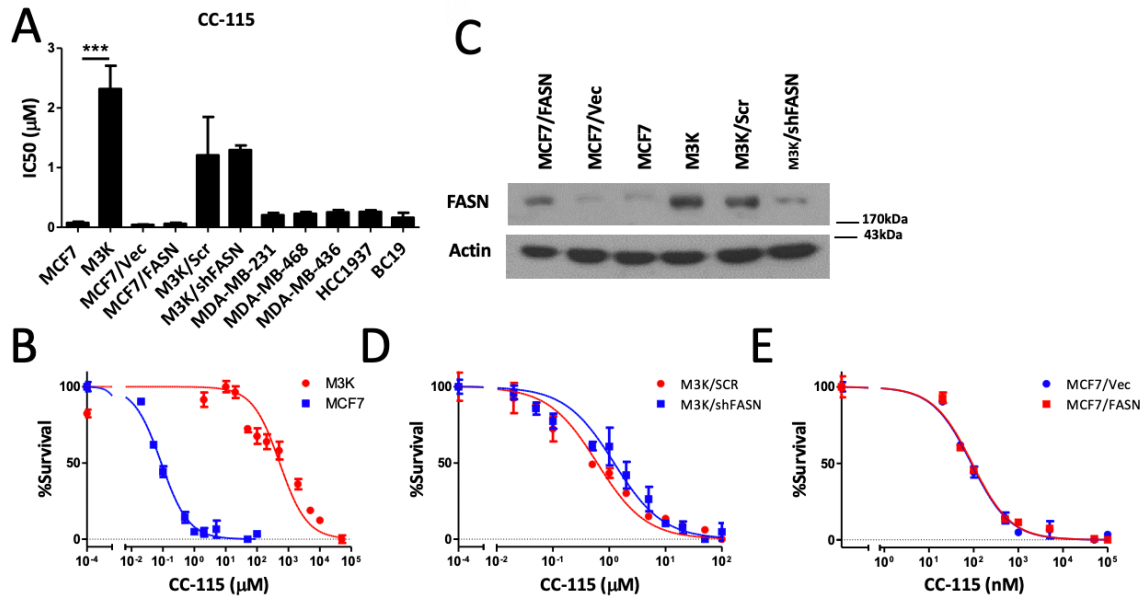


Figure 26: FASN does not affect the potency of CC-115 - A) IC₅₀ values to dual DNA-PK/mTOR inhibitor CC-115 determined by methylene blue in each cell line. (n=3) B) Survival curve for MCF7 (■) and M3K (●) cells treated with CC-115. C) FASN expression in MCF7/Vec, MCF7/FASN, MCF7, M3K, M3K/Scr, and, M3K/shFASN cell lines. Survival curves for D) M3K/Scr (●) vs. M3K/shFASN (■) and E) MCF7/Vec (■) and MCF7/FASN (●). An ANOVA was used for statistical analysis in (A), followed by a T-test to compare MCF7 (parent) to M3K (Doxorubicin resistant clone). P<0.05 = *, P<0.01 = **, and P<0.001 = ***

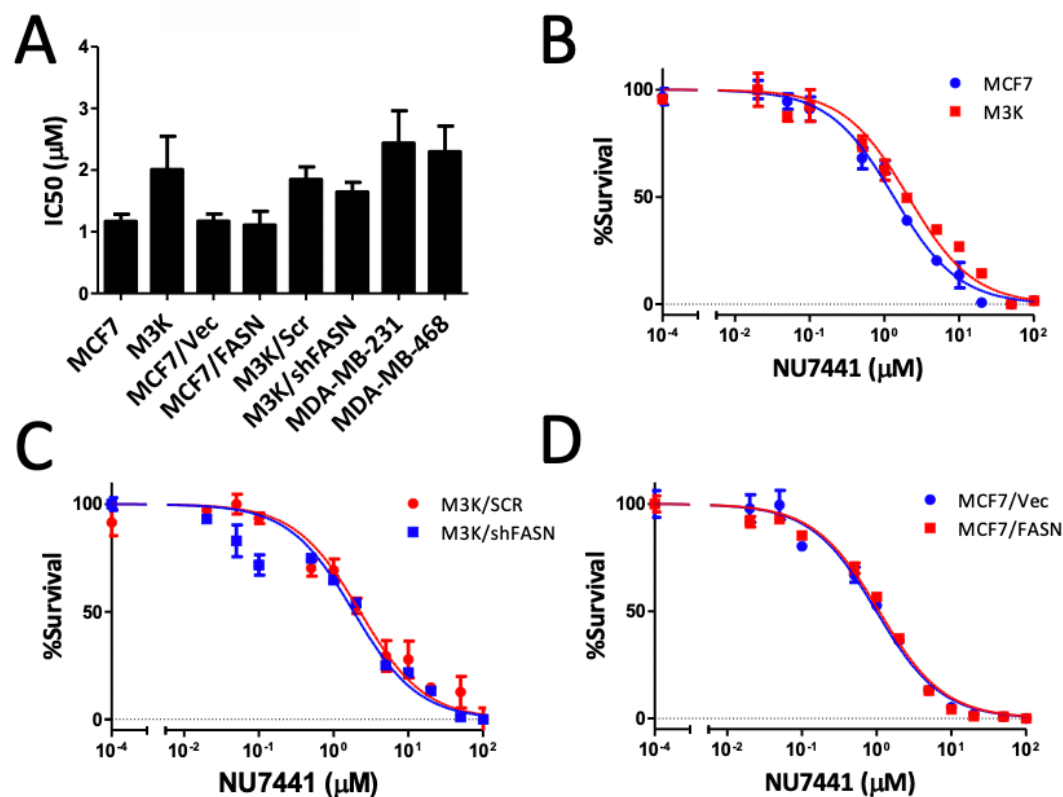


Figure 27: FASN does not affect the potency of DNA-PK specific inhibitor NU7441 - A) IC₅₀ values to DNA-PK inhibitor Nu7441 determined by methylene blue. Survival curves for (n=3) B) MCF7 (■) and M3K (●), C) M3K/Scr (●) and M3K/shFASN (■), and D) MCF7/Vec (■) vs MCF7/FASN (●). An ANOVA was performed on (A) and no statistically significant difference was found.

Being that CC-115 is a dual mTOR/DNA-PK inhibitor, we next tested if its inhibition of mTOR pathway was impaired in the drug resistant M3K cells. To do this we treated cells for 2-hours and monitored for phosphorylation of certain proteins. Specifically, we probed for phosphorylation at Thr389 on S6K, which is indicative of phosphorylation by mTOR, and Ser235/236 on S6, indicative of phosphorylation by S6K [214]. As shown in Figure 28A, CC-115 inhibition of constitutive activation of S6K and phosphorylation of S6, downstream targets of mTOR, were significantly impaired in M3K compared with MCF7 cells. The western blot for S6K and P-S6K has two bands because the antibody can also

detect p85. Based on these findings, we conclude that FASN does not play a role in DNA-PK inhibitor resistance.

3.B.2 Identification of ABCG2 as a contributor to CC-115 resistance

Due to the short treatment in the above study, lack of mTOR inhibition, 50-fold increase in resistance, and, the known role of efflux pumps in resistance [275-278], we decided to determine if an efflux pump could be playing a role in this resistance. First, it has been previously shown that M3K cells overexpress ABCG2 [279]. We also tested the expression of ABCB1 and ABCC1 shown in Figure 28B. This matched with early studies which indicated M3K acquired resistance through overexpression of ABCG2 and not ABCB1 and ABCC1 [280].

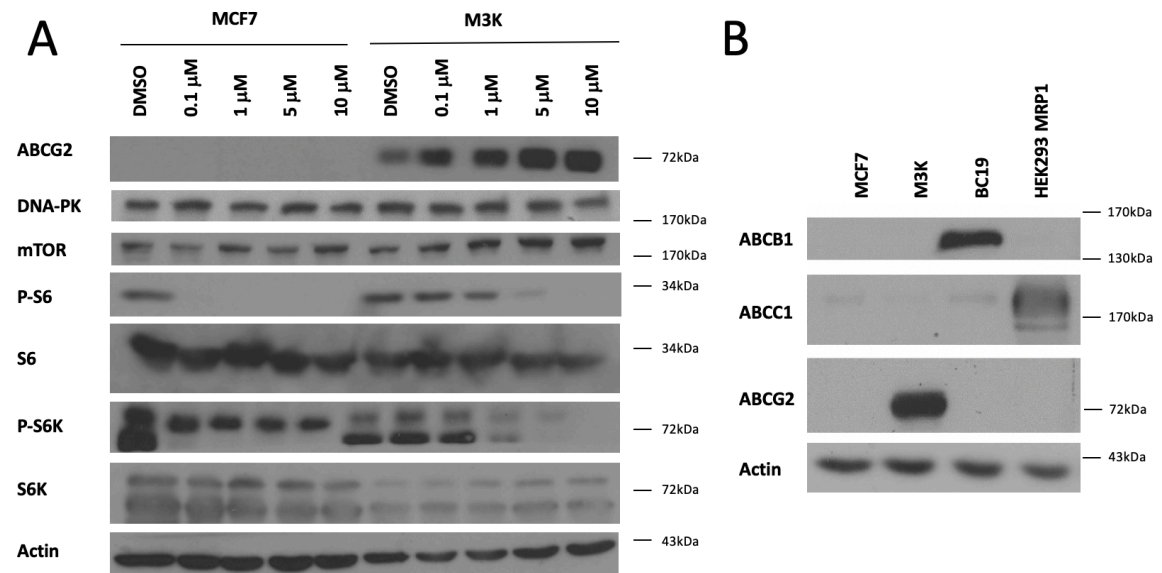


Figure 28: CC-115 inhibition of mTOR and expression profile of efflux pumps - A) CC-115 inhibition of mTOR, monitored by phosphorylation of S6 and S6K. **B)** Expression profile of ABCB1, ABCC1, and ABCG2. (S6K and P-S6K also detects p85)

To determine cellular accumulation of CC-115, I first had to determine if CC-115 was a fluorescent molecule. To do this, I used spectrophotometer with a small amount of sample (0.33mM) and measured the absorbance at different wavelengths along the spectrum. Based on the absorbance shown in Figure 29A CC-115 absorbs light at about 340-400 nm. Knowing this absorbance allowed me to use a fluorescence spectrophotometer (Cary Eclipse Varian) and measure the emission at a specific excitation wavelength. Excitation at a wavelength of 386 nm yielded the emission spectra shown in Figure 29B. The fluorescent property of CC-115 provides the opportunity of using flow cytometry to measure cellular accumulation of drug.

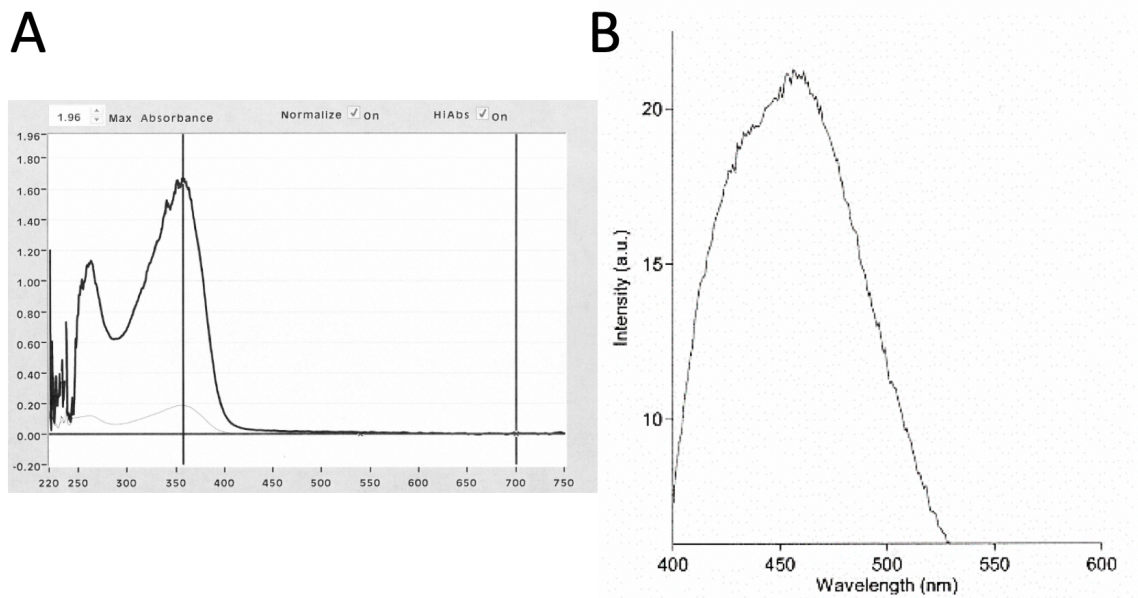


Figure 29: Absorbance and Fluorescence of CC-115 - A) Absorbance spectrum for CC-115 B) Emission spectrum at excitation 386 nm.

To test the ability of flow to measure differences in accumulation of CC-115 I first tested DMSO control versus CC-115 treatment in MCF7 cells. Using the excitation and emission data for CC-115, it was decided with help from the flow cytometry lab to use

BD LSR II analyzer at excitation wavelength of 405 nm and an emission of 421 nm. Cells were treated with 10 μ M CC-115 or DMSO as a control for 30 min. After 30 min cells were collected and washed with PBS. Cells were then resuspended in 500 μ L PBS and filter through 5 mL polystyrene round-bottom tube with cell-strainer cap for flow cytometry. Using these parameters, we could see a significant difference in fluorescence intensity of MCF7 cells exposed to drug versus DMSO control. This is shown in Figure 30A and B. Furthermore, there was a significant difference in CC-115 accumulation between MCF7 and M3K cells. This is shown in Figure 30C and D, M3K cells accumulated about ~20% the amount of CC-115 as was seen in MCF7 cells. Here, only MCF7 treated with DMSO as a negative control is shown due to the overlap of MCF7 and M3K negative controls.

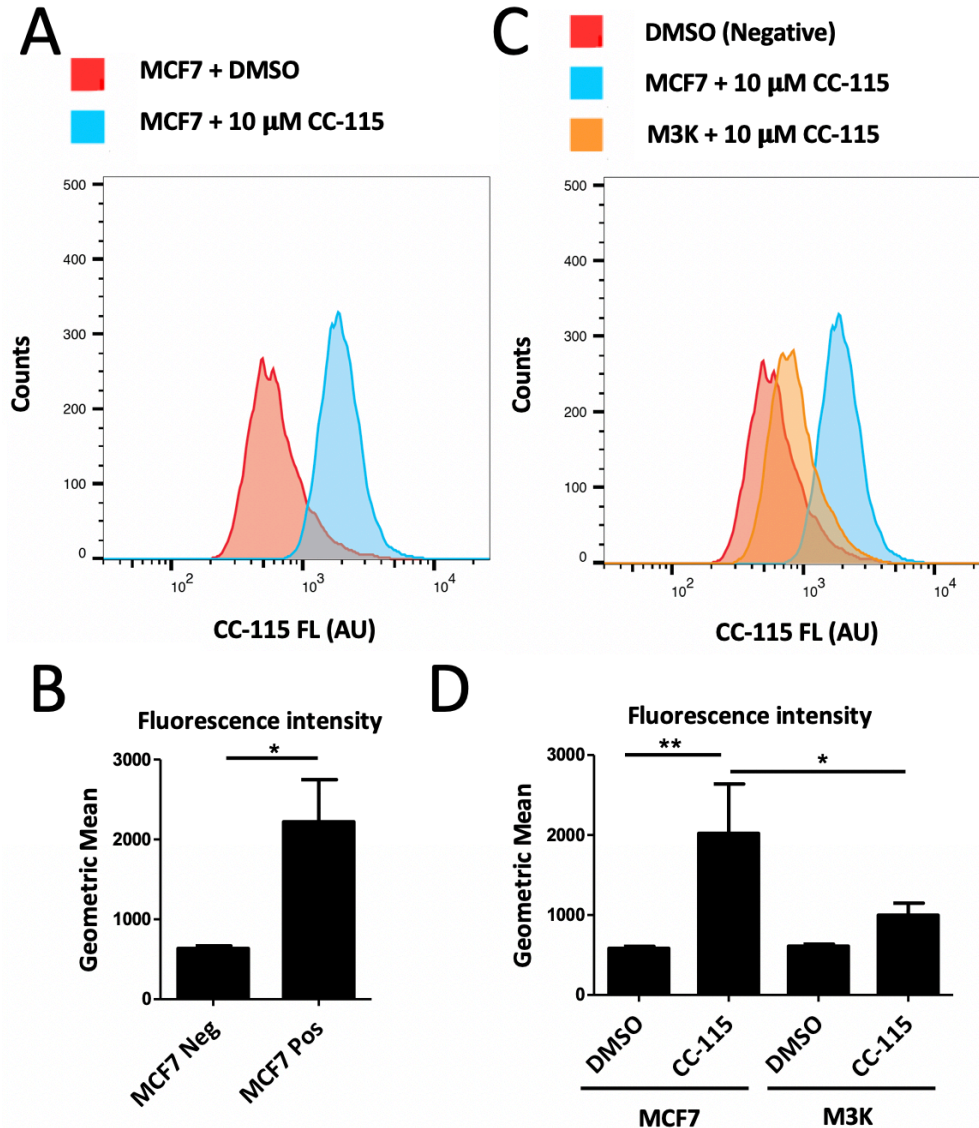


Figure 30: CC-115 Accumulation is decreased in M3K cells as compared to MCF7 - Accumulation of CC-115 can be detected in cells with flow cytometry using excitation wavelength 405 nm and emission max filter at 421 nm. A) shows the separation of cells treated with CC-115 versus those treated with DMSO control and B) is the quantification of the fluorescence intensity. Panel C) shows an increase in accumulation of CC-115 in MCF7 cells as compared to less accumulation in M3K cells with quantification in D. (n=3) Statistical analysis using a T-test comparing negative and positive controls in (C) and ANOVA comparing all groups (D) was utilized. $P < 0.05 = *$, $P < 0.01 = **$, and $P < 0.001 = ***$

3.B.3 Inhibition of ABCG2 reverses CC-115 resistance by increasing accumulation of drug

To evaluate the role of ABCG2 in the efflux of CC-115, we employed the use of two ABCG2 inhibitors: fumitremorgin C (FTC) [257], which is commercially available, and C8, an inhibitor developed in our lab [259]. First, the inhibitors were used to measure the accumulation of CC-115 within M3K cells treated with 1 μ M and 5 μ M inhibitor. Cells were collected and incubated with inhibitor for 15 minutes before exposure to CC-115 for 30 min. As shown in Figure 31A-C, there was a dose dependent increase in CC-115 accumulation in M3K cells. As discussed above, M3K cells had about a 79% decrease in CC-115 accumulation as compared to MCF7 cells. When M3K cells are first treated with 1 μ M and 5 μ M C8 this decrease was reduced to ~45% and ~14% respectively. Treatment with FTC had a similar effect with a decrease of only ~30% and ~0.5% with 1 μ M and 5 μ M, respectively.

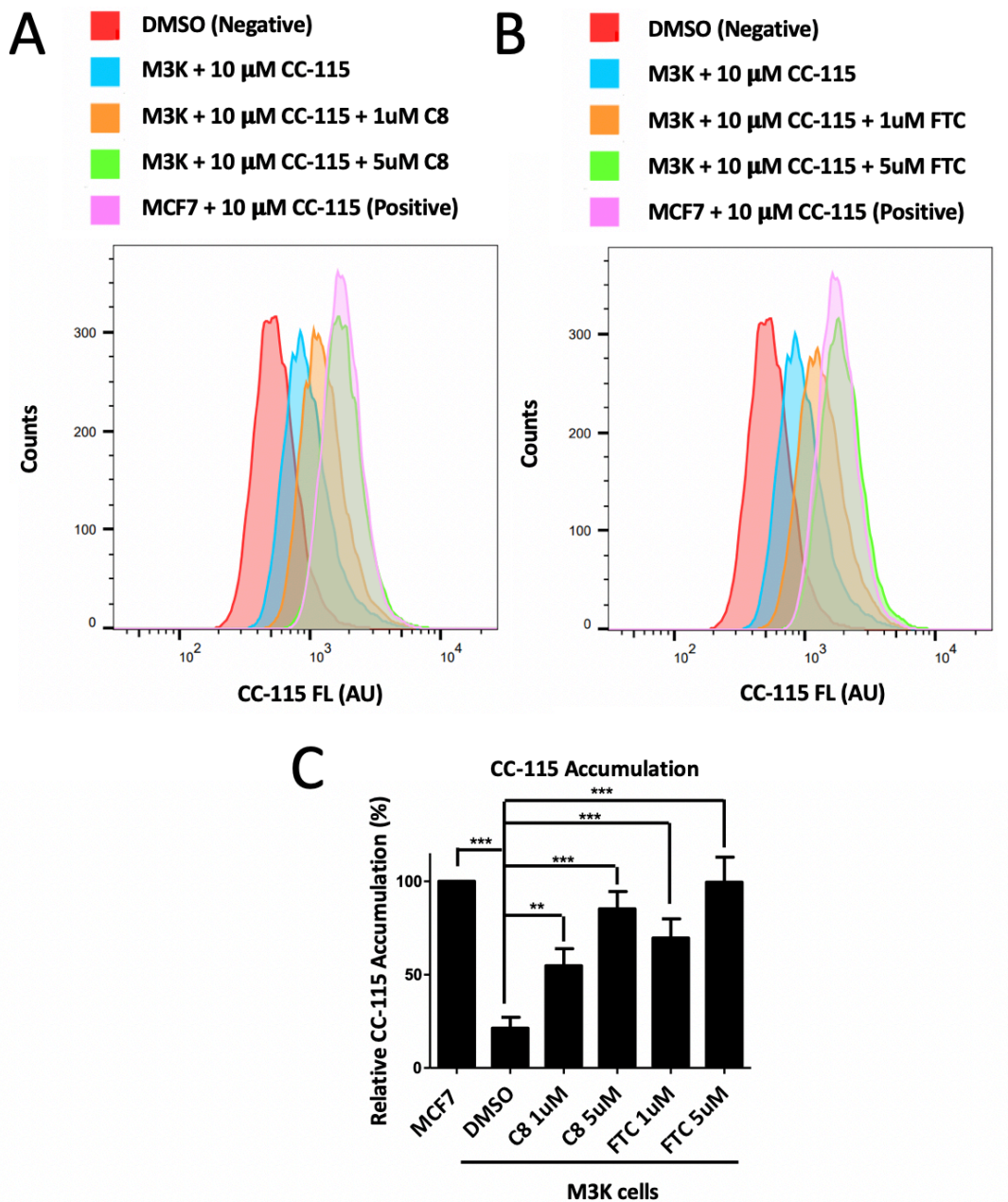


Figure 31: ABCG2 decreases cellular accumulation of CC-115 - CC-115 accumulation in M3K cells was measured after inhibition of ABCG2 by C8 (A) and FTC (B) using 1 μ M and 5 μ M concentration of inhibitor. C) Quantification of CC-115 accumulation. (n=3) An ANOVA comparing all groups was used in (C) for statistical analysis. $P < 0.05 = *$, $P < 0.01 = **$, and $P < 0.001 = ***$

Furthermore, ABCG2 inhibition by C8 sensitized M3K cells to CC-115 inhibition of mTOR signaling (Figure 32A). M3K cells treated with 1 μ M of C8 in combination with increasing concentrations of CC-115 for 2 hours decreased S6K and S6 phosphorylation. Inhibition of ABCG2, using 1 μ M C8 or FTC, in a methylene blue assay lead to a 10-fold decrease in IC₅₀ value in M3K cells (Figure 32B and C). Treatment with 1 μ M C8 or FTC alone did not affect growth of M3K cells as evidenced by similar proliferations rates as control.

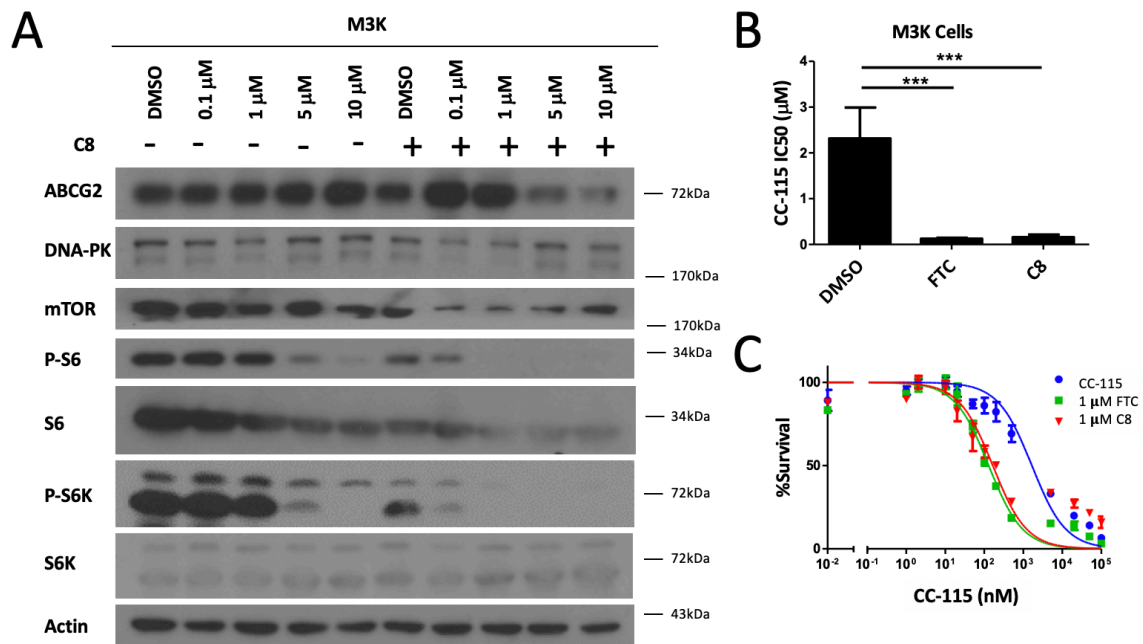


Figure 32: Inhibition of ABCG2 sensitizes M3K cells to CC-115 and increases inhibition of mTOR signaling - A) Western blot measuring mTOR activation through P-S6K and P-S6 in the absence or presence of 1 μM C8 B) Sensitization of M3K cells to CC-115 treatment in the presence of 1 μM FTC or C8 C) Potency index to CC-115 in M3K cells treated with vehicle (●), C8 (▼) and FTC (■) at 1 μM. (n=3) ANOVA was utilized in (B) to determine statistical significance. P<0.05 = *, P<0.01 = **, and P<0.001 = ***

3.B.4 Overexpression of ABCG2 in MCF7 and HEK293 cells increases resistance to CC-115

To further validate ABCG2's role in CC-115 efflux and resistance HEK293/Vec vs HEK293/ABCG2 and MCF7/Vec vs MCF7/ABCG2 (Figure 33A) were generated. HEK293 cells were transfected with a venus tagged ABCG2 for better visualization. A western blot confirming overexpression of ABCG2 in these cell lines is in Figure 33A. The IC₅₀ to CC-115 was then determined by MTT and methylene blue respectively. Both ABCG2 overexpression cell lines had a significant increase in resistance to CC-115 treatment (Figure 33B and C). Then accumulation of CC-115 was measured in the different cell

lines using FACs. Figure 33D and E shows that both HEK293/Vec and MCF7/Vec had a greater accumulation of drug as compared to their paired counterparts HEK293/ABCG2 and MCF7/ABCG2. The ability of CC-115 to inhibit the mTOR pathway was again measured by phosphorylation of S6K and S6 (Figure 34A-B). HEK/ABCG2 and MCF7/ABCG2 required more drug to achieve the same amount of inhibition as was seen in their vector control cells respectively.

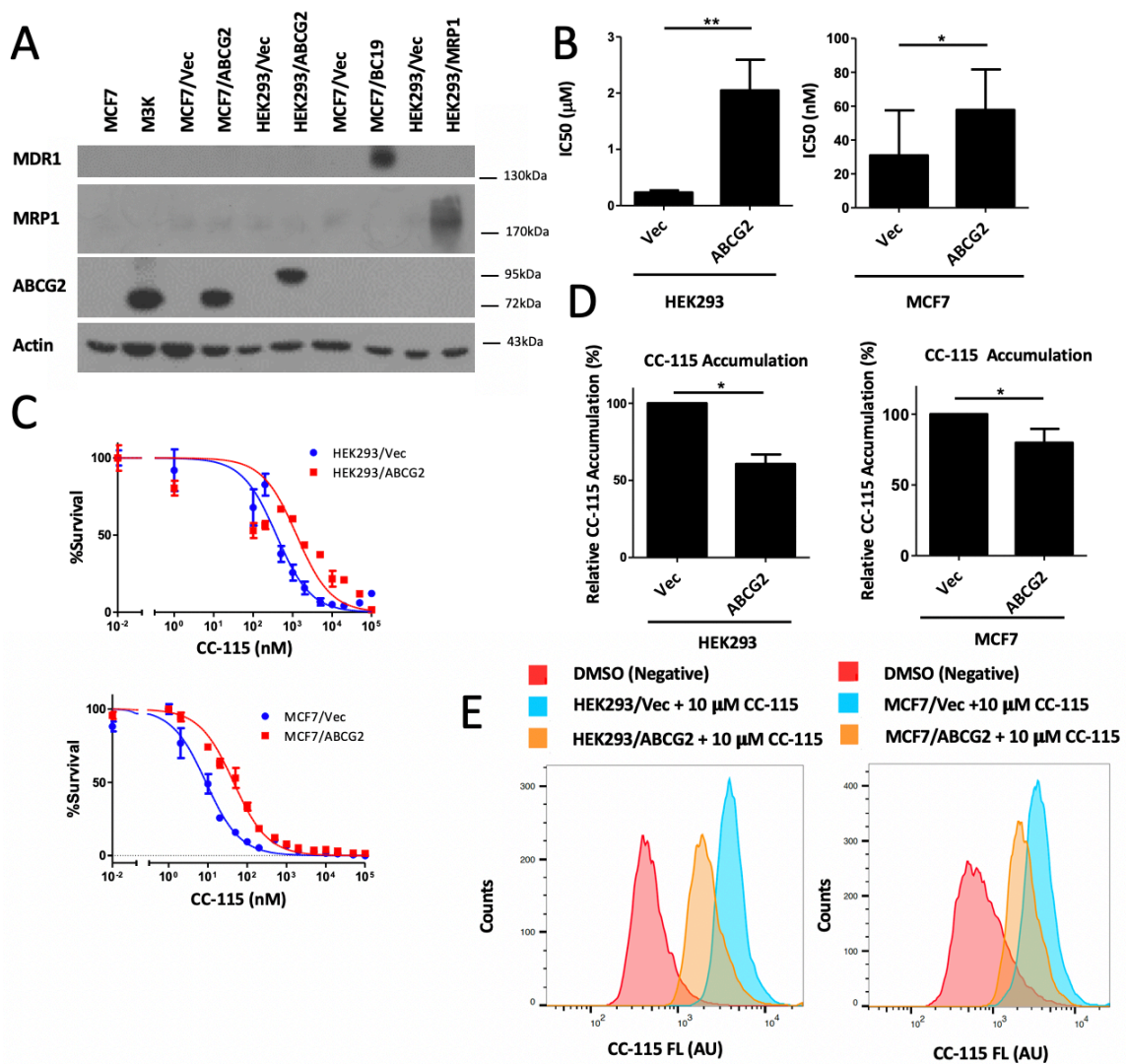


Figure 33: Overexpression of ABCG2 in HEK293 and MCF7 cells reduces accumulation increases resistance to CC-115 - A) Expression of efflux pumps ABCB1, ABCC1, and ABCG2. (ABCG2 in HEK293 cells is venus tagged increasing its molecular weight) B) IC₅₀ to CC-115 in HEK293/Vec vs HEK293/ABCG2 by MTT and MCF7/Vec vs MCF7/ABCG2 by methylene blue Assay. C) Representative survival curve for Vec (●) and ABCG2 (■) overexpression cells treated with CC-115 in HEK293 and MCF7. D) and E) CC-115 accumulation measured by flow cytometry with quantification. (n=3) Statistical analysis using a T-test comparing IC₅₀ to CC-115 in Vec and ABCG2 overexpressing cells (B) and relative accumulation (D) was used to determine significance. P<0.05 = *, P<0.01 = **, and P<0.001 = ***

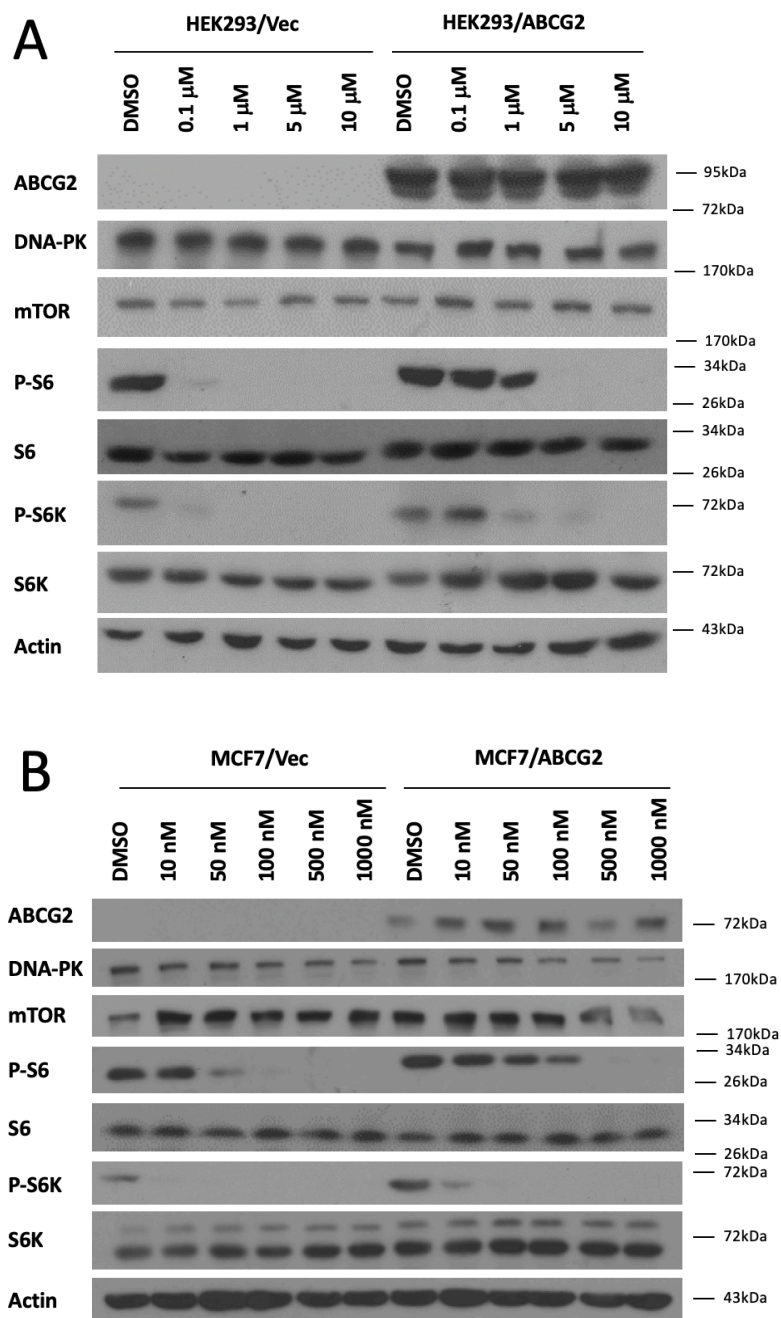


Figure 34: ABCG2 increases resistance to CC-115 inhibition of mTOR - A) CC-115 inhibition of mTOR in HEK293 cells and B) MCF7 cells. Cells were treated with CC-115 for 2 hours and then cell pellets were collected for analysis. (n=4)

To confirm ABCG2's role in CC-115 resistance HEK293/ABCG2 cells were used with ABCG2 inhibitors. The HEK293/ABCG2 cells were chosen based on ABCG2 expression levels confirmed via western blot analysis. ABCG2 expression in MCF7/ABCG2 was much lower than that observed in M3K and HEK293/ABCG2 cells (Figure 35). MCF7/ABCG2 cells while still having a significant difference in IC_{50} , about 2-fold, and accumulation of CC-115, reduction of about 21%, it was much less than was observed for M3K cells at 79%. Due to the lower expression of ABCG2 it may be hard to see a significant difference when using inhibitors. Additionally, HEK293/ABCG2 cells showed about a 45% reduction in accumulation in CC-115 as compared to M3K cells, 79%. M3K cells were acquired by stepwise selection and may have additional changes occurring within the cells that may increase resistance other than ABCG2 expression. Furthermore, it is known that ABCG2 in M3K cells carries an arginine to threonine mutation at position 482 [281] which may increase its ability to efflux CC-115.

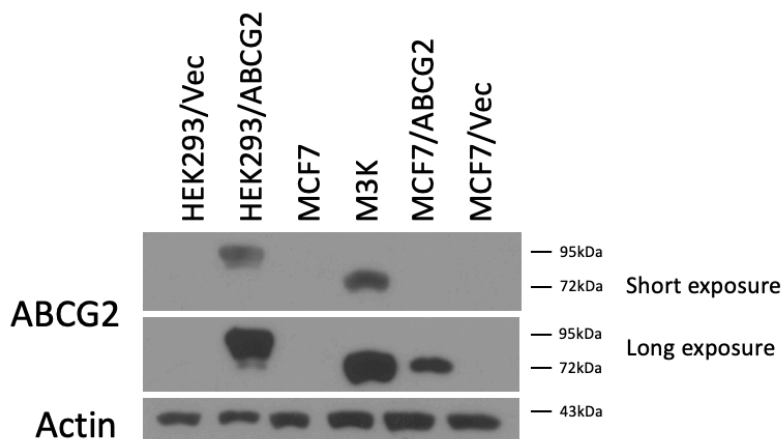


Figure 35: ABCG2 expression (ABCG2 in HEK293 cells is venus tagged increasing its molecular weight)

Using the same method as above HEK293/ABCG2 cells were pre-incubated with 1 μ M and 5 μ M C8 or FTC for 10 min and then 10 μ M CC-115 was added for 30 min to measure accumulation. As shown in Figure 36A-C there was a dose dependent increase in CC-115 accumulation with inhibition of ABCG2 by either inhibitor. Introducing either 1 μ M C8 or FTC into the IC₅₀ assay (MTT) caused a sensitization to CC-115 treatment (Figure 37B and C). Inhibition of the mTOR pathway was also reduced with addition of 1 μ M C8. This was determined by again measuring the phosphorylation of S6k and S6 (Figure 37A).

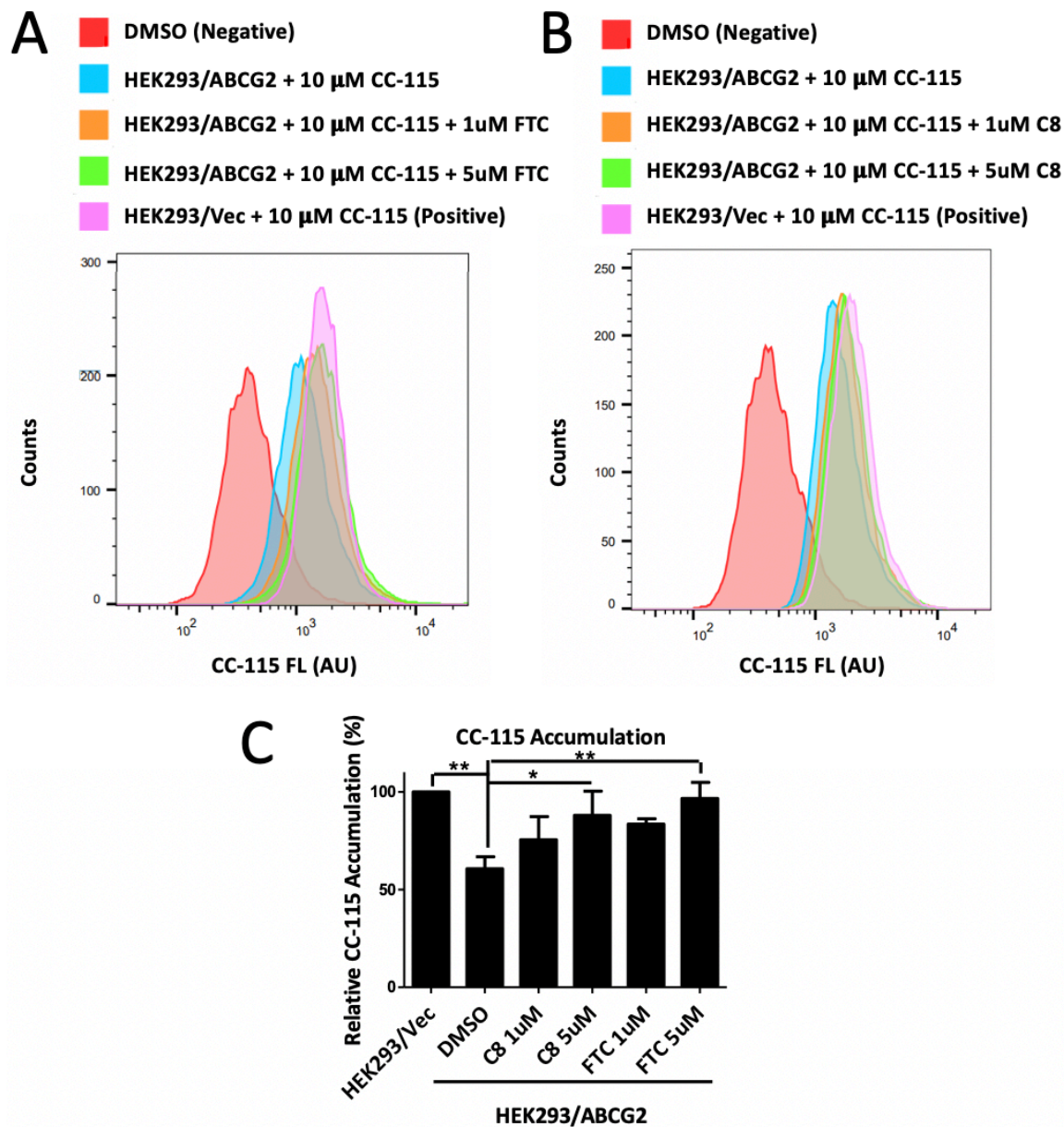


Figure 36: Inhibition of ABCG2 in HEK293 cells restores CC-115 accumulation - A) and B) dose response to ABCG2 inhibitors C8 and FTC, using 1 μ M and 5 μ M, in restoring CC-115 accumulation in HEK293/ABCG2 cells with quantification C). (n=3) An ANOVA comparing all groups was used in (C) for statistical analysis. $P < 0.05 = *$, $P < 0.01 = **$, and $P < 0.001 = *$**

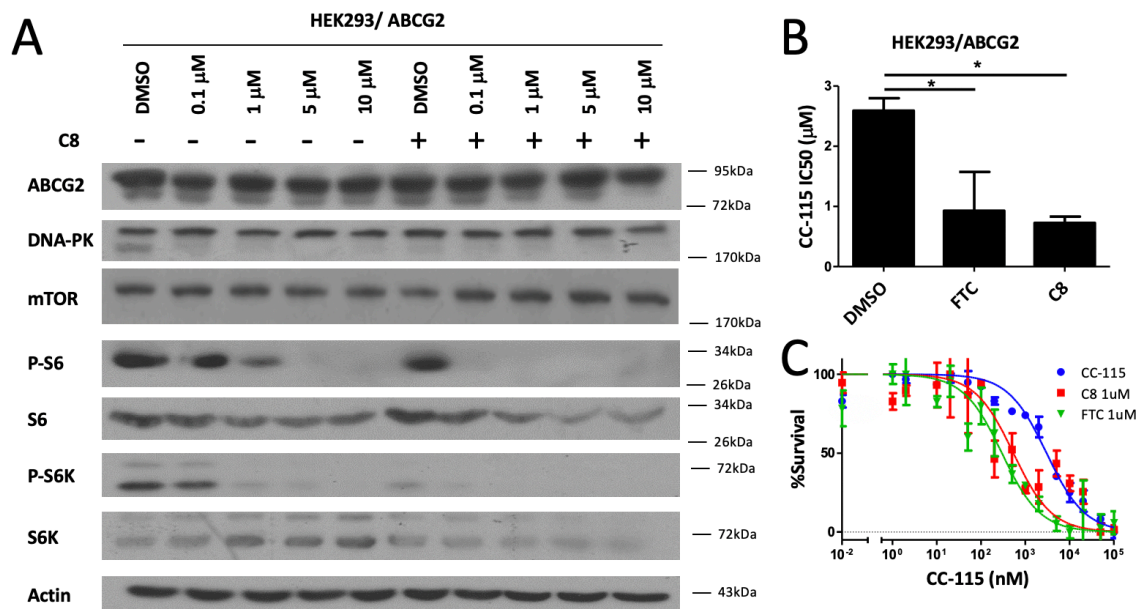


Figure 37: Inhibition of ABCG2 in HEK293 cells reverses mTOR inhibition and sensitizes HEK293/ABCG2 to CC-115 - A) Analysis of CC-115 inhibition of mTOR using ABCG2 inhibitor C8 at a concentration of 1 μ M by western blot B) Sensitization to CC-115 treatment in HEK293/ABCG2 cells using ABCG2 inhibitors C8 and FTC at 1 μ M concentration. C) Representative survival curve of HEK293/ABCG2 cells treated with CC-115 - vehicle (●), C8 (▼) and FTC (■) at 1 μ M. (n=3) An ANOVA comparing all groups in (B) was utilized for statistical analysis. P<0.05 = *, P<0.01 = **, and P<0.001 = ***

3.B.5 CC-115 is also a substrate of ABCB1

It is known that ABC transporters involved in drug resistance have overlapping substrates, therefore, we next tested if other ABC transporters such as ABCB1 may also contribute to CC-115 resistance. For this purpose, we took advantage of MCF7 cells that overexpress ectopic ABCB1 (BC19 cells) (Figure 38A) and tested CC-115 accumulation and resistance compared with vector-transfected MCF7 cells (MCF7/Vec). As shown in Figure 38B-C, CC-115 accumulation is significantly reduced in BC19 compared with the control MCF7/Vec cells. The IC₅₀ of CC-115 was also significantly increased in BC19 cells

compared with the MCF7/Vec cells. (Figure 38D-E) Thus, ABCB1, in addition to ABCG2, may also contribute to CC-115 resistance by reducing its intracellular accumulation.

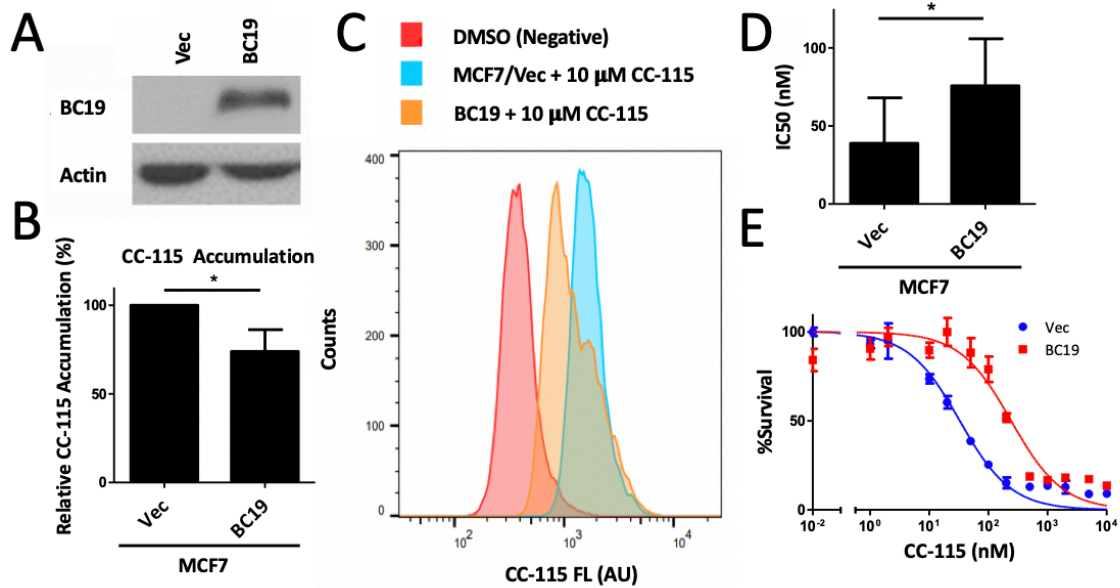


Figure 38: CC-115 is a substrate for ABCB1 - A) Expression of ABCB1. B) and C) Accumulation of CC-115 in MCF7/Vec versus MCF7/BC19 with D) IC₅₀ to CC-115 in MCF7 with Vec or ABCB1 overexpression. E) Representative survival curve for MCF7 cell treated with CC-115 – Vec (●) and ABCB1 (■). (n=3) Statistical analysis was performed using a T-test to compare relative accumulation (B) and IC₅₀. P<0.05 = *, P<0.01 = **, and P<0.001 = ***

3.B.6 Summary

Here we identified a mechanism of resistance that can be utilized by cancer cells to overcome the drug CC-115, which is currently in clinical trials. ABCG2 removes CC-115 from within cells preventing its interaction with target proteins as shown by a lack of mTOR inhibition. Inhibition of ABCG2 using small molecule inhibitors C8 and FTC increased accumulation of CC-115 and increased the inhibition of mTOR in cells with overexpression of ABCG2. While ABCG2 has been identified as a mechanism of resistance for a variety of anticancer drugs there is still no clinically approved drug inhibiting its activity. However, ABCG2 status can be assessed to stratify patients into treatment groups. Additionally, ABCB1 a second efflux pump, removes CC-115 from cells and may also be contributing to resistance.

CHAPTER 4: DISCUSSION

Section 4.A: 5-hydroxy lansoprazole Sulfide

Currently, FDA-approved PPI's could be quickly implemented in the treatment of TNBC. In a current clinical trial, patients are receiving 80 mg omeprazole twice a day which is four times the optimal dose in the treatment of *Helicobacter pylori* [282]. While PPI's may be effective, if 5-hydroxy lansoprazole sulfide is largely responsible for the positive effects, it may be most beneficial to directly give patients this compound. The use of 5-hydroxy lansoprazole sulfide in the treatment of TNBC could prove to be beneficial; however, there are many obstacles that will need to be overcome and addressed first. The major obstacle will be the delivery method of 5-hydroxy lansoprazole sulfide. Pharmacokinetic studies in mouse models will need to be utilized to determine the best route of administration, half-life, and elimination. Additionally, while lansoprazole has been FDA-approved, indicating there are acceptable side effects, its metabolite, 5-hydroxy lansoprazole sulfide, has not. Even though it seems counterintuitive that there would be additional side effects from 5-hydroxy lansoprazole sulfide over lansoprazole, that may not be the case. Only about 15-25% of lansoprazole is converted to the 5-hydroxylated metabolite and excreted in the urine [283, 284]. Therefore, a maximum tolerated dose will need to be determined to insure there are no ill effects from using 5-hydroxy lansoprazole sulfide at higher concentrations than are typically seen in the body when using parent compound lansoprazole. Once an effective administration route and MTD is determined, the effect of 5-hydroxy lansoprazole

sulfide treatment on TNBC will need to be assessed in xenograft mouse models of this disease.

The use of 5-hydroxy lansoprazole sulfide may also be an effective treatment strategy for cancer cells that have defects in other DNA repair pathways, such as mutations in BRAC1/2, leading to defects in the homologous repair mechanism. Due to the inhibition of NHEJ caused by 5-hydroxy lansoprazole sulfide, cells that have known defects in HR may be more sensitive to treatment and be susceptible to synthetic lethality. This has been observed in cells using PARP inhibitors [285]. For this reason, it may be important to look at the effect in other cancers. Furthermore, the synergistic effect of 5-hydroxy lansoprazole sulfide with current chemotherapy, doxorubicin, will need to be assessed. This can be done first in cell lines and, then, with promising results, could be moved into a mouse model of TNBC.

During experimentation, as shown in Figure 8, it was observed that there was a difference in response to lansoprazole and 5-hydroxy lansoprazole sulfide in TNBC but not in luminal A MCF7 cells. While it is unclear if this is due to differences between TNBC and luminal A type breast cancers, another intriguing possibility is differences in CYP enzymes within these cell lines. While CYP enzymes are mostly expressed in the liver, they are also expressed in cancer tissues. One study showed that there are differences in expression of CYP enzymes between paired benign and cancer tissues and that these changes may play a role in cancer cell survival by either eliminating toxins or preventing prodrugs from being converted to their active metabolite at the tumor site [286, 287]. Differences in expression profiles of CYPs in breast cancer showed that expression could

be clustered into different ethnic groups [288]. However, further studies are required to determine if this creates differences in clinical outcome. Studies have shown that changes in CYP2D6 efficiency has an effect on clinical outcomes of breast cancer patients. Tamoxifen is typically given as an antiestrogen in the case of estrogen receptor positive breast cancer [289]. While tamoxifen does have some activity against the estrogen receptor, its metabolite, endoxifen, formed from CYP3A4 and CYP2D6, is 100 times more potent [290]. Women with mutations in CYP2D6, which cause decreased activity, were more likely to have relapse of their breast cancer over those who showed normal activity of CYP2D6 [291]. Additionally, a retrospective study looking at the use of CYP2D6 inhibitors and tamoxifen treatment concluded that the benefits of tamoxifen were significantly decreased with concurrent use [292]. While we did not test the CYP profile in the cell lines used in this thesis, this might be a direction to take this research in the future. A genome-wide approach showed that there was an association between TNBC and CYP2C19 deletion [293]. It is possible that the CYP profile in TNBC differs from that in luminal A breast cancer cell lines. If this is the case, MCF7 may convert the parent compound to 5-hydroxy lansoprazole sulfide more efficiently than TNBC cell lines, creating a similar effect as the parent compound.

To test this possibility, it is important to first check the expression of different CYP's and also to determine if there are any mutations which might affect activity. While expression may not be changed there are known mutations that can increase or decrease CYP activity which will have an effect on drug conversion [294]. While this is one possibility for the difference in luminal A versus TNBC it may not be the only

explanation. 5-hydroxy lansoprazole sulfide may be more effective in TNBC because it is leading to synthetic lethality similar to that seen in cells with mutations in HR. This could be a factor in MDA-MB-436 and HCC1937 cell lines as both harbor a mutation in BRCA1. Additionally, some cell lines will exhibit a 'BRCAness' phenotype in which they display similar features of cells with mutations in BRCA1 but the exact cause of the phenotype may not be known [295]. While the two main cell lines used in this work, MDA-MB-231 and MDA-MB-468, do not carry any known mutations in HR pathway, studies have shown that treatment with specific agents can cause a conversion to a 'BRCAness' state [296-298]. This leaves the possibility that 5-hydroxy lansoprazole sulfide may also be affecting HR in TNBC and well as NHEJ leading to synthetic lethality. Furthermore, a study of TNBC 'BRCAness' in 3 different patient cohorts looked at BRCA1 mutation status, BRCA1 methylation patterns, and a specific BRCA-1 like pattern by comparative genomic hybridization found that the majority of TNBC exhibit a 'BRCAness' phenotype. Therefore, it is possible that TNBC is more sensitive to treatment due to this feature. The 'BRCAness' status in these cell lines after treatment with 5-hydroxy lansoprazole sulfide should therefore be assessed.

FASN regulation of PARP expression is a relatively new concept and has not been fully explored. While it is currently unknown how this may be occurring, there are a few possibilities. It is possible that the FASN molecule itself is somehow interacting with transcription factors involved in regulation of PARP such as SP1 [299], AP-2 [300], YY1 [301], and Ets [302]. It is also possible that FASN itself does not interact with these transcription factors, but, rather, its end-product, palmitate, could be affecting the

activity of one of these transcription factors. Further studies are necessary to determine how this phenomenon might occur. The first experiment to be performed to determine how this might be occurring would be to look at expression levels of these transcription factors when FASN is overexpressed and knocked down in different cells lines. Addition of a gene reporter activity assay for these promoters will indicate which transcription factors are activated by FASN overexpression and knockdown. A pull-down experiment could be used to see if FASN directly interacts with SP1, AP-2, YY1 or Ets. Furthermore, FASN may not directly interact with these transcription factors but rather, its end product, palmitate, could be used to modify these transcription factors increasing activity or affect its expression. One way to determine if regulation is occurring by end product starvation is to supplement the media with palmitate in cells with FASN inhibition to determine if this will reverse the observed decrease in PARP after FASN inhibition. Additionally, our previous paper indicates that FASN may also be affecting PARP expression by relieving NF- κ B inhibition on PARP transcription [128]. Therefore, NF- κ B expression and activity should also be assessed in the same way. These tests will also help to determine if FASN is not regulating PARP expression. It is possible that the decrease observed in PARP protein levels is due to PARP cleavage and not a decrease in expression. Additionally, while mRNA data indicates that PARP transcription is decreasing this could be caused by the late, 72-hour, analysis time. Cells that are being treated with drug are starting to die at 72 hours which would affect transcription and potentially that is why there was a decrease. These experiments should be run again at 24 and 48 hours to see if the same result is obtained.

Based on this data, it appears that 5-hydroxy lansoprazole sulfide prevents the repair of DNA DSBs potentially through regulation of PARP expression. If this is the case, while inhibition of DNA DSBs plays a role in cell death, a decrease in PARP expression can also affect other DNA repair pathways. PARP plays a significant role in single strand DNA break repair, base excision repair (BER), and nucleotide excision repair (NER) [303-305]. BER is typically utilized by cells to remove damage caused by oxidation, alkylation, and deamination [306]. These types of DNA lesions can occur via ROS, environmental factors, radiation, or a natural result of DNA decay [307]. On the other hand, NER removes bulky DNA lesions such as inter- and intra- DNA crosslinks created by UV irradiation and chemotherapeutics [308, 309]. While activity of these pathways was not tested, a decrease in PARP expression may not only be affecting NHEJ but also these other forms of DNA repair leading to increase in DNA damage, mutation, and cell death. It is possible that the increase in DNA DSBs observed after treatment of 5-hydroxy lansoprazole sulfide may be caused by cells not repairing damaged bases or removing bulky adducts.

One way in which DSBs can arise is through reactive oxygen species causing damage to DNA bases, which, when not repaired can be converted to DSBs during replication. While it is possible 5-hydroxy lansoprazole sulfide causes DNA damage via another mechanism it is clear that 5-hydroxy lansoprazole sulfide itself is not producing reactive oxygen species. It is also possible that 5-hydroxy lansoprazole sulfide does not produce DNA damage at all but rather the DNA damage is due to the inhibition of NHEJ repair. DSBs created by reactive oxygen species produced by normal metabolic activity

are unable to be repaired, leading to their accumulation. This could be due to ROS or it could be due to natural DNA decay failing to be repaired. Previous studies have indicated that cells with deficient NHEJ repair develop spontaneous DNA DSBs [310, 311]. DNA DSB can arise naturally in the cell by DNA decay or by the production of reactive oxygen species during normal metabolic processes [269, 312, 313]. In replicating MEFs, it has been shown that DNA damage caused by oxidative stress led to cellular senescence [314]. Cells with a defect in DNA repair pathways reached their replicative limit quicker than wild-type cells, implicating repair mechanisms as a way in which cells overcome oxidative damage. Oxidative stress still occurs in non-replicating cells. In MEFs and primary human fibroblasts defective in some aspect of NHEJ repair, there was an increased accumulation of γ H2AX over time [269]. To confirm cells with deficiencies in NHEJ repair did not have increase γ H2AX due to an increase in ROS, fibroblasts lacking glutathione synthetase were utilized as a positive control for ROS and oxidation of proteins was monitored. Cells with defects in NHEJ repair did not have an increase in oxidation of proteins as compared to control. This indicated that there is not an increase in ROS as compared to WT and suggests that the DNA damage is occurring due to the cells inability to repair damaged DNA. Additionally, the glutathione synthetase lacking fibroblasts did not have an increase in γ H2AX over time. This may be due to an active WT NHEJ repair pathway.

Furthermore, in addition to fibroblasts, neuronal cells that do not have a functioning NHEJ repair pathway begin to show an increase in chromosomal breaks over time. These lesions led to an apoptotic event [312]. Based on this data, it is possible that

the inhibition of NHEJ by 5-hydroxy lansoprazole sulfide leads to an increase in DNA DSBs due to the inability of these cells to repair damage caused by reactive oxygen species produced by normal cellular metabolic activity. This provides one possible explanation for the protective effect NAC has on both preventing DSBs, as indicated by γ H2AX, and against apoptosis in cells treated with 5-hydroxy lansoprazole sulfide. The NAC may protect cells against reactive oxygen species produced during normal metabolic activity.

It is also possible that 5-hydroxy lansoprazole sulfide is leading to DNA damage via other means, and reactive oxygen scavenger NAC is protective in some other way. For example, ROS have also been implicated in mediating apoptosis within cells. Cell death by apoptosis can be triggered by things like DNA damage, ROS, hypoxia, and heat shock [315]. Specifically, ROS has been shown to induce apoptosis through both intrinsic and extrinsic pathways [316]. ROS can lead to activation of p53 and, ultimately, to an increase in pro-apoptotic bcl-2 proteins, as well as causing oxidation of cardiolipin releasing cytochrome C and causing mitochondrial depolarization. Additionally, ROS can activate death receptors on the membrane, leading to apoptosis through the extrinsic pathway [317]. NAC could also have a protective effect in cells by preventing activation of these pathways by ROS scavenging and not just by preventing DNA damage. Additionally, NAC has a reactive thiol group that could also be interacting with 5-hydroxy lansoprazole sulfide preventing its antitumor activities [318]. In this way NAC helps to prevent DNA damage and apoptosis by inactivating 5-hydroxy lansoprazole sulfide rather than by reducing ROS. To determine if this inactivation is in fact occurring,

a nonthiol antioxidant could be utilized to see if the same results are obtained for DNA damage and apoptosis. These antioxidants include MnTBAP, butylated hydroxyanisole, mannitol, and Trolox.

There were observed differences in cancer cells versus benign epithelial cell lines in terms of DNA damage caused and IC₅₀ values. Benign epithelial cell lines did not have an induction of γ H2AX and there was about a 2.5-fold increase in IC₅₀ to 5-hydroxy lansoprazole sulfide. Due to the inhibition of FASN by 5-hydroxy lansoprazole sulfide, the differences observed between cancer and benign cells may be caused by differences in metabolic activities within these cells. It is known that cancer cells take up a large amount of glucose and utilize this glucose in anaerobic respiration to produce energy, while non-cancerous cells utilize aerobic respiration. These differences in metabolic activity could account for differences in reactive oxygen species and the amount of DNA damage produced when cells are treated with 5-hydroxy lansoprazole sulfide.

Section 4.B: CC-115

In this study, we showed that ABCG2 expression plays a major role in CC-115 resistance by reducing its intracellular accumulation and its inhibition of mTOR pathway. ABCB1, to a lesser extent, may also contribute to CC-115 resistance via a similar mechanism. Clearly, CC-115 may be a substrate of multiple ABC transporters, and reduced clinical responses are expected in patients that express any of these ABC transporters.

Based on these findings, it is tempting to speculate that ABCG2 and ABCB1 may be utilized as markers to stratify patients into treatment groups for future clinical trials.

The observed variability in CLL patient response in a past trial may possibly be due to different expression of ABCG2 or ABCB1. Previously, it has been found that ABCG2 and ABCB1 are expressed in leukemia patients by comparing expression levels in cancer patients and healthy donor controls. Their expression influences the outcome of these patients who were subjected to chemotherapy [319-321]. Currently, there is an ongoing clinical trial of CC-115 for glioblastoma. However, it is also well known that ABCG2 and ABCB1 are both highly expressed in the endothelial cells of the blood brain barrier preventing drug entry [236], which may affect the outcome of this trial. Unfortunately, there are no FDA-approved drugs to target ABCG2 or ABCB1, due to neurotoxicity, low specificity, and unachievable clinical IC₅₀ [322]. While FTC cannot be used in the clinic due to neurotoxicity, C8 has not moved passed *in vitro* studies [259]. Further *in vivo* studies would need to be conducted to access pharmacokinetic properties before testing in a clinical setting. Lack of clinically available inhibitors limits combined treatment strategies for patients with ABCG2 or ABCB1 overexpression and efforts have shifted to produce new treatments that are not substrates for these efflux pumps [323].

Despite the fact that FASN up-regulates DNA-PK activity [229], FASN over-expression does not appear to contribute to cellular resistance to the DNA-PK inhibitory activity of CC-115 or a DNA-PK selective inhibitor, NU7441. We have proven that FASN over-expression causes resistance to DNA damaging drugs [126] and inhibitors of PARP1 (manuscript submitted), a mediator of FASN-induced up-regulation of DNA-PK activity [229]. Although it remains to be determined, the failure of FASN over-expression in resistance to DNA-PK inhibition may be due to the fact that FASN overexpression only

leads to an increase in activity and not expression of DNA-PK, which may be insufficient to overcome the effect of DNA-PK inhibition.

Future Directions

Based on this work, there are a few directions and loose ends that should be addressed. First, as discussed above, the expression levels of CYP3A4 and CYP2C19 may be able to explain the difference in sensitivity to lansoprazole and 5-hydroxy lansoprazole sulfide. Knowing this information in a patient population can help to predict the most effective treatment strategy. Second, while this thesis shows that 5-hydroxy lansoprazole sulfide causes apoptosis, the exact mechanism of how this is occurring is still unknown. It is also possible that 5-hydroxy lansoprazole sulfide is causing cell death through other pathways such as necroptosis. In the case of apoptosis, it would be interesting to see if the DNA damage created by 5-hydroxy lansoprazole sulfide is causing activation of p53 and, then, when cells are unable to repair DNA, there is a upregulation of pro-apoptotic proteins such as Bak and Bax [324]. Expression of these pro-apoptotic proteins could be the mechanism behind apoptosis caused by 5-hydroxy lansoprazole sulfide inducing mitochondrial permeabilization and release of cytochrome C. However, it is also known that p53 is frequently mutated in TNBC [325, 326], as is the case for the TNBC cell lines used in this thesis. It does not rule out the possibility that p53 family members, such as p73, are activated in place of p53 itself, which has been shown in the literature.

Another possibility is that FASN inhibition effects cellular membranes, leading to dysfunction of the mitochondria and release of cytochrome C, resulting in apoptosis. A

previous paper had shown that knockdown of FASN led to mitochondrial impairment and apoptosis [129]. Inhibition of FASN by 5-hydroxy lansoprazole sulfide could alter the membrane make-up of the mitochondrial membrane, leaving cells susceptible to apoptosis. A previous study revealed that inhibition of FASN led to activation of the intrinsic apoptosis pathway, with release of cytochrome c and activation of caspase 3, independent of p53, and mitochondrial permeability transition by altering fatty acid composition of the mitochondrial membrane [327, 328].

Additionally, is apoptosis caused by 5-hydroxy lansoprazole sulfide completely caspase dependent? Or, are there additional pathways that are activated and culminate in cell death? While this thesis indicates that ROS is playing a role in DNA damage, as 5 mM NAC treatment reduced γ H2AX, it is not clear if ROS is playing another role in reversing apoptosis outside of DNA damage response. Further studies are needed to elucidate whether one or a combined effort of these two mechanisms are leading to apoptosis by 5-hydroxy lansoprazole sulfide.

Necroptosis is another form of cell death that could be occurring after treatment with 5-hydroxy lansoprazole sulfide. The flow cytometry graphs in Figures 11, 12 and 18 indicate that treatment with 5-hydroxy lansoprazole sulfide causes cells to be in late apoptosis or necrotic state. This could indicate that cells are going through not just apoptosis but also necroptosis. Necroptosis is another form of programmed cell death. The main players in cell death by necroptosis are RIPK3 and MLKL [329]. Activation of necroptosis is caspase independent and mimics necrosis [330, 331].

To determine what role apoptosis and necroptosis are playing in cell death caused by 5-hydroxy lansoprazole sulfide the first experiments to answer this question would be to inhibit activation of caspases using a pan-caspase inhibitor and determine if cell death is still occurring. If cells are continuing to die even in the presence of caspase inhibitors it would indicate that cell death is caspase independent and likely occurring through another mechanism. To test for necroptosis cells can be treated with RIPK1 inhibitor necrostatin-1 [330]. RIPK1 is upstream of RIPK3 activation and inhibition of RIPK1 will inhibit the process of necroptosis [329]. In this way necroptosis and apoptosis can be analyzed to determine their contribution to cell death by 5-hydroxy lansoprazole sulfide.

Inhibition of FASN by 5-hydroxy lansoprazole sulfide may also affect other cellular membranes besides the mitochondrial membrane. Will 5-hydroxy lansoprazole sulfide also affect the fluidity of the membrane and increase penetrance of chemotherapeutic drugs as seen previously by inhibiting ACC and FASN [127]? As discussed briefly above, will 5-hydroxy lansoprazole sulfide have a synergistic effect when used in combination with not only doxorubicin, but also with other DNA damaging agents? With the known role of 5-hydroxy lansoprazole sulfide inhibition of NHEJ repair and the potential ability of FASN inhibition to increase drug penetrance, the implications for future treatment strategies could be significant. To proceed in this direction, these pathways and possibilities need further investigation. Moving forward, a mouse model of disease will need to be used to determine effect *in vivo* and to identify if combination therapy is effective. To determine the effect that 5-hydroxy lansoprazole sulfide has on

cellular membranes mass spectrometry can be utilized to analyze the composition of lipids in specific membranes, as was done by Zecchin et al. to analyze the composition change in the mitochondria membrane of melanoma cells after orlistat treatment [327]. Additionally, since FASN inhibition affects lipid raft formation, lipid rafts on the membrane can be analyzed using fluorescent glycol chitosan derivatives [332]. Affecting lipid raft formations could have significant implications in cell signaling and survival.

Due to the decrease in PARP expression and its role in DNA repair, will overexpression of PARP reverse some of the effects observed by 5-hydroxy lansoprazole sulfide? This experiment would help to determine the exact mechanism of how 5-hydroxy lansoprazole sulfide is leading to cell death. If DNA damage is an important factor in cell death by 5-hydroxy lansoprazole sulfide then an increase in expression of PARP should increase NHEJ repair and decrease DNA damage as was seen previously [128]. If PARP overexpression increases NHEJ and reduces DNA damage but cell death is still occurring another mechanism, such as changes in cellular membrane structures may be the driving force for cell death. These experiments will also help to determine if PARP is truly being decreased by treatment or if the decrease is caused by an increase in cleavage. If PARP overexpression can reverse damage and apoptosis it could indicate that PARP is being decreased by treatment. If, however, it cannot reverse damage and apoptosis it may indicate that PARP is being cleaved leading to cell death and that the observed decrease is actually due to cleavage and not down regulation. Furthermore, inhibition of NHEJ repair by 5-hydroxy lansoprazole sulfide may be an effective way to treat cancers with defects in other DNA repair pathways, as discussed briefly above.

Expanding these findings to other cancers that may have these same defects or overexpression of FASN may lead to advanced treatments.

Lastly, there are several ways in which the above thesis could be improved. The first being that several of these experiments used a set concentration of drug during experimentation. While this is an effective way to show differences in the treatment groups it is not necessarily the best. It does not provide a way to easily correlate cytotoxic effects with DNA damage and cleavage of proteins. It is difficult to normalize findings and directly compare efficacy of the treatment groups and control. In the future it would be a good idea to use IC_{25} , IC_{50} , and IC_{75} values for each treatment. In this way it is much easier to compare the effect each drug is having at comparable concentrations and correlate cytotoxicity to the observed effects. The use of multiple types of reactive oxygen species scavengers to assess the effect on DNA damage and apoptosis should have been used in order to rule out the possibility that NAC is reacting with 5-hydroxy lansoprazole sulfide. Additionally, other assays should be utilized to confirm FASN inhibition. These assays include binding assays, FASN activity assays, and more specifically activity assays assessing the TE domain of FASN. While the decrease in free fatty acids indicates that 5-hydroxy lansoprazole sulfide is inhibiting FASN it does not confirm how this is occurring. Experiments determining how 5-hydroxy lansoprazole sulfide is affecting other DNA repair pathways may also provide insight into how DNA damage and apoptosis are occurring.

REFERENCES

1. Hanahan, D. and R.A. Weinberg, *The hallmarks of cancer*. Cell, 2000. **100**(1): p. 57-70.
2. Bougie, O. and J.I. Weberpals, *Clinical Considerations of BRCA1- and BRCA2-Mutation Carriers: A Review*. Int J Surg Oncol, 2011. **2011**: p. 374012.
3. Peshkin, B.N., M.L. Alabek, and C. Isaacs, *BRCA1/2 mutations and triple negative breast cancers*. Breast Dis, 2010. **32**(1-2): p. 25-33.
4. Carriaga, M.T. and D.E. Henson, *The histologic grading of cancer*. Cancer, 1995. **75**(1 Suppl): p. 406-21.
5. Rakha, E.A., J.S. Reis-Filho, F. Baehner, et al., *Breast cancer prognostic classification in the molecular era: the role of histological grade*. Breast Cancer Res, 2010. **12**(4): p. 207.
6. Cianfrocca, M. and L.J. Goldstein, *Prognostic and predictive factors in early-stage breast cancer*. Oncologist, 2004. **9**(6): p. 606-16.
7. Feng, Y., M. Spezia, S. Huang, et al., *Breast cancer development and progression: Risk factors, cancer stem cells, signaling pathways, genomics, and molecular pathogenesis*. Genes Dis, 2018. **5**(2): p. 77-106.
8. Khamis, Z.I., Z.J. Sahab, and Q.X. Sang, *Active roles of tumor stroma in breast cancer metastasis*. Int J Breast Cancer, 2012. **2012**: p. 574025.
9. Easton, D.F., *The inherited component of cancer*. Br Med Bull, 1994. **50**(3): p. 527-35.
10. Hulka, B.S., *Epidemiology of susceptibility to breast cancer*. Prog Clin Biol Res, 1996. **395**: p. 159-74.
11. Campbell, I.G., S.E. Russell, D.Y. Choong, et al., *Mutation of the PIK3CA gene in ovarian and breast cancer*. Cancer Res, 2004. **64**(21): p. 7678-81.
12. de Jong, M.M., I.M. Nolte, G.J. te Meerman, et al., *Genes other than BRCA1 and BRCA2 involved in breast cancer susceptibility*. J Med Genet, 2002. **39**(4): p. 225-42.
13. Karsli-Ceppioglu, S., et al., *Epigenetic mechanisms of breast cancer: an update of the current knowledge*. Epigenomics, 2014. **6**(6): p. 651+.
14. Martin-Sanchez, E., S. Mendaza, A. Ulazia-Garmendia, et al., *CHL1 hypermethylation as a potential biomarker of poor prognosis in breast cancer*. Oncotarget, 2017. **8**(9): p. 15789-15801.
15. Stirzaker, C., E. Zotenko, J.Z. Song, et al., *Methylome sequencing in triple-negative breast cancer reveals distinct methylation clusters with prognostic value*. Nat Commun, 2015. **6**: p. 5899.
16. Pasculli, B., R. Barbano, and P. Parrella, *Epigenetics of breast cancer: Biology and clinical implication in the era of precision medicine*. Semin Cancer Biol, 2018. **51**: p. 22-35.
17. Byler, S., S. Goldgar, S. Heerboth, et al., *Genetic and epigenetic aspects of breast cancer progression and therapy*. Anticancer Res, 2014. **34**(3): p. 1071-7.

18. Severi, G., M.C. Southey, D.R. English, et al., *Epigenome-wide methylation in DNA from peripheral blood as a marker of risk for breast cancer*. Breast Cancer Res Treat, 2014. **148**(3): p. 665-73.
19. Fleischer, T., A. Frigessi, K.C. Johnson, et al., *Genome-wide DNA methylation profiles in progression to in situ and invasive carcinoma of the breast with impact on gene transcription and prognosis*. Genome Biol, 2014. **15**(8): p. 435.
20. Bediaga, N.G., A. Acha-Sagredo, I. Guerra, et al., *DNA methylation epigenotypes in breast cancer molecular subtypes*. Breast Cancer Res, 2010. **12**(5): p. R77.
21. Parrella, P., M.L. Poeta, A.P. Gallo, et al., *Nonrandom distribution of aberrant promoter methylation of cancer-related genes in sporadic breast tumors*. Clin Cancer Res, 2004. **10**(16): p. 5349-54.
22. van Hoesel, A.Q., C.J. van de Velde, P.J. Kuppen, et al., *Hypomethylation of LINE-1 in primary tumor has poor prognosis in young breast cancer patients: a retrospective cohort study*. Breast Cancer Res Treat, 2012. **134**(3): p. 1103-14.
23. Hoque, M.O., M. Prencipe, M.L. Poeta, et al., *Changes in CpG islands promoter methylation patterns during ductal breast carcinoma progression*. Cancer Epidemiol Biomarkers Prev, 2009. **18**(10): p. 2694-700.
24. Temian, D.C., L.A. Pop, A.I. Irimie, et al., *The Epigenetics of Triple-Negative and Basal-Like Breast Cancer: Current Knowledge*. J Breast Cancer, 2018. **21**(3): p. 233-243.
25. Bannister, A.J. and T. Kouzarides, *Regulation of chromatin by histone modifications*. Cell Res, 2011. **21**(3): p. 381-95.
26. Messier, T.L., J.A. Gordon, J.R. Boyd, et al., *Histone H3 lysine 4 acetylation and methylation dynamics define breast cancer subtypes*. Oncotarget, 2016. **7**(5): p. 5094-109.
27. Chen, X., H. Hu, L. He, et al., *A novel subtype classification and risk of breast cancer by histone modification profiling*. Breast Cancer Res Treat, 2016. **157**(2): p. 267-279.
28. Sotiriou, C. and L. Pusztai, *Gene-expression signatures in breast cancer*. N Engl J Med, 2009. **360**(8): p. 790-800.
29. Russnes, H.G., O.C. Lingjaerde, A.L. Borresen-Dale, et al., *Breast Cancer Molecular Stratification: From Intrinsic Subtypes to Integrative Clusters*. Am J Pathol, 2017. **187**(10): p. 2152-2162.
30. Chin, K., S. DeVries, J. Fridlyand, et al., *Genomic and transcriptional aberrations linked to breast cancer pathophysiologies*. Cancer Cell, 2006. **10**(6): p. 529-41.
31. Chin, S.F., A.E. Teschendorff, J.C. Marioni, et al., *High-resolution aCGH and expression profiling identifies a novel genomic subtype of ER negative breast cancer*. Genome Biol, 2007. **8**(10): p. R215.
32. Weigelt, B., F.C. Geyer, and J.S. Reis-Filho, *Histological types of breast cancer: how special are they?* Mol Oncol, 2010. **4**(3): p. 192-208.
33. Creighton, C.J., *The molecular profile of luminal B breast cancer*. Biologics, 2012. **6**: p. 289-97.
34. Yersal, O. and S. Barutca, *Biological subtypes of breast cancer: Prognostic and therapeutic implications*. World J Clin Oncol, 2014. **5**(3): p. 412-24.

35. Tong, C.W.S., M. Wu, W.C.S. Cho, et al., *Recent Advances in the Treatment of Breast Cancer*. Front Oncol, 2018. **8**: p. 227.
36. Waks, A.G. and E.P. Winer, *Breast Cancer Treatment: A Review*. JAMA, 2019. **321**(3): p. 288-300.
37. Yager, J.D. and N.E. Davidson, *Estrogen carcinogenesis in breast cancer*. N Engl J Med, 2006. **354**(3): p. 270-82.
38. Tran, B. and P.L. Bedard, *Luminal-B breast cancer and novel therapeutic targets*. Breast Cancer Res, 2011. **13**(6): p. 221.
39. Li, Z.H., P.H. Hu, J.H. Tu, et al., *Luminal B breast cancer: patterns of recurrence and clinical outcome*. Oncotarget, 2016. **7**(40): p. 65024-65033.
40. Roskoski, R., Jr., *The ErbB/HER family of protein-tyrosine kinases and cancer*. Pharmacol Res, 2014. **79**: p. 34-74.
41. Appert-Collin, A., P. Hubert, G. Cremel, et al., *Role of ErbB Receptors in Cancer Cell Migration and Invasion*. Front Pharmacol, 2015. **6**: p. 283.
42. Ghosh, R., A. Narasanna, S.E. Wang, et al., *Trastuzumab has preferential activity against breast cancers driven by HER2 homodimers*. Cancer Res, 2011. **71**(5): p. 1871-82.
43. Krishnamurti, U. and J.F. Silverman, *HER2 in breast cancer: a review and update*. Adv Anat Pathol, 2014. **21**(2): p. 100-7.
44. Kallioniemi, O.P., A. Kallioniemi, W. Kurisu, et al., *ERBB2 amplification in breast cancer analyzed by fluorescence in situ hybridization*. Proc Natl Acad Sci U S A, 1992. **89**(12): p. 5321-5.
45. Slamon, D.J., G.M. Clark, S.G. Wong, et al., *Human breast cancer: correlation of relapse and survival with amplification of the HER-2/neu oncogene*. Science, 1987. **235**(4785): p. 177-82.
46. Goldenberg, M.M., *Trastuzumab, a recombinant DNA-derived humanized monoclonal antibody, a novel agent for the treatment of metastatic breast cancer*. Clin Ther, 1999. **21**(2): p. 309-18.
47. von Minckwitz, G., C.S. Huang, M.S. Mano, et al., *Trastuzumab Emtansine for Residual Invasive HER2-Positive Breast Cancer*. N Engl J Med, 2018.
48. Memon, A.A., B.S. Sorensen, P. Melgard, et al., *Expression of HER3, HER4 and their ligand heregulin-4 is associated with better survival in bladder cancer patients*. Br J Cancer, 2004. **91**(12): p. 2034-41.
49. Arkhipov, A., Y. Shan, E.T. Kim, et al., *Her2 activation mechanism reflects evolutionary preservation of asymmetric ectodomain dimers in the human EGFR family*. Elife, 2013. **2**: p. e00708.
50. Shi, Y., J. Jin, W. Ji, et al., *Therapeutic landscape in mutational triple negative breast cancer*. Mol Cancer, 2018. **17**(1): p. 99.
51. Changavi, A.A., A. Shashikala, and A.S. Ramji, *Epidermal Growth Factor Receptor Expression in Triple Negative and Nontriple Negative Breast Carcinomas*. J Lab Physicians, 2015. **7**(2): p. 79-83.
52. Nakai, K., M.C. Hung, and H. Yamaguchi, *A perspective on anti-EGFR therapies targeting triple-negative breast cancer*. Am J Cancer Res, 2016. **6**(8): p. 1609-23.

53. Foulkes, W.D., I.E. Smith, and J.S. Reis-Filho, *Triple-negative breast cancer*. N Engl J Med, 2010. **363**(20): p. 1938-48.
54. Wright, W.D., S.S. Shah, and W.D. Heyer, *Homologous recombination and the repair of DNA double-strand breaks*. J Biol Chem, 2018. **293**(27): p. 10524-10535.
55. Chang, H.H.Y., N.R. Pannunzio, N. Adachi, et al., *Non-homologous DNA end joining and alternative pathways to double-strand break repair*. Nat Rev Mol Cell Biol, 2017. **18**(8): p. 495-506.
56. Byrski, T., T. Huzarski, R. Dent, et al., *Response to neoadjuvant therapy with cisplatin in BRCA1-positive breast cancer patients*. Breast Cancer Res Treat, 2009. **115**(2): p. 359-63.
57. Kuhajda, F.P., S. Piantadosi, and G.R. Pasternack, *Haptoglobin-related protein (Hpr) epitopes in breast cancer as a predictor of recurrence of the disease*. N Engl J Med, 1989. **321**(10): p. 636-41.
58. Shurbaji, M.S., F.P. Kuhajda, G.R. Pasternack, et al., *Expression of oncogenic antigen 519 (OA-519) in prostate cancer is a potential prognostic indicator*. Am J Clin Pathol, 1992. **97**(5): p. 686-91.
59. Shurbaji, M.S., J.H. Kalbfleisch, and T.S. Thurmond, *Immunohistochemical detection of a fatty acid synthase (OA-519) as a predictor of progression of prostate cancer*. Hum Pathol, 1996. **27**(9): p. 917-21.
60. Jensen, V., M. Ladekarl, P. Holm-Nielsen, et al., *The prognostic value of oncogenic antigen 519 (OA-519) expression and proliferative activity detected by antibody MIB-1 in node-negative breast cancer*. J Pathol, 1995. **176**(4): p. 343-52.
61. Gansler, T.S., W. Hardman, 3rd, D.A. Hunt, et al., *Increased expression of fatty acid synthase (OA-519) in ovarian neoplasms predicts shorter survival*. Hum Pathol, 1997. **28**(6): p. 686-92.
62. Kuhajda, F.P., K. Jenner, F.D. Wood, et al., *Fatty acid synthesis: a potential selective target for antineoplastic therapy*. Proc Natl Acad Sci U S A, 1994. **91**(14): p. 6379-83.
63. Kuhajda, F.P., *Fatty-acid synthase and human cancer: new perspectives on its role in tumor biology*. Nutrition, 2000. **16**(3): p. 202-8.
64. Ookhtens, M., R. Kannan, I. Lyon, et al., *Liver and adipose tissue contributions to newly formed fatty acids in an ascites tumor*. Am J Physiol, 1984. **247**(1 Pt 2): p. R146-53.
65. Akram, M., *Citric acid cycle and role of its intermediates in metabolism*. Cell Biochem Biophys, 2014. **68**(3): p. 475-8.
66. Kersten, S., *Mechanisms of nutritional and hormonal regulation of lipogenesis*. EMBO Rep, 2001. **2**(4): p. 282-6.
67. Hellerstein, M.K., *De novo lipogenesis in humans: metabolic and regulatory aspects*. Eur J Clin Nutr, 1999. **53 Suppl 1**: p. S53-65.
68. Houten, S.M. and R.J. Wanders, *A general introduction to the biochemistry of mitochondrial fatty acid beta-oxidation*. J Inherit Metab Dis, 2010. **33**(5): p. 469-77.
69. Tong, L., *Acetyl-coenzyme A carboxylase: crucial metabolic enzyme and attractive target for drug discovery*. Cell Mol Life Sci, 2005. **62**(16): p. 1784-803.

70. Smith, S., *The animal fatty acid synthase: one gene, one polypeptide, seven enzymes*. FASEB J, 1994. **8**(15): p. 1248-59.
71. Wakil, S.J., J.K. Stoops, and V.C. Joshi, *Fatty acid synthesis and its regulation*. Annu Rev Biochem, 1983. **52**: p. 537-79.
72. Wakil, S.J., *Fatty acid synthase, a proficient multifunctional enzyme*. Biochemistry, 1989. **28**(11): p. 4523-30.
73. Hudgins, L.C., M. Hellerstein, C. Seidman, et al., *Human fatty acid synthesis is stimulated by a eucaloric low fat, high carbohydrate diet*. J Clin Invest, 1996. **97**(9): p. 2081-91.
74. Guan, X. and C.A. Fierke, *Understanding Protein Palmitoylation: Biological Significance and Enzymology*. Sci China Chem, 2011. **54**(12): p. 1888-1897.
75. Iwanaga, T., R. Tsutsumi, J. Noritake, et al., *Dynamic protein palmitoylation in cellular signaling*. Prog Lipid Res, 2009. **48**(3-4): p. 117-27.
76. Conibear, E. and N.G. Davis, *Palmitoylation and depalmitoylation dynamics at a glance*. J Cell Sci, 2010. **123**(Pt 23): p. 4007-10.
77. Sprecher, H., D.L. Luthria, B.S. Mohammed, et al., *Reevaluation of the pathways for the biosynthesis of polyunsaturated fatty acids*. J Lipid Res, 1995. **36**(12): p. 2471-7.
78. Leonard, A.E., S.L. Pereira, H. Sprecher, et al., *Elongation of long-chain fatty acids*. Prog Lipid Res, 2004. **43**(1): p. 36-54.
79. Joseph, S.B., B.A. Laffitte, P.H. Patel, et al., *Direct and indirect mechanisms for regulation of fatty acid synthase gene expression by liver X receptors*. J Biol Chem, 2002. **277**(13): p. 11019-25.
80. Foretz, M., C. Guichard, P. Ferre, et al., *Sterol regulatory element binding protein-1c is a major mediator of insulin action on the hepatic expression of glucokinase and lipogenesis-related genes*. Proc Natl Acad Sci U S A, 1999. **96**(22): p. 12737-42.
81. Shimomura, I., Y. Bashmakov, S. Ikemoto, et al., *Insulin selectively increases SREBP-1c mRNA in the livers of rats with streptozotocin-induced diabetes*. Proc Natl Acad Sci U S A, 1999. **96**(24): p. 13656-61.
82. Foretz, M., C. Pacot, I. Dugail, et al., *ADD1/SREBP-1c is required in the activation of hepatic lipogenic gene expression by glucose*. Mol Cell Biol, 1999. **19**(5): p. 3760-8.
83. Espenshade, P.J., *SREBPs: sterol-regulated transcription factors*. J Cell Sci, 2006. **119**(Pt 6): p. 973-6.
84. Rawson, R.B., *The SREBP pathway--insights from Insigs and insects*. Nat Rev Mol Cell Biol, 2003. **4**(8): p. 631-40.
85. Brownsey, R.W., A.N. Boone, J.E. Elliott, et al., *Regulation of acetyl-CoA carboxylase*. Biochem Soc Trans, 2006. **34**(Pt 2): p. 223-7.
86. Mihaylova, M.M. and R.J. Shaw, *The AMPK signalling pathway coordinates cell growth, autophagy and metabolism*. Nature Cell Biology, 2011. **13**: p. 1016.
87. Munday, M.R., *Regulation of mammalian acetyl-CoA carboxylase*. Biochem Soc Trans, 2002. **30**(Pt 6): p. 1059-64.

88. Weiss, L., G.E. Hoffmann, R. Schreiber, et al., *Fatty-acid biosynthesis in man, a pathway of minor importance. Purification, optimal assay conditions, and organ distribution of fatty-acid synthase*. Biol Chem Hoppe Seyler, 1986. **367**(9): p. 905-12.
89. Kusakabe, T., M. Maeda, N. Hoshi, et al., *Fatty Acid Synthase Is Expressed Mainly in Adult Hormone-sensitive Cells or Cells with High Lipid Metabolism and in Proliferating Fetal Cells*. 2000. **48**(5): p. 613-622.
90. Aarsland, A., D. Chinkes, and R.R. Wolfe, *Hepatic and whole-body fat synthesis in humans during carbohydrate overfeeding*. Am J Clin Nutr, 1997. **65**(6): p. 1774-82.
91. Chascione, C., D.H. Elwyn, M. Davila, et al., *Effect of carbohydrate intake on de novo lipogenesis in human adipose tissue*. Am J Physiol, 1987. **253**(6 Pt 1): p. E664-9.
92. Anderson, S.M., M.C. Rudolph, J.L. McManaman, et al., *Key stages in mammary gland development. Secretory activation in the mammary gland: it's not just about milk protein synthesis!* Breast Cancer Res, 2007. **9**(1): p. 204.
93. Pizer, E.S., R.J. Kurman, G.R. Pasternack, et al., *Expression of fatty acid synthase is closely linked to proliferation and stromal decidualization in cycling endometrium*. Int J Gynecol Pathol, 1997. **16**(1): p. 45-51.
94. Chirala, S.S., H. Chang, M. Matzuk, et al., *Fatty acid synthesis is essential in embryonic development: fatty acid synthase null mutants and most of the heterozygotes die in utero*. Proc Natl Acad Sci U S A, 2003. **100**(11): p. 6358-63.
95. Wagle, S., A. Bui, P.L. Ballard, et al., *Hormonal regulation and cellular localization of fatty acid synthase in human fetal lung*. Am J Physiol, 1999. **277**(2): p. L381-90.
96. Vander Heiden, M.G., L.C. Cantley, and C.B. Thompson, *Understanding the Warburg effect: the metabolic requirements of cell proliferation*. Science, 2009. **324**(5930): p. 1029-33.
97. Warburg, O., *The Metabolism of Carcinoma Cells*. 1925. **9**(1): p. 148-163.
98. Shestov, A.A., X. Liu, Z. Ser, et al., *Quantitative determinants of aerobic glycolysis identify flux through the enzyme GAPDH as a limiting step*. Elife, 2014. **3**.
99. Patra, K.C. and N. Hay, *The pentose phosphate pathway and cancer*. Trends Biochem Sci, 2014. **39**(8): p. 347-54.
100. Jiang, P., W. Du, and M. Wu, *Regulation of the pentose phosphate pathway in cancer*. Protein Cell, 2014. **5**(8): p. 592-602.
101. Swinnen, J.V., P.P. Van Veldhoven, L. Timmermans, et al., *Fatty acid synthase drives the synthesis of phospholipids partitioning into detergent-resistant membrane microdomains*. Biochem Biophys Res Commun, 2003. **302**(4): p. 898-903.
102. Heemers, H., B. Maes, F. Foufelle, et al., *Androgens stimulate lipogenic gene expression in prostate cancer cells by activation of the sterol regulatory element-binding protein cleavage activating protein/sterol regulatory element-binding protein pathway*. Mol Endocrinol, 2001. **15**(10): p. 1817-28.
103. Swinnen, J.V., W. Ulrix, W. Heyns, et al., *Coordinate regulation of lipogenic gene expression by androgens: evidence for a cascade mechanism involving sterol*

- regulatory element binding proteins*. Proc Natl Acad Sci U S A, 1997. **94**(24): p. 12975-80.
104. Van de Sande, T., E. De Schrijver, W. Heyns, et al., *Role of the phosphatidylinositol 3'-kinase/PTEN/Akt kinase pathway in the overexpression of fatty acid synthase in LNCaP prostate cancer cells*. Cancer Res, 2002. **62**(3): p. 642-6.
 105. Yang, Y.A., W.F. Han, P.J. Morin, et al., *Activation of fatty acid synthesis during neoplastic transformation: role of mitogen-activated protein kinase and phosphatidylinositol 3-kinase*. Exp Cell Res, 2002. **279**(1): p. 80-90.
 106. Bandyopadhyay, S., S.K. Pai, M. Watabe, et al., *FAS expression inversely correlates with PTEN level in prostate cancer and a PI 3-kinase inhibitor synergizes with FAS siRNA to induce apoptosis*. Oncogene, 2005. **24**(34): p. 5389-95.
 107. Cheng, C.S., Z. Wang, and J. Chen, *Targeting FASN in Breast Cancer and the Discovery of Promising Inhibitors from Natural Products Derived from Traditional Chinese Medicine*. Evid Based Complement Alternat Med, 2014. **2014**: p. 232946.
 108. Chen, T., L. Zhou, H. Li, et al., *Fatty acid synthase affects expression of ErbB receptors in epithelial to mesenchymal transition of breast cancer cells and invasive ductal carcinoma*. Oncol Lett, 2017. **14**(5): p. 5934-5946.
 109. Bollu, L.R., R.R. Katreddy, A.M. Blessing, et al., *Intracellular activation of EGFR by fatty acid synthase dependent palmitoylation*. Oncotarget, 2015. **6**(33): p. 34992-5003.
 110. Shah, U.S., R. Dhir, S.M. Gollin, et al., *Fatty acid synthase gene overexpression and copy number gain in prostate adenocarcinoma*. Hum Pathol, 2006. **37**(4): p. 401-9.
 111. Buckley, D., G. Duke, T.S. Heuer, et al., *Fatty acid synthase - Modern tumor cell biology insights into a classical oncology target*. Pharmacol Ther, 2017. **177**: p. 23-31.
 112. Crispino, P., P.L. Alo, M. Rivera, et al., *Evaluation of fatty acid synthase expression in oesophageal mucosa of patients with oesophagitis, Barrett's oesophagus and adenocarcinoma*. J Cancer Res Clin Oncol, 2009. **135**(11): p. 1533-41.
 113. Myers, R.B., D.K. Oelschlager, H.L. Weiss, et al., *Fatty acid synthase: an early molecular marker of progression of prostatic adenocarcinoma to androgen independence*. J Urol, 2001. **165**(3): p. 1027-32.
 114. Rashid, A., E.S. Pizer, M. Moga, et al., *Elevated expression of fatty acid synthase and fatty acid synthetic activity in colorectal neoplasia*. Am J Pathol, 1997. **150**(1): p. 201-8.
 115. Milgram, L.Z., L.A. Witters, G.R. Pasternack, et al., *Enzymes of the fatty acid synthesis pathway are highly expressed in in situ breast carcinoma*. Clin Cancer Res, 1997. **3**(11): p. 2115-20.
 116. Menendez, J.A., J.P. Decker, and R. Lupu, *In support of fatty acid synthase (FAS) as a metabolic oncogene: extracellular acidosis acts in an epigenetic fashion activating FAS gene expression in cancer cells*. J Cell Biochem, 2005. **94**(1): p. 1-4.

117. Vazquez-Martin, A., R. Colomer, J. Brunet, et al., *Overexpression of fatty acid synthase gene activates HER1/HER2 tyrosine kinase receptors in human breast epithelial cells*. Cell Prolif, 2008. **41**(1): p. 59-85.
118. Gonzalez-Guerrico, A.M., I. Espinoza, B. Schroeder, et al., *Suppression of endogenous lipogenesis induces reversion of the malignant phenotype and normalized differentiation in breast cancer*. Oncotarget, 2016. **7**(44): p. 71151-71168.
119. Fiorentino, M., G. Zadra, E. Palescandolo, et al., *Overexpression of fatty acid synthase is associated with palmitoylation of Wnt1 and cytoplasmic stabilization of beta-catenin in prostate cancer*. Lab Invest, 2008. **88**(12): p. 1340-8.
120. Zhan, T., N. Rindtorff, and M. Boutros, *Wnt signaling in cancer*. Oncogene, 2017. **36**(11): p. 1461-1473.
121. Krishnamurthy, N. and R. Kurzrock, *Targeting the Wnt/beta-catenin pathway in cancer: Update on effectors and inhibitors*. Cancer Treat Rev, 2018. **62**: p. 50-60.
122. Liu, H., Y. Liu, and J.T. Zhang, *A new mechanism of drug resistance in breast cancer cells: fatty acid synthase overexpression-mediated palmitate overproduction*. Mol Cancer Ther, 2008. **7**(2): p. 263-70.
123. Meena, A.S., A. Sharma, R. Kumari, et al., *Inherent and acquired resistance to paclitaxel in hepatocellular carcinoma: molecular events involved*. PLoS One, 2013. **8**(4): p. e61524.
124. Yang, Y., H. Liu, Z. Li, et al., *Role of fatty acid synthase in gemcitabine and radiation resistance of pancreatic cancers*. Int J Biochem Mol Biol, 2011. **2**(1): p. 89-98.
125. Kao, Y.C., S.W. Lee, L.C. Lin, et al., *Fatty acid synthase overexpression confers an independent prognosticator and associates with radiation resistance in nasopharyngeal carcinoma*. Tumour Biol, 2013. **34**(2): p. 759-68.
126. Liu, H., X. Wu, Z. Dong, et al., *Fatty acid synthase causes drug resistance by inhibiting TNF-alpha and ceramide production*. J Lipid Res, 2013. **54**(3): p. 776-85.
127. Rysman, E., K. Brusselmans, K. Scheys, et al., *De novo lipogenesis protects cancer cells from free radicals and chemotherapeutics by promoting membrane lipid saturation*. Cancer Res, 2010. **70**(20): p. 8117-26.
128. Wu, X., Z. Dong, C.J. Wang, et al., *FASN regulates cellular response to genotoxic treatments by increasing PARP-1 expression and DNA repair activity via NF-kB and SP1*. 2016. **113**(45): p. E6965-E6973.
129. Chajes, V., M. Cambot, K. Moreau, et al., *Acetyl-CoA carboxylase alpha is essential to breast cancer cell survival*. Cancer Res, 2006. **66**(10): p. 5287-94.
130. Wang, H., Q. Xi, and G. Wu, *Fatty acid synthase regulates invasion and metastasis of colorectal cancer via Wnt signaling pathway*. Cancer Med, 2016. **5**(7): p. 1599-606.
131. Seong-Hoon Yun, S.-W.S., Joo-In Park, *Expression of fatty acid synthase is regulated by PGC-1alpha and contributes to increased cell proliferation*. Oncology Reports, 2017. **36**(6): p. 3497-3506.
132. Sun, L., Y. yao, G. Pan, et al., *Small interfering RNA-mediated knockdown of fatty acid synthase attenuates the proliferation and metastasis of human gastric*

- cancer cells via mTOR/Gli1 signaling pathway* Oncology Letters, 2018. **16**(1): p. 594-602.
133. De Schrijver, E., K. Brusselmans, W. Heyns, et al., *RNA interference-mediated silencing of the fatty acid synthase gene attenuates growth and induces morphological changes and apoptosis of LNCaP prostate cancer cells*. Cancer Res, 2003. **63**(13): p. 3799-804.
 134. Chen, H.W., Y.F. Chang, H.Y. Chuang, et al., *Targeted therapy with fatty acid synthase inhibitors in a human prostate carcinoma LNCaP/tk-luc-bearing animal model*. Prostate Cancer Prostatic Dis, 2012. **15**(3): p. 260-4.
 135. Knowles, L.M. and J.W. Smith, *Genome-wide changes accompanying knockdown of fatty acid synthase in breast cancer*. BMC Genomics, 2007. **8**: p. 168.
 136. Menendez, J.A., R. Lupu, and R. Colomer, *Inhibition of tumor-associated fatty acid synthase hyperactivity induces synergistic chemosensitization of HER -2/ neu -overexpressing human breast cancer cells to docetaxel (taxotere)*. Breast Cancer Res Treat, 2004. **84**(2): p. 183-95.
 137. Menendez, J.A., L. Vellon, R. Colomer, et al., *Pharmacological and small interference RNA-mediated inhibition of breast cancer-associated fatty acid synthase (oncogenic antigen-519) synergistically enhances Taxol (paclitaxel)-induced cytotoxicity*. Int J Cancer, 2005. **115**(1): p. 19-35.
 138. Heuer, T.S., R. Ventura, K. Mordec, et al., *Abstract 4446: Discovery of tumor types highly susceptible to FASN inhibition and biomarker candidates for clinical analysis*. 2015. **75**(15 Supplement): p. 4446-4446.
 139. Funabashi, H., A. Kawaguchi, H. Tomoda, et al., *Binding site of cerulenin in fatty acid synthetase*. J Biochem, 1989. **105**(5): p. 751-5.
 140. Pizer, E.S., F.D. Wood, G.R. Pasternack, et al., *Fatty acid synthase (FAS): a target for cytotoxic antimetabolites in HL60 promyelocytic leukemia cells*. Cancer Res, 1996. **56**(4): p. 745-51.
 141. Ho, T.S., Y.P. Ho, W.Y. Wong, et al., *Fatty acid synthase inhibitors cerulenin and C75 retard growth and induce caspase-dependent apoptosis in human melanoma A-375 cells*. Biomed Pharmacother, 2007. **61**(9): p. 578-87.
 142. Pizer, E.S., C. Jackisch, F.D. Wood, et al., *Inhibition of fatty acid synthesis induces programmed cell death in human breast cancer cells*. Cancer Res, 1996. **56**(12): p. 2745-7.
 143. Murata, S., K. Yanagisawa, K. Fukunaga, et al., *Fatty acid synthase inhibitor cerulenin suppresses liver metastasis of colon cancer in mice*. Cancer Sci, 2010. **101**(8): p. 1861-5.
 144. Furuya, Y., S. Akimoto, K. Yasuda, et al., *Apoptosis of androgen-independent prostate cell line induced by inhibition of fatty acid synthesis*. Anticancer Res, 1997. **17**(6D): p. 4589-93.
 145. Corominas-Faja, B., L. Vellon, E. Cuyas, et al., *Clinical and therapeutic relevance of the metabolic oncogene fatty acid synthase in HER2+ breast cancer*. Histol Histopathol, 2017. **32**(7): p. 687-698.

146. Zhou, W., P.J. Simpson, J.M. McFadden, et al., *Fatty acid synthase inhibition triggers apoptosis during S phase in human cancer cells*. *Cancer Res*, 2003. **63**(21): p. 7330-7.
147. Wang, X. and W. Tian, *Green tea epigallocatechin gallate: a natural inhibitor of fatty-acid synthase*. *Biochem Biophys Res Commun*, 2001. **288**(5): p. 1200-6.
148. Puig, T., J. Relat, and R. Colomer, *Green Tea Catechin Inhibits Fatty Acid Synthase without Stimulating Carnitine Palmitoyltransferase-1 or Inducing Weight Loss in Experimental Animals*. *Anticancer Res*, 2008. **28**: p. 3671-3676.
149. Brusselmans, K., E. De Schrijver, W. Heyns, et al., *Epigallocatechin-3-gallate is a potent natural inhibitor of fatty acid synthase in intact cells and selectively induces apoptosis in prostate cancer cells*. *Int J Cancer*, 2003. **106**(6): p. 856-62.
150. Zhang, Z., M. Garzotto, T.M. Beer, et al., *Effects of omega-3 Fatty Acids and Catechins on Fatty Acid Synthase in the Prostate: A Randomized Controlled Trial*. *Nutr Cancer*, 2016. **68**(8): p. 1309-1319.
151. Vazquez, M.J., W. Leavens, R. Liu, et al., *Discovery of GSK837149A, an inhibitor of human fatty acid synthase targeting the beta-ketoacyl reductase reaction*. *FEBS J*, 2008. **275**(7): p. 1556-67.
152. Hardwicke, M.A., A.R. Rendina, S.P. Williams, et al., *A human fatty acid synthase inhibitor binds beta-ketoacyl reductase in the keto-substrate site*. *Nat Chem Biol*, 2014. **10**(9): p. 774-9.
153. Alwarawrah, Y., P. Hughes, D. Loiselle, et al., *Fasnall, a Selective FASN Inhibitor, Shows Potent Anti-tumor Activity in the MMTV-Neu Model of HER2(+) Breast Cancer*. *Cell Chem Biol*, 2016. **23**(6): p. 678-88.
154. Kridel, S.J., F. Axelrod, N. Rozenkrantz, et al., *Orlistat is a novel inhibitor of fatty acid synthase with antitumor activity*. *Cancer Res*, 2004. **64**(6): p. 2070-5.
155. Carvalho, M.A., K.G. Zecchin, F. Seguin, et al., *Fatty acid synthase inhibition with Orlistat promotes apoptosis and reduces cell growth and lymph node metastasis in a mouse melanoma model*. *Int J Cancer*, 2008. **123**(11): p. 2557-65.
156. Dowling, S., J. Cox, and R.J. Cenedella, *Inhibition of fatty acid synthase by Orlistat accelerates gastric tumor cell apoptosis in culture and increases survival rates in gastric tumor bearing mice in vivo*. *Lipids*, 2009. **44**(6): p. 489-98.
157. Zhi, J., A.T. Melia, C. Funk, et al., *Metabolic profiles of minimally absorbed orlistat in obese/overweight volunteers*. *J Clin Pharmacol*, 1996. **36**(11): p. 1006-11.
158. Zhi, J., A.T. Melia, H. Eggers, et al., *Review of limited systemic absorption of orlistat, a lipase inhibitor, in healthy human volunteers*. *J Clin Pharmacol*, 1995. **35**(11): p. 1103-8.
159. Hollywood, A. and J. Ogden, *Taking Orlistat: Predicting Weight Loss over 6 Months*. *J Obes*, 2011. **2011**: p. 806896.
160. Richardson, R.D., G. Ma, Y. Oyola, et al., *Synthesis of novel beta-lactone inhibitors of fatty acid synthase*. *J Med Chem*, 2008. **51**(17): p. 5285-96.
161. Purohit, V.C., R.D. Richardson, J.W. Smith, et al., *Practical, catalytic, asymmetric synthesis of beta-lactones via a sequential ketene dimerization/hydrogenation*

- process: inhibitors of the thioesterase domain of fatty acid synthase. *J Org Chem*, 2006. **71**(12): p. 4549-58.
162. Zhang, W., R.D. Richardson, S. Chamni, et al., *Beta-lactam congeners of orlistat as inhibitors of fatty acid synthase*. *Bioorg Med Chem Lett*, 2008. **18**(7): p. 2491-4.
 163. Ma, G., M. Zancanella, Y. Oyola, et al., *Total synthesis and comparative analysis of orlistat, valilactone, and a transposed orlistat derivative: Inhibitors of fatty acid synthase*. *Org Lett*, 2006. **8**(20): p. 4497-500.
 164. Liu, B., Y. Wang, K.L. Fillgrove, et al., *Triclosan inhibits enoyl-reductase of type I fatty acid synthase in vitro and is cytotoxic to MCF-7 and SKBr-3 breast cancer cells*. *Cancer Chemother Pharmacol*, 2002. **49**(3): p. 187-93.
 165. Oku, H., S. Wongtangtharn, H. Iwasaki, et al., *Conjugated linoleic acid (CLA) inhibits fatty acid synthetase activity in vitro*. *Biosci Biotechnol Biochem*, 2003. **67**(7): p. 1584-6.
 166. Zhao, W.H., J.F. Zhang, W. Zhe, et al., *The extract of leaves of Acer truncatum Bunge: A natural inhibitor of fatty acid synthase with antitumor activity*. *J Enzyme Inhib Med Chem*, 2006. **21**(5): p. 589-96.
 167. Zhao, W.H., C. Gao, Y.X. Zhang, et al., *Evaluation of the inhibitory activities of aceraceous plants on fatty acid synthase*. *J Enzyme Inhib Med Chem*, 2007. **22**(4): p. 501-10.
 168. Zhao, W.H., C.Y. Zhao, L.F. Gao, et al., *The novel inhibitory effect of Pangdahai on fatty acid synthase*. *IUBMB Life*, 2008. **60**(3): p. 185-94.
 169. Oh, J., I.H. Hwang, C.-E. Hong, et al., *Inhibition of fatty acid synthase by ginkgolic acids from the leaves of Ginkgo biloba and their cytotoxic activity*. *Journal of Enzyme Inhibition and Medicinal Chemistry*, 2013. **28**(3): p. 565-568.
 170. Wang, Y., W.X. Tian, and X.F. Ma, *Inhibitory effects of onion (Allium cepa L.) extract on proliferation of cancer cells and adipocytes via inhibiting fatty acid synthase*. *Asian Pac J Cancer Prev*, 2012. **13**(11): p. 5573-9.
 171. Richardson, R.D. and J.W. Smith, *Novel antagonists of the thioesterase domain of human fatty acid synthase*. *Mol Cancer Ther*, 2007. **6**(7): p. 2120-6.
 172. Rivkin, A., Y.R. Kim, M.T. Goulet, et al., *3-Aryl-4-hydroxyquinolin-2(1H)-one derivatives as type I fatty acid synthase inhibitors*. *Bioorganic & Medicinal Chemistry Letters*, 2006. **16**(17): p. 4620-4623.
 173. Zeng, X.F., W.W. Li, H.J. Fan, et al., *Discovery of novel fatty acid synthase (FAS) inhibitors based on the structure of ketoacyl synthase (KS) domain*. *Bioorg Med Chem Lett*, 2011. **21**(16): p. 4742-4.
 174. *A Phase 1, First-In-Human Study of Escalating Doses of Oral TVB-2640 in Patients With Solid Tumors.*
 175. *TVB 2640 for Resectable Colon Cancer Other Resectable Cancers; a Window Trial.*
 176. *FASN Inhibitor TVB-2640, Paclitaxel, and Trastuzumab in Treating Patients With HER2 Positive Advanced Breast Cancer.*
 177. *TVB- 2640 in Combination With Bevacizumab in Patients With First Relapse of High Grade Astrocytoma.*

178. Fako, V.E., X. Wu, B. Pflug, et al., *Repositioning proton pump inhibitors as anticancer drugs by targeting the thioesterase domain of human fatty acid synthase*. J Med Chem, 2015. **58**(2): p. 778-84.
179. Strand, D.S., D. Kim, and D.A. Peura, *25 Years of Proton Pump Inhibitors: A Comprehensive Review*. Gut Liver, 2017. **11**(1): p. 27-37.
180. Sachs, G., J.M. Shin, and C.W. Howden, *Review article: the clinical pharmacology of proton pump inhibitors*. Aliment Pharmacol Ther, 2006. **23 Suppl 2**: p. 2-8.
181. Sachs, G., J.M. Shin, C. Briving, et al., *The pharmacology of the gastric acid pump: the H⁺,K⁺ ATPase*. Annu Rev Pharmacol Toxicol, 1995. **35**: p. 277-305.
182. Thomson, A.B., M.D. Sauve, N. Kassam, et al., *Safety of the long-term use of proton pump inhibitors*. World Journal of Gastroenterology 2010. **16**(19): p. 2323-2330.
183. Luciani, F., M. Spada, A. De Milito, et al., *Effect of proton pump inhibitor pretreatment on resistance of solid tumors to cytotoxic drugs*. J Natl Cancer Inst, 2004. **96**(22): p. 1702-13.
184. Li, X., M.L. Yan, and Q. Yu, *Identification of candidate drugs for the treatment of metastatic osteosarcoma through a subpathway analysis method*. Oncol Lett, 2017. **13**(6): p. 4378-4384.
185. Lugini, L., I. Sciamanna, C. Federici, et al., *Antitumor effect of combination of the inhibitors of two new oncotargets: proton pumps and reverse transcriptase*. Oncotarget, 2017. **8**(3): p. 4147-4155.
186. Azzarito, T., G. Venturi, A. Cesolini, et al., *Lansoprazole induces sensitivity to suboptimal doses of paclitaxel in human melanoma*. Cancer Lett, 2015. **356**(2 Pt B): p. 697-703.
187. De Milito, A., E. Iessi, M. Logozzi, et al., *Proton pump inhibitors induce apoptosis of human B-cell tumors through a caspase-independent mechanism involving reactive oxygen species*. Cancer Res, 2007. **67**(11): p. 5408-17.
188. De Milito, A., R. Canese, M.L. Marino, et al., *pH-dependent antitumor activity of proton pump inhibitors against human melanoma is mediated by inhibition of tumor acidity*. Int J Cancer, 2010. **127**(1): p. 207-19.
189. Tan, Q., A.M. Joshua, J.K. Saggarr, et al., *Effect of pantoprazole to enhance activity of docetaxel against human tumour xenografts by inhibiting autophagy*. Br J Cancer, 2015. **112**(5): p. 832-40.
190. Yu, M., C. Lee, M. Wang, et al., *Influence of the proton pump inhibitor lansoprazole on distribution and activity of doxorubicin in solid tumors*. Cancer Sci, 2015. **106**(10): p. 1438-47.
191. Barar, J. and Y. Omid, *Dysregulated pH in Tumor Microenvironment Checkmates Cancer Therapy*. Bioimpacts, 2013. **3**(4): p. 149-62.
192. Tredan, O., C.M. Galmarini, K. Patel, et al., *Drug resistance and the solid tumor microenvironment*. J Natl Cancer Inst, 2007. **99**(19): p. 1441-54.
193. Fais, S., G. Venturi, and B. Gatenby, *Microenvironmental acidosis in carcinogenesis and metastases: new strategies in prevention and therapy*. Cancer Metastasis Rev, 2014. **33**(4): p. 1095-108.

194. Fais, S., A. De Milito, H. You, et al., *Targeting Vacuolar H⁺-ATPases as a New Strategy against Cancer*. 2007. **67**(22): p. 10627-10630.
195. Schempp, C.M., K. von Schwarzenberg, L. Schreiner, et al., *V-ATPase inhibition regulates anoikis resistance and metastasis of cancer cells*. *Mol Cancer Ther*, 2014. **13**(4): p. 926-37.
196. Sennoune, S.R., K. Bakunts, G.M. Martinez, et al., *Vacuolar H⁺-ATPase in human breast cancer cells with distinct metastatic potential: distribution and functional activity*. *Am J Physiol Cell Physiol*, 2004. **286**(6): p. C1443-52.
197. Martinez-Zaguilan, R., N. Raghunand, R.M. Lynch, et al., *pH and drug resistance. I. Functional expression of plasmalemmal V-type H⁺-ATPase in drug-resistant human breast carcinoma cell lines*. *Biochem Pharmacol*, 1999. **57**(9): p. 1037-46.
198. Spugnini, E.P., P. Sonveaux, C. Stock, et al., *Proton channels and exchangers in cancer*. *Biochim Biophys Acta*, 2015. **1848**(10 Pt B): p. 2715-26.
199. Pauli-Magnus, C., S. Rekersbrink, U. Klotz, et al., *Interaction of omeprazole, lansoprazole and pantoprazole with P-glycoprotein*. *Naunyn Schmiedebergs Arch Pharmacol*, 2001. **364**(6): p. 551-7.
200. Darby, R., R. Callaghan, and R. McMahon, *P-glycoprotein Inhibition: The Past, the Present and the Future*. *Current Drug Metabolism*, 2011. **12**(8): p. 722-731.
201. Spugnini, E.P., A. Baldi, S. Buglioni, et al., *Lansoprazole as a rescue agent in chemoresistant tumors: a phase I/II study in companion animals with spontaneously occurring tumors*. *Journal of Translational Medicine*, 2011. **9**(1): p. 221.
202. Spugnini, E.P., S. Buglioni, F. Carocci, et al., *High dose lansoprazole combined with metronomic chemotherapy: a phase I/II study in companion animals with spontaneously occurring tumors*. *J Transl Med*, 2014. **12**: p. 225.
203. *Pantoprazole and Docetaxel for Men With Metastatic Castration-Resistant Prostate Cancer*.
204. *Pantoprazole With Doxorubicin for Advanced Cancer Patients With Extension Cohort of Patients With Solid Tumours*.
205. Wang, B.Y., J. Zhang, J.L. Wang, et al., *Intermittent high dose proton pump inhibitor enhances the antitumor effects of chemotherapy in metastatic breast cancer*. *J Exp Clin Cancer Res*, 2015. **34**: p. 85.
206. *Inhibiting Fatty Acid Synthase to Improve Efficacy of Neoadjuvant Chemotherapy*.
207. Lugini, L., C. Federici, M. Borghi, et al., *Proton pump inhibitors while belonging to the same family of generic drugs show different anti-tumor effect*. *Journal of Enzyme Inhibition and Medicinal Chemistry*, 2016. **31**(4): p. 538-545.
208. Lovejoy, C.A. and D. Cortez, *Common mechanisms of PIKK regulation*. *DNA Repair (Amst)*, 2009. **8**(9): p. 1004-8.
209. Hammel, M., Y. Yu, B.L. Mahaney, et al., *Ku and DNA-dependent protein kinase dynamic conformations and assembly regulate DNA binding and the initial non-homologous end joining complex*. *J Biol Chem*, 2010. **285**(2): p. 1414-23.
210. Hung, C.M., L. Garcia-Haro, C.A. Sparks, et al., *mTOR-dependent cell survival mechanisms*. *Cold Spring Harb Perspect Biol*, 2012. **4**(12).

211. Feng, Y.L., J.F. Xiang, S.C. Liu, et al., *H2AX facilitates classical non-homologous end joining at the expense of limited nucleotide loss at repair junctions*. Nucleic Acids Res, 2017. **45**(18): p. 10614-10633.
212. Redon, C.E., A.J. Nakamura, Y.W. Zhang, et al., *Histone gammaH2AX and poly(ADP-ribose) as clinical pharmacodynamic biomarkers*. Clin Cancer Res, 2010. **16**(18): p. 4532-42.
213. An, J., Y.C. Huang, Q.Z. Xu, et al., *DNA-PKcs plays a dominant role in the regulation of H2AX phosphorylation in response to DNA damage and cell cycle progression*. BMC Mol Biol, 2010. **11**: p. 18.
214. Showkat, M., M.A. Beigh, and K.I. Andrabi, *mTOR Signaling in Protein Translation Regulation: Implications in Cancer Genesis and Therapeutic Interventions*. Mol Biol Int, 2014. **2014**: p. 686984.
215. Populo, H., J.M. Lopes, and P. Soares, *The mTOR signalling pathway in human cancer*. Int J Mol Sci, 2012. **13**(2): p. 1886-918.
216. Harnor, S.J., A. Brennan, and C. Cano, *Targeting DNA-Dependent Protein Kinase for Cancer Therapy*. ChemMedChem, 2017. **12**(12): p. 895-900.
217. Gaillard, H., T. Garcia-Muse, and A. Aguilera, *Replication stress and cancer*. Nat Rev Cancer, 2015. **15**(5): p. 276-89.
218. Yanai, M., H. Makino, B. Ping, et al., *DNA-PK Inhibition by NU7441 Enhances Chemosensitivity to Topoisomerase Inhibitor in Non-Small Cell Lung Carcinoma Cells by Blocking DNA Damage Repair*. Yonago Acta Med, 2017. **60**(1): p. 9-15.
219. Davidson, D., L. Amrein, L. Panasci, et al., *Small Molecules, Inhibitors of DNA-PK, Targeting DNA Repair, and Beyond*. Front Pharmacol, 2013. **4**: p. 5.
220. Gustafsson, A.S., A. Abramenkova, and B. Stenerlow, *Suppression of DNA-dependent protein kinase sensitize cells to radiation without affecting DSB repair*. Mutat Res, 2014. **769**: p. 1-10.
221. Yuan, T.L. and L.C. Cantley, *PI3K pathway alterations in cancer: variations on a theme*. Oncogene, 2008. **27**(41): p. 5497-510.
222. Mortensen, D.S., S.M. Perrin-Ninkovic, G. Shevlin, et al., *Optimization of a Series of Triazole Containing Mammalian Target of Rapamycin (mTOR) Kinase Inhibitors and the Discovery of CC-115*. J Med Chem, 2015. **58**(14): p. 5599-608.
223. Tsuji, T., L.M. Sapinoso, T. Tran, et al., *CC-115, a dual inhibitor of mTOR kinase and DNA-PK, blocks DNA damage repair pathways and selectively inhibits ATM-deficient cell growth in vitro*. Oncotarget, 2017. **8**(43): p. 74688-74702.
224. Munster, P.N., A. Mahipal, J.J. Nemunaitis, et al., *Phase I trial of a dual TOR kinase and DNA-PK inhibitor (CC-115) in advanced solid and hematologic cancers*. Journal of Clinical Oncology, 2016. **34**(15_suppl): p. 2505-2505.
225. Thijssen, R., J. Ter Burg, B. Garrick, et al., *Dual TORC/DNA-PK inhibition blocks critical signaling pathways in chronic lymphocytic leukemia*. Blood, 2016. **128**(4): p. 574-83.
226. Schiffer, C.A., J.E. Cortes, A. Hochhaus, et al., *Lymphocytosis after treatment with dasatinib in chronic myeloid leukemia: Effects on response and toxicity*. Cancer, 2016. **122**(9): p. 1398-407.

227. Rossi, D. and G. Gaidano, *Lymphocytosis and ibrutinib treatment of CLL*. Blood, 2014. **123**(12): p. 1772-4.
228. Woyach, J.A., K. Smucker, L.L. Smith, et al., *Prolonged lymphocytosis during ibrutinib therapy is associated with distinct molecular characteristics and does not indicate a suboptimal response to therapy*. Blood, 2014. **123**(12): p. 1810-7.
229. Wu, X., Z. Dong, C.J. Wang, et al., *FASN regulates cellular response to genotoxic treatments by increasing PARP-1 expression and DNA repair activity via NF-kappaB and SP1*. Proc Natl Acad Sci U S A, 2016. **113**: p. E6965–E6973.
230. Schinkel, A.H. and J.W. Jonker, *Mammalian drug efflux transporters of the ATP binding cassette (ABC) family: an overview*. Adv Drug Deliv Rev, 2003. **55**(1): p. 3-29.
231. Dubyak, G.R., *Ion homeostasis, channels, and transporters: an update on cellular mechanisms*. Adv Physiol Educ, 2004. **28**(1-4): p. 143-54.
232. Benga, G., *Water channel proteins (later called aquaporins) and relatives: past, present, and future*. IUBMB Life, 2009. **61**(2): p. 112-33.
233. Lewinson, O. and N. Livnat-Levanon, *Mechanism of Action of ABC Importers: Conservation, Divergence, and Physiological Adaptations*. J Mol Biol, 2017. **429**(5): p. 606-619.
234. Vasiliou, V., K. Vasiliou, and D.W. Nebert, *Human ATP-binding cassette (ABC) transporter family*. Hum Genomics, 2009. **3**(3): p. 281-90.
235. Gradhand, U. and R.B. Kim, *Pharmacogenomics of MRP transporters (ABCC1-5) and BCRP (ABCG2)*. Drug Metab Rev, 2008. **40**(2): p. 317-54.
236. Loscher, W. and H. Potschka, *Blood-brain barrier active efflux transporters: ATP-binding cassette gene family*. NeuroRx, 2005. **2**(1): p. 86-98.
237. Riordan, J.R., K. Deuchars, N. Kartner, et al., *Amplification of P-glycoprotein genes in multidrug-resistant mammalian cell lines*. Nature, 1985. **316**(6031): p. 817-9.
238. Doyle, L.A., W. Yang, L.V. Abruzzo, et al., *A multidrug resistance transporter from human MCF-7 breast cancer cells*. Proc Natl Acad Sci U S A, 1998. **95**(26): p. 15665-70.
239. Robey, R.W., K.K. To, O. Polgar, et al., *ABCG2: a perspective*. Adv Drug Deliv Rev, 2009. **61**(1): p. 3-13.
240. Woodward, O.M., A. Kottgen, J. Coresh, et al., *Identification of a urate transporter, ABCG2, with a common functional polymorphism causing gout*. Proc Natl Acad Sci U S A, 2009. **106**(25): p. 10338-42.
241. Hamdan, A.M., S. Koyanagi, E. Wada, et al., *Intestinal expression of mouse Abcg2/breast cancer resistance protein (BCRP) gene is under control of circadian clock-activating transcription factor-4 pathway*. J Biol Chem, 2012. **287**(21): p. 17224-31.
242. Cisternino, S., C. Mercier, F. Bourasset, et al., *Expression, up-regulation, and transport activity of the multidrug-resistance protein Abcg2 at the mouse blood-brain barrier*. Cancer Res, 2004. **64**(9): p. 3296-301.
243. Krishnamurthy, P. and J.D. Schuetz, *Role of ABCG2/BCRP in biology and medicine*. Annu Rev Pharmacol Toxicol, 2006. **46**: p. 381-410.

244. Krishnamurthy, P., D.D. Ross, T. Nakanishi, et al., *The stem cell marker Bcrp/ABCG2 enhances hypoxic cell survival through interactions with heme*. J Biol Chem, 2004. **279**(23): p. 24218-25.
245. Keogh, J.P., *Membrane transporters in drug development*. Adv Pharmacol, 2012. **63**: p. 1-42.
246. Nakanishi, T. and D.D. Ross, *Breast cancer resistance protein (BCRP/ABCG2): its role in multidrug resistance and regulation of its gene expression*. Chin J Cancer, 2012. **31**(2): p. 73-99.
247. Abbott, B.L., A.M. Colapietro, Y. Barnes, et al., *Low levels of ABCG2 expression in adult AML blast samples*. Blood, 2002. **100**(13): p. 4594-601.
248. Suvannasankha, A., H. Minderman, K.L. O'Loughlin, et al., *Breast cancer resistance protein (BCRP/MXR/ABCG2) in acute myeloid leukemia: discordance between expression and function*. Leukemia, 2004. **18**(7): p. 1252-7.
249. van den Heuvel-Eibrink, M.M., E.A. Wiemer, A. Prins, et al., *Increased expression of the breast cancer resistance protein (BCRP) in relapsed or refractory acute myeloid leukemia (AML)*. Leukemia, 2002. **16**(5): p. 833-9.
250. Benderra, Z., A.M. Faussat, L. Sayada, et al., *Breast cancer resistance protein and P-glycoprotein in 149 adult acute myeloid leukemias*. Clin Cancer Res, 2004. **10**(23): p. 7896-902.
251. Jordanides, N.E., H.G. Jorgensen, T.L. Holyoake, et al., *Functional ABCG2 is overexpressed on primary CML CD34+ cells and is inhibited by imatinib mesylate*. Blood, 2006. **108**(4): p. 1370-3.
252. Rinaldetti, S., M. Pfirrmann, K. Manz, et al., *Effect of ABCG2, OCT1, and ABCB1 (MDR1) Gene Expression on Treatment-Free Remission in a EURO-SKI Subtrial*. Clin Lymphoma Myeloma Leuk, 2018. **18**(4): p. 266-271.
253. Diestra, J.E., G.L. Scheffer, I. Catala, et al., *Frequent expression of the multi-drug resistance-associated protein BCRP/MXR/ABCP/ABCG2 in human tumours detected by the BXP-21 monoclonal antibody in paraffin-embedded material*. J Pathol, 2002. **198**(2): p. 213-9.
254. Kim, Y.H., G. Ishii, K. Goto, et al., *Expression of breast cancer resistance protein is associated with a poor clinical outcome in patients with small-cell lung cancer*. Lung Cancer, 2009. **65**(1): p. 105-11.
255. Ota, S., G. Ishii, K. Goto, et al., *Immunohistochemical expression of BCRP and ERCC1 in biopsy specimen predicts survival in advanced non-small-cell lung cancer treated with cisplatin-based chemotherapy*. Lung Cancer, 2009. **64**(1): p. 98-104.
256. Rabindran, S.K., H. He, M. Singh, et al., *Reversal of a novel multidrug resistance mechanism in human colon carcinoma cells by fumitremorgin C*. Cancer Res, 1998. **58**(24): p. 5850-8.
257. Rabindran, S.K., D.D. Ross, L.A. Doyle, et al., *Fumitremorgin C reverses multidrug resistance in cells transfected with the breast cancer resistance protein*. Cancer Res, 2000. **60**(1): p. 47-50.
258. Allen, J.D., A. van Loevezijn, J.M. Lakhai, et al., *Potent and specific inhibition of the breast cancer resistance protein multidrug transporter in vitro and in mouse*

- intestine by a novel analogue of fumitremorgin C. *Mol Cancer Ther*, 2002. **1**(6): p. 417-25.
259. Peng, H., Z. Dong, J. Qi, et al., *A novel two mode-acting inhibitor of ABCG2-mediated multidrug transport and resistance in cancer chemotherapy*. *PLoS One*, 2009. **4**(5): p. e5676.
 260. Woehlecke, H., H. Osada, A. Herrmann, et al., *Reversal of breast cancer resistance protein-mediated drug resistance by tryprostatin A*. *Int J Cancer*, 2003. **107**(5): p. 721-8.
 261. Lee, J.S., S. Scala, Y. Matsumoto, et al., *Reduced drug accumulation and multidrug resistance in human breast cancer cells without associated P-glycoprotein or MRP overexpression*. *J Cell Biochem*, 1997. **65**(4): p. 513-26.
 262. Horton, J.K., C.G. Vanoye, and L. Reuss, *Swelling-activated chloride currents in a drug-sensitive cell line and a P glycoprotein-expressing derivative are underlied by channels with the same pharmacological properties*. *Cell Physiol Biochem*, 1998. **8**(5): p. 246-60.
 263. Kumar, B., M. Prasad, P. Bhat-Nakshatri, et al., *Normal Breast-Derived Epithelial Cells with Luminal and Intrinsic Subtype-Enriched Gene Expression Document Interindividual Differences in Their Differentiation Cascade*. *Cancer Res*, 2018. **78**(17): p. 5107-5123.
 264. Oliver, M.H., N.K. Harrison, J.E. Bishop, et al., *A rapid and convenient assay for counting cells cultured in microwell plates: application for assessment of growth factors*. *J Cell Sci*, 1989. **92 (Pt 3)**: p. 513-8.
 265. Nagelkerke, A. and P.N. Span, *Staining Against Phospho-H2AX (gamma-H2AX) as a Marker for DNA Damage and Genomic Instability in Cancer Tissues and Cells*. *Adv Exp Med Biol*, 2016. **899**: p. 1-10.
 266. Mariotti, L.G., G. Pirovano, K.I. Savage, et al., *Use of the γ -H2AX Assay to Investigate DNA Repair Dynamics Following Multiple Radiation Exposures*. *PLOS ONE*, 2013. **8**(11): p. e79541.
 267. Stiff, T., M. O'Driscoll, N. Rief, et al., *ATM and DNA-PK function redundantly to phosphorylate H2AX after exposure to ionizing radiation*. *Cancer Res*, 2004. **64**(7): p. 2390-6.
 268. Keogh, M.C., J.A. Kim, M. Downey, et al., *A phosphatase complex that dephosphorylates gammaH2AX regulates DNA damage checkpoint recovery*. *Nature*, 2006. **439**(7075): p. 497-501.
 269. Woodbine, L., H. Brunton, A.A. Goodarzi, et al., *Endogenously induced DNA double strand breaks arise in heterochromatic DNA regions and require ataxia telangiectasia mutated and Artemis for their repair*. *Nucleic Acids Res*, 2011. **39**(16): p. 6986-97.
 270. Di Meo, S., T.T. Reed, P. Venditti, et al., *Role of ROS and RNS Sources in Physiological and Pathological Conditions*. *Oxid Med Cell Longev*, 2016. **2016**: p. 1245049.
 271. Davis, A.J. and D.J. Chen, *DNA double strand break repair via non-homologous end-joining*. *Transl Cancer Res*, 2013. **2**(3): p. 130-143.

272. Couto, C.A., H.Y. Wang, J.C. Green, et al., *PARP regulates nonhomologous end joining through retention of Ku at double-strand breaks*. J Cell Biol, 2011. **194**(3): p. 367-75.
273. Boeckman, H.J., K.S. Trego, and J.J. Turchi, *Cisplatin sensitizes cancer cells to ionizing radiation via inhibition of nonhomologous end joining*. Mol Cancer Res, 2005. **3**(5): p. 277-85.
274. Mehta, A. and J.E. Haber, *Sources of DNA double-strand breaks and models of recombinational DNA repair*. Cold Spring Harb Perspect Biol, 2014. **6**(9): p. a016428.
275. Robey, R.W., O. Polgar, J. Deeken, et al., *ABCG2: determining its relevance in clinical drug resistance*. Cancer Metastasis Rev, 2007. **26**(1): p. 39-57.
276. Seamon, J.A., C.A. Rugg, S. Emanuel, et al., *Role of the ABCG2 drug transporter in the resistance and oral bioavailability of a potent cyclin-dependent kinase/Aurora kinase inhibitor*. Mol Cancer Ther, 2006. **5**(10): p. 2459-67.
277. Ee, P.L., X. He, D.D. Ross, et al., *Modulation of breast cancer resistance protein (BCRP/ABCG2) gene expression using RNA interference*. Mol Cancer Ther, 2004. **3**(12): p. 1577-83.
278. Gottesman, M.M. and I.H. Pastan, *The Role of Multidrug Resistance Efflux Pumps in Cancer: Revisiting a JNCI Publication Exploring Expression of the MDR1 (P-glycoprotein) Gene*. J Natl Cancer Inst, 2015. **107**(9).
279. Liu, Y., H. Peng, and J.T. Zhang, *Expression profiling of ABC transporters in a drug-resistant breast cancer cell line using AmpArray*. Mol Pharmacol, 2005. **68**(2): p. 430-8.
280. Litman, T., M. Brangi, E. Hudson, et al., *The multidrug-resistant phenotype associated with overexpression of the new ABC half-transporter, MXR (ABCG2)*. J Cell Sci, 2000. **113 (Pt 11)**: p. 2011-21.
281. Alqawi, O., S. Bates, and E. Georges, *Arginine482 to threonine mutation in the breast cancer resistance protein ABCG2 inhibits rhodamine 123 transport while increasing binding*. Biochem J, 2004. **382**(Pt 2): p. 711-6.
282. Manes, G., O. Pieramico, F. Perri, et al., *Twice-daily standard dose of omeprazole achieves the necessary level of acid inhibition for Helicobacter pylori eradication. A randomized controlled trial using standard and double doses of omeprazole in triple therapy*. Dig Dis Sci, 2005. **50**(3): p. 443-8.
283. Landes, B.D., J.P. Petite, and B. Flouvat, *Clinical pharmacokinetics of lansoprazole*. Clin Pharmacokinet, 1995. **28**(6): p. 458-70.
284. Karol, M.D., G.R. Granneman, and K. Alexander, *Determination of lansoprazole and five metabolites in plasma by high-performance liquid chromatography*. J Chromatogr B Biomed Appl, 1995. **668**(1): p. 182-6.
285. Dziadkowiec, K.N., E. Gasiorowska, E. Nowak-Markwitz, et al., *PARP inhibitors: review of mechanisms of action and BRCA1/2 mutation targeting*. Prz Menopauzalny, 2016. **15**(4): p. 215-219.
286. Molina-Ortiz, D., R. Camacho-Carranza, J.F. Gonzalez-Zamora, et al., *Differential expression of cytochrome P450 enzymes in normal and tumor tissues from childhood rhabdomyosarcoma*. PLoS One, 2014. **9**(4): p. e93261.

287. Oyama, T., N. Kagawa, N. Kunugita, et al., *Expression of cytochrome P450 in tumor tissues and its association with cancer development*. Front Biosci, 2004. **9**: p. 1967-76.
288. Li, Y., A. Steppi, Y. Zhou, et al., *Tumoral expression of drug and xenobiotic metabolizing enzymes in breast cancer patients of different ethnicities with implications to personalized medicine*. Sci Rep, 2017. **7**(1): p. 4747.
289. Sporn, M., *Agents for Chemoprevention and their Mechanisms of Action*, in *Cancer Medicine*. 2003.
290. Squirewell, E.J., X. Qin, and M.W. Duffel, *Endoxifen and other metabolites of tamoxifen inhibit human hydroxysteroid sulfotransferase 2A1 (hSULT2A1)*. Drug Metab Dispos, 2014. **42**(11): p. 1843-50.
291. Goetz, M.P., J.M. Rae, V.J. Suman, et al., *Pharmacogenetics of tamoxifen biotransformation is associated with clinical outcomes of efficacy and hot flashes*. J Clin Oncol, 2005. **23**(36): p. 9312-8.
292. Singh, M.S., P.A. Francis, and M. Michael, *Tamoxifen, cytochrome P450 genes and breast cancer clinical outcomes*. Breast, 2011. **20**(2): p. 111-8.
293. Tervasmaki, A., R. Winqvist, A. Jukkola-Vuorinen, et al., *Recurrent CYP2C19 deletion allele is associated with triple-negative breast cancer*. BMC Cancer, 2014. **14**: p. 902.
294. Preissner, S.C., M.F. Hoffmann, R. Preissner, et al., *Polymorphic cytochrome P450 enzymes (CYPs) and their role in personalized therapy*. PLoS One, 2013. **8**(12): p. e82562.
295. Lord, C.J. and A. Ashworth, *BRCAness revisited*. Nat Rev Cancer, 2016. **16**(2): p. 110-20.
296. Liu, L., W. Zhou, C.T. Cheng, et al., *TGFbeta induces "BRCAness" and sensitivity to PARP inhibition in breast cancer by regulating DNA-repair genes*. Mol Cancer Res, 2014. **12**(11): p. 1597-609.
297. Wiegman, A.P., P.Y. Yap, A. Ward, et al., *Differences in Expression of Key DNA Damage Repair Genes after Epigenetic-Induced BRCAness Dictate Synthetic Lethality with PARP1 Inhibition*. Mol Cancer Ther, 2015. **14**(10): p. 2321-31.
298. Zhang, X., S. Hofmann, N. Harbeck, et al., *Impact of Etoposide on BRCA1 Expression in Various Breast Cancer Cell Lines*. Drugs R D, 2017. **17**(4): p. 569-583.
299. Zaniolo, K., S. Desnoyers, S. Leclerc, et al., *Regulation of poly(ADP-ribose) polymerase-1 (PARP-1) gene expression through the post-translational modification of Sp1: a nuclear target protein of PARP-1*. BMC Mol Biol, 2007. **8**: p. 96.
300. Yokoyama, Y., T. Kawamoto, Y. Mitsuuchi, et al., *Human poly(ADP-ribose) polymerase gene. Cloning of the promoter region*. Eur J Biochem, 1990. **194**(2): p. 521-6.
301. Oei, S.L., J. Griesenbeck, M. Schweiger, et al., *Interaction of the transcription factor YY1 with human poly(ADP-ribosyl) transferase*. Biochem Biophys Res Commun, 1997. **240**(1): p. 108-11.

302. Soldatenkov, V.A., A. Albor, B.K. Patel, et al., *Regulation of the human poly(ADP-ribose) polymerase promoter by the ETS transcription factor*. *Oncogene*, 1999. **18**(27): p. 3954-62.
303. Caldecott, K.W., S. Aoufouchi, P. Johnson, et al., *XRCC1 polypeptide interacts with DNA polymerase beta and possibly poly (ADP-ribose) polymerase, and DNA ligase III is a novel molecular 'nick-sensor' in vitro*. *Nucleic Acids Res*, 1996. **24**(22): p. 4387-94.
304. Satoh, M.S. and T. Lindahl, *Role of poly(ADP-ribose) formation in DNA repair*. *Nature*, 1992. **356**(6367): p. 356-8.
305. Flohr, C., A. Burkle, J.P. Radicella, et al., *Poly(ADP-ribosyl)ation accelerates DNA repair in a pathway dependent on Cockayne syndrome B protein*. *Nucleic Acids Res*, 2003. **31**(18): p. 5332-7.
306. Krokan, H.E. and M. Bjoras, *Base excision repair*. *Cold Spring Harb Perspect Biol*, 2013. **5**(4): p. a012583.
307. Lindahl, T., *Instability and decay of the primary structure of DNA*. *Nature*, 1993. **362**(6422): p. 709-15.
308. Scharer, O.D., *Nucleotide excision repair in eukaryotes*. *Cold Spring Harb Perspect Biol*, 2013. **5**(10): p. a012609.
309. Jena, N.R., *DNA damage by reactive species: Mechanisms, mutation and repair*. *J Biosci*, 2012. **37**(3): p. 503-17.
310. Karanjawala, Z.E., U. Grawunder, C.L. Hsieh, et al., *The nonhomologous DNA end joining pathway is important for chromosome stability in primary fibroblasts*. *Curr Biol*, 1999. **9**(24): p. 1501-4.
311. Difilippantonio, M.J., J. Zhu, H.T. Chen, et al., *DNA repair protein Ku80 suppresses chromosomal aberrations and malignant transformation*. *Nature*, 2000. **404**(6777): p. 510-4.
312. Karanjawala, Z.E., N. Murphy, D.R. Hinton, et al., *Oxygen metabolism causes chromosome breaks and is associated with the neuronal apoptosis observed in DNA double-strand break repair mutants*. *Curr Biol*, 2002. **12**(5): p. 397-402.
313. Phaniendra, A., D.B. Jestadi, and L. Periyasamy, *Free radicals: properties, sources, targets, and their implication in various diseases*. *Indian J Clin Biochem*, 2015. **30**(1): p. 11-26.
314. Parrinello, S., E. Samper, A. Krtolica, et al., *Oxygen sensitivity severely limits the replicative lifespan of murine fibroblasts*. *Nat Cell Biol*, 2003. **5**(8): p. 741-7.
315. Fulda, S., A.M. Gorman, O. Hori, et al., *Cellular stress responses: cell survival and cell death*. *Int J Cell Biol*, 2010. **2010**: p. 214074.
316. Redza-Dutordoir, M. and D.A. Averill-Bates, *Activation of apoptosis signalling pathways by reactive oxygen species*. *Biochim Biophys Acta*, 2016. **1863**(12): p. 2977-2992.
317. Pallepati, P. and D.A. Averill-Bates, *Mild thermotolerance induced at 40 degrees C protects HeLa cells against activation of death receptor-mediated apoptosis by hydrogen peroxide*. *Free Radic Biol Med*, 2011. **50**(6): p. 667-79.
318. Sun, S.Y., *N-acetylcysteine, reactive oxygen species and beyond*. *Cancer Biol Ther*, 2010. **9**(2): p. 109-10.

319. Svirnovski, A.I., T.V. Shman, T.F. Serhiyenka, et al., *ABCB1 and ABCG2 proteins, their functional activity and gene expression in concert with drug sensitivity of leukemia cells*. Hematology, 2009. **14**(4): p. 204-12.
320. Mo, W. and J.T. Zhang, *Human ABCG2: structure, function, and its role in multidrug resistance*. Int J Biochem Mol Biol, 2012. **3**(1): p. 1-27.
321. Olarte Carrillo, I., C. Ramos Peñafiel, E. Miranda Peralta, et al., *Clinical significance of the ABCB1 and ABCG2 gene expression levels in acute lymphoblastic leukemia*. Hematology, 2017. **22**(5): p. 286-291.
322. Toyoda, Y., T. Takada, and H. Suzuki, *Inhibitors of Human ABCG2: From Technical Background to Recent Updates With Clinical Implications*. Front Pharmacol, 2019. **10**: p. 208.
323. Westover, D. and F. Li, *New trends for overcoming ABCG2/BCRP-mediated resistance to cancer therapies*. J Exp Clin Cancer Res, 2015. **34**: p. 159.
324. Nowsheen, S. and E.S. Yang, *The intersection between DNA damage response and cell death pathways*. Exp Oncol, 2012. **34**(3): p. 243-54.
325. Duffy, M.J., N.C. Synnott, P.M. McGowan, et al., *p53 as a target for the treatment of cancer*. Cancer Treat Rev, 2014. **40**(10): p. 1153-60.
326. Oakman, C., G. Viale, and A. Di Leo, *Management of triple negative breast cancer*. Breast, 2010. **19**(5): p. 312-21.
327. Zecchin, K.G., L.C. Alberici, M.F. Riccio, et al., *Visualizing inhibition of fatty acid synthase through mass spectrometric analysis of mitochondria from melanoma cells*. Rapid Commun Mass Spectrom, 2011. **25**(3): p. 449-52.
328. Zecchin, K.G., F.A. Rossato, H.F. Raposo, et al., *Inhibition of fatty acid synthase in melanoma cells activates the intrinsic pathway of apoptosis*. Lab Invest, 2011. **91**(2): p. 232-40.
329. Galluzzi, L., O. Kepp, F.K. Chan, et al., *Necroptosis: Mechanisms and Relevance to Disease*. Annu Rev Pathol, 2017. **12**: p. 103-130.
330. Weinlich, R., A. Oberst, H.M. Beere, et al., *Necroptosis in development, inflammation and disease*. Nat Rev Mol Cell Biol, 2017. **18**(2): p. 127-136.
331. Najafov, A., H. Chen, and J. Yuan, *Necroptosis and Cancer*. Trends Cancer, 2017. **3**(4): p. 294-301.
332. Jiang, Y.W., H.Y. Guo, Z. Chen, et al., *In Situ Visualization of Lipid Raft Domains by Fluorescent Glycol Chitosan Derivatives*. Langmuir, 2016. **32**(26): p. 6739-45.

CURRICULUM VITAE

Jennifer Diane Beebe

EDUCATION

- 2013 – 2019 **Doctor of Philosophy in Pharmacology**
Minor: Cancer Biology
Indiana University
Indianapolis, IN
Mentor – Jian-Ting Zhang, Ph.D.
- 2008 – 2012 **B.S. Genomics and Molecular Genetics**
Minor: Spanish
Michigan State University
East Lansing, MI

PROFESSIONAL EXPERIENCE

- 2013 – 2019 **Graduate Student Researcher**
Indiana University School of Medicine, Indianapolis, IN
Department of Pharmacology
Mentor: Jian-Ting Zhang
- 2012 – 2013 **Research Associate**
Pfizer, Kalamazoo, MI
Bioprocess Genetics Group
- 2011 – 2012 **Undergraduate Research Assistant**
Michigan State University, East Lansing, MI
Department of Microbiology
Mentor: Terence Marsh
- 2012 **Teaching Assistant**
Michigan State University, East Lansing, MI
Department of Microbiology

PUBLICATIONS

- Beebe, J;** Dong, Z.; Zhang, J.T. (2019) Lansoprazole and its metabolites in the treatment of TNBC. (manuscript in preparation)
- Beebe, J;** Zhang, J.T. (2019) ABCG2 contributes to resistance to CC-115 a dual mTOR/DNA-PK inhibitor. JPET (under revision)
- Qin, L.; Hao Liu, **Beebe J.**; *et al.* and Zhang, J.T. (2019) PDGFD over-expression due to reversible promoter demethylation contributes gemcitabine resistance via STAT3 in both autocrine and paracrine manners. (manuscript submitted)

Beebe, J.; Zhang, J.T. (2018) Two decades of research in discovery of anticancer drugs targeting STAT3, how close are we? *Pharmacology Therapeutics* 191:74-91

Chen, Y., et al., **Beebe, J.;** Zhang, J.T. (2017). 14-3-3 σ contributes to radioresistance by regulating DNA repair and cell cycle via PARP1 and CHK2. *Molecular Cancer Research* 15(4): 418-428

PRESENTATIONS

Oral Presentations

Beebe J., et al. and Zhang JT. Lansoprazole and its metabolites in the treatment of triple-negative breast cancer. May 2019. Dissertation Defense, Indianapolis, IN.

Beebe J., et al. and Zhang JT. Inhibition of FASN TE domain by PPI sensitizes breast cancer to chemotherapeutics. April 2019. Department of Pharmacology Student Seminar Series, Indianapolis, IN.

Beebe J., et al. and Zhang JT. Targeted approaches to overcome resistance in breast cancer. December 2017. Department of Pharmacology Student Seminar Series, Indianapolis, IN.

Beebe J., et al. and Zhang JT. Inhibition of FASN TE domain by PPI sensitizes breast cancer to chemotherapeutics. April 2017. Department of Pharmacology Student Seminar Series, Indianapolis, IN.

Beebe J. et al. and Zhang JT. PDGF-D overexpression contributes to gemcitabine resistance in pancreatic cancer. March 2016. Department of Pharmacology Student Seminar Series, Indianapolis, IN.

Poster Presentations

Beebe J., Zhang JT. ABCG2 contributes to resistance to CC-115 a dual mTOR/DNA-PK inhibitor. September 2018, Chinese Society of Clinical Oncology Annual Meeting, Xiamen, China.

Beebe J., Zhang JT. ABCG2 contributes to resistance to CC-115 a dual mTOR/DNA-PK inhibitor. May 2018, Great Lakes Drug Metabolism Conference Annual Meeting, Indianapolis, IN.

Beebe J., Zhang JT. ABCG2 contributes to resistance to CC-115 a dual mTOR/DNA-PK inhibitor. April 2018, American Association for Cancer Research Annual Meeting, Chicago, IL.

Beebe J., Zhang JT. Role of PDGF-D in Gemcitabine Resistance in PDAC. September 2016, Pharmacology Poster Presentation Day, Indianapolis, IN.

Beebe J. Zhang JT. Role of PDGF-D in Gemcitabine Resistance in PDAC. May 2015, IU Simon Cancer Center Research Day, Indianapolis IN.

Beebe J. Zhang JT. Role of PDGF-D in Gemcitabine Resistance in PDAC. May 2015, Great Lakes Drug Metabolism Conference Annual Meeting, Ann Arbor, MI.

ACADEMIC and PROFESSIONAL HONORS

Travel Grant Awards

- | | |
|----------------|---|
| September 2018 | CSCO travel grant award to attend Chinese Society of Clinical Oncology conference |
| April 2018 | IUSM travel grant award to Attend AACR |

Fellowships

- | | |
|-----------|---|
| 2014-2015 | IU Simon Cancer Center - Cancer Biology Training Program Fellowship |
| 2016 | Sole nominee for PhRMA foundation Pre-doctoral Fellowship from IUSM |

SERVICE

- | | |
|----------------|--|
| 2017 - 2018 | President of NetworkIN
Indiana University School of Medicine
Indianapolis, IN |
| 2015 - Present | NetworkIN Committee Member
Indiana University School of Medicine
Indianapolis, IN |
| 2017 - 2018 | Graduate Student President
Department of Pharmacology and Toxicology
Indiana University School of Medicine
Indianapolis, IN |
| 2014 – Present | Graduate Student Mentor
Indiana University School of Medicine
Indianapolis, IN |